EPFL

Thèse n° 9266

Mitochondrial respiratory chain dysfunction disrupts intracellular cholesterol homeostasis

Présentée le 25 février 2022

Faculté des sciences de la vie
Programme doctoral en approches moléculaires du vivant

pour l'obtention du grade de Docteur ès Sciences

par

Christopher Tadhg James WALL

Acceptée sur proposition du jury

Prof. E. Oricchio, présidente du jury
Dr A. Wiederkehr, Prof. D. M. Suter, directeurs de thèse
Prof. N. Zelcer, rapporteur
Prof. M. Campanella, rapporteur
Prof. G. D'Angelo, rapporteur

École polytechnique fédérale de Lausanne

2022

Is fada an bóthar
nach bhfuil aon chasadh ann
It's a long road that has no turn in it

To my parents
To my grandparents
To my siblings
To my cousins
To my aunt and uncle

Acknowledgements

The journey of obtaining a PhD is one that is not completed alone. Along the way many people believed in me or stood by my side. First of all, my sincere gratitude goes to Andreas Wiederkehr and Jaime Santo-Domingo who must have seen some potential in me the day I came to NIHS, on the 16th of September in 2017. They gave me the opportunity to come to Switzerland and do my doctoral studies at EPFL and Nestlé. This moment was a pivotal moment both in my career and in my life as this brought me into the world of metabolism and gave me my basic training as a scientist. This chance brought me in contact with so many fantastic people that I can not express enough gratitude. Jaime is great scientist and a wonderful supervisor. I could always count on Jaime to discuss ideas and experiments and was always ready to help with his impressive ready knowledge of the literature. Especially in the first part of my PhD Jaime and I set up the cellular models and Jaime directed me into the right direction. Jaime gave me lots of freedom to develop my own ideas and learn at my own pace and from this liberty the best ideas came forth. Andreas has also been the best supervisor I could have wished for. Always open to ideas but indicating boundaries when he felt the idea would not produce results. Andreas was nothing but supportive throughout the entire PhD, always thinking the best of people and supervising in a sympathetic and motivating way. Especially in the last part of the PhD when we worked more closely together Andreas was patient and willing to listen even when my ideas maybe get too wild sometimes. A big thank you to Philipp Gut, who even with his packed schedule still takes the time to be involved and helpful in individual projects. Philipp was always very supportive of my PhD and enabled a lot of very fruitful and essential experiments in my PhD with his useful feedback and endorsements. Thank you to my EPFL supervisor professor David Suter, who enabled me to do a PhD at the world-class university of EPFL. David was always ready in case I needed help and in the last years of my PhD dedicated resources in his own lab to help in my project. Thank you Robin Willows for your incredible knowledge in biochemistry and helping me specifically with advising on making the knockout clones. Thanks to Robin's advice I was able to make these cell lines without trouble, avoiding some major pitfalls. Thank you, Gregory Lefebvre, for in the first year taking the time to explain statistical principles of RNAseq, hereby sparking an interest that I think will take me in a whole new direction. Special thanks to Carles, who puts himself out there for all PhD students and always ready to help scientifically with any project. Thank you Steve Laussueur who's help and teachings in the beginning were the kickstart for

my technical development in the lab.

Secondly to all my NIHS friends, everyone who helped me become who I am today. A PhD is not just a scientific development, it's a personal development. You are faced with your own strengths and weaknesses and no-one else to hold responsible but yourself. Having wonderful peers around you is key to success to pick you up when you fail. It's like a child learning from its parents and peers in a different way. I have been very lucky in meeting some of the greatest people. Thank you of course to mamen Philipp Rhein, who teamed up with me from the very start and together we did embark on many adventures, professional and personal. It made all of my active PhD like a pleasure to do. Philipp is a friend for life. Thank you to my other partner in crime, Margherita. Mags is a fantastic creature with a very bright mind and an incredible work ethic. She would support me when things would get tough and would always be there for me in the end. I am sure she will be very successful in her work and her life. Thank you, Lucie Chanvillard, pelo, with whom I can't stop laughing. Lucie has an amazing and inspiring positive attitude in life and is always a great pleasure to share thoughts with about the quest for personal development. Thanks to the greatest gentleman of all time dadash Omid Mashinchian, who is a one-of-a-kind of person, where kindness, ambition and intelligence are combined. Omid is always ready for a joke or to give advice and will always be ready to help you. Thank you Melanie Buisson, who's energy and drive are unmatched. Mel is an extremely driven person who can get anything done and it was a great pleasure running the YSN together with you and Phil. Thank you to Angelique Cercillieux, who was in this journey together with me and will hand in the thesis at the same time. Angelique is the sweetest person and was a great point of reflection throughout the course of the PhD on where we are and where we are going. Thank you to Katyayanee Neopane who I really got to know working in the same team, running western blots back-to-back. Katya missed me so much she had to build a glovebox-puppet on my desk beside hers, but also used it as a wall when I wás there. Thank you to Miriam Valera Alberni, who is my role model mitochondria scientist. Miriam would never shy away form a discussion on mitochondrial biology and metabolism, but also always there to help. Thank you Anna Weiser, who's down to earth attitude is always a refreshing factor that grounded me and put things back into perspective for me. Thank you Romy, for becoming a close friend in no time and always there to talk or hang out.

Then a word of gratitude to all the friends made at the EPFL. Key to me retaining partial sanity was the strong friend base that I built up in Lausanne, turning the town into home in no time. Special thanks to Kevin, Sam, Remco, Valeria with whom I have countless adventures shared and are fantastic friends. Charalampos Koutsoulas, who is basically a Greek version of myself and a fantastic friend. Charis always listens, never judges and supports no matter what. I wish I could find a wife like you! Francesco, Stefan, Thibaud, true bothers until the end. Larise, Daniele, Amber, Fabio, Irene, Celine, Barnaby, Otto, Joanna thank you for being such a good friends! Forgive me if I forgot you, reader!

Lausanne, November 17, 2021 Christopher T.J. Wall

Abstract

Mitochondrial diseases are rare and severe conditions with debilitating symptoms. Biochemical defects in mitochondria however are common. The difference between these two frequencies is suspected to lie in the capability of the cells to adapt to the homeostatic disbalance. Cells activate retrograde signalling pathways in response to mitochondrial dysfunction, activating cellular transcriptional programs to correct for the disbalance. The full extent of the retrograde signals that are induced by mitochondrial dysfunctions still remains unknown. Studying these retrograde signalling pathways can lead to insights how to make the difference between restoring the homeostasis and a detrimental disease. Investigating the transcriptional responses to artificially induced mitochondrial dysfunction has proven to be lucrative in unveiling novel responses to mitochondrial defects. In this work we studied the transcriptional responses to three chemical models of mitochondrial respiratory chain dysfunction. In line with recently published work, we found a commonly upregulated stress response in all models. Interestingly, shared between all the models was a downregulation of genes enriched in cholesterol biosynthesis pathways. Upon closer examination this encompassed, almost without exception, all transcripts of the mevalonate pathway. This coordinated downregulation of transcripts had functional consequences on the output of the pathway, lowering the abundance of cholesterol precursor metabolites. Other metabolites in more upstream regions of the pathway were changed differently depending on the complex affected, suggesting other regulatory influences involved. Upon closer mechanistic investigation to the cause of the transcriptional suppression we found the main transcription factor responsible for mevalonate pathway gene transcription, the Sterol Response Element Binding Protein 2 (SREBP2), to be inhibited during complex I impairment. This was most evident in sterol depleted conditions where SREBP2 did not activate to normal levels. A decreased activation of SREBP2 is signature for an elevated concentration of ER-cholesterol. Indeed, other ER-bound cholesterol sensitive proteins confirmed this, showing a similar decreased abundance following complex I impairment in both normal and low lipid conditions. To investigate the source of this cholesterol we measured various cholesterol levels. No changes in the levels of total cholesterol (free cholesterol plus esterified cholesterol) were detected. Also, the fraction of free cholesterol was not significantly affected by complex I inhibition. Using the fluorescent cholesterol stain filipin, we were able to measure a modest but reproducible increase in intracellular free cholesterol. This provided

novel mechanistic insight into the inhibition of ER sterol sensors and mevalonate pathway activity by mitochondrial dysfunction. Several well-known retrograde signalling pathways AMPK, ISR and mTOR did not explain the changes observed. The exact mechanism through which mitochondria incite an increase in intracellular free cholesterol remains unknown. Taken together this work can provide a mechanistic link between mitochondrial function and intracellular cholesterol homeostasis and could possibly link mitochondrial function to circulating lipoprotein homeostasis. Further work should focus on elucidating the possible mechanism, where differences in complex functions could provide a hint in the right direction.

Key words: Mitochondria, mitochondrial dysfunction, respiratory chain, retrograde signalling, cholesterol metabolism, mevalonate pathway, SREBP2

Résumé

Les maladies mitochondriales sont des affections rares et graves dont les symptômes sont débilitants. Les cellules activent des voies de signalisation rétrograde en réponse au dysfonctionnement mitochondrial, activant les programmes de transcription cellulaire pour corriger le déséquilibre. L'étude de ces voies de signalisation rétrograde peut permettre de comprendre comment faire la différence entre le rétablissement de l'homéostasie et une maladie préjudiciable. L'étude des réponses transcriptionnelles au dysfonctionnement mitochondrial induit artificiellement s'est avérée très lucrative pour dévoiler de nouvelles réponses aux défauts mitochondriaux. Dans ce travail, nous avons étudié les réponses transcriptionnelles communes à trois modèles chimiques de dysfonctionnement de la chaîne respiratoire mitochondriale. En accord avec les travaux récemment publiés, nous avons trouvé une réponse au stress communément régulée dans tous les modèles. Il est intéressant de noter que tous les modèles partagent une régulation négative des gènes enrichis dans les voies de biosynthèse du cholestérol. Cette régulation coordonnée à la baisse des transcrits a eu des conséquences fonctionnelles sur la sortie de la voie, diminuant l'abondance des métabolites précurseurs du cholestérol. D'autres métabolites dans des régions plus en amont de la voie ont été modifiés différemment selon le complexe affecté, ce qui suggère d'autres influences régulatrices impliquées. En examinant de plus près les mécanismes à l'origine de la suppression de la transcription, nous avons découvert que le principal facteur de transcription responsable de la transcription des gènes de la voie du mévalonate, la protéine 2 de liaison aux éléments de réponse aux stérols (SREBP2), était inhibé lors de l'altération du complexe I. Ce phénomène était le plus évident dans les cas de carence en stérols. Une diminution de l'activation de SREBP2 et la réduction consécutive des transcrits de mévalonate sont la signature d'une concentration élevée de cholestérol du réticulum endoplasmique (RE). En effet, d'autres protéines sensibles au cholestérol lié au RE l'ont confirmé, montrant une diminution similaire de l'abondance suite à l'altération du complexe I. Aucun changement dans les niveaux de cholestérol total n'a été détecté. De même, la sous-fraction de cholestérol libre n'a pas été significativement affectée par l'inhibition du complexe I. En utilisant la filipin, un colorant fluorescent qui peut se lier au cholestérol libre, nous avons pu mesurer une augmentation modeste mais reproductible du cholestérol libre intracellulaire. Ceci a fourni un nouvel aperçu mécanistique de l'inhibition des capteurs de stérol du RE et de l'activité de la voie du mévalonate par le

dysfonctionnement mitochondrial. Plusieurs voies de signalisation rétrograde bien connues, AMPK, ISR et mTOR, n'ont pas expliqué les changements observés. Le mécanisme exact par lequel les mitochondries incitent à une augmentation du cholestérol libre intracellulaire reste inconnu. Dans l'ensemble, ce travail peut fournir un lien mécaniste entre la fonction mitochondriale et l'homéostasie du cholestérol intracellulaire et pourrait éventuellement relier la fonction mitochondriale à l'homéostasie des lipoprotéines circulantes. Les travaux futurs devraient se concentrer sur l'élucidation du mécanisme possible, où les différences dans les fonctions complexes pourraient fournir un indice dans la bonne direction.

Mots clefs : Mitochondries, dysfonctionnement mitochondrial, signalisation rétrograde, métabolisme du cholestérol, voie du mévalonate, SREBP2.

Contents

Acknowledgements i

Abstract (English/Français) iii

List of figures xi

List of tables xiii

List of abbreviations xv

1 Introduction 1

1.1 Mitochondrial function and oxidative phosphorylation . . . 1

1.1.1 The respiratory chain complexes . . . 2

1.1.2 Beyond oxidative phosphorylation . . . 4

1.2 Mitochondrial dysfunction . . . 5

1.2.1 Clinical epidemiology of mitochondrial diseases . . . 5

1.2.2 Biochemical consequences . . . 6

1.3 Retrograde signalling . . . 6

1.3.1 Retrograde signalling in mitochondrial dysfunction . . . 7

1.3.2 Targeting retrograde signalling . . . 10

1.4 Cholesterol metabolism . . . 11

1.4.1 Cholesterol distribution . . . 11

1.4.2 The mevalonate pathway . . . 12

1.4.3 The biological relevance of mevalonate pathway metabolites . . . 14

1.4.4 Regulation of the mevalonate pathway activity . . . 15

1.4.5 Intracellular cholesterol trafficking . . . 20

1.4.6 Mitochondrial cholesterol . . . 23

1.5 Outline of the thesis project . . . 24

2 Pharmacological models of respiratory chain dysfunction 27

2.1 Dose finding . . . 28

2.2 Further phenotyping of the models . . . 30

2.3 Conclusion . . . 30

3 Transcriptional profile of mitochondrial respiratory chain dysfunction 33
3.1 Exploratory data analysis . . . 33
3.2 The mevalonate pathway . . . 34
3.3 Validation . . . 36
3.4 Conclusion . . . 38

4 Metabolic profile of mitochondrial respiratory chain dysfunction 41
4.1 Exploratory data analysis and validation . . . 41
4.2 Isoprenoids . . . 42
4.3 Ubiquinone . . . 43
4.4 Sterol intermediates . . . 44
4.5 Conclusion . . . 44

5 Genetic models of mitochondrial respiratory chain dysfunction 47
5.1 Validation of knockout models . . . 47
5.2 Further characterisation of the genetic models . . . 49
5.3 Expression of mevalonate pathway genes . . . 49
5.4 Conclusion . . . 50

6 Investigation of upstream signalling pathways 53
6.1 Integrated stress response . . . 53
6.2 AMPK . . . 55
6.3 mTOR . . . 56
6.4 Conclusion . . . 57

7 Characterisation of cholesterol signalling 59
7.1 Changes in SREBP2 activation . . . 59
7.2 Adaptations to rapid cholesterol changes . . . 61
7.3 Cholesterol sensing enzymes on ER membrane . . . 63
7.4 Conclusion . . . 64

8 Intracellular cholesterol levels 67
8.1 Changes in total cellular cholesterol . . . 67
8.2 Intracellular free cholesterol . . . 69
8.3 Intracellular trafficking . . . 69
8.4 Conclusion . . . 70

9 Complex I dysfunction in hepatocarcinoma cells 71
9.1 Mevalonate pathway transcripts . . . 71
9.2 Changes in SREBP2 activation . . . 71
9.3 Cholesterol sensing enzymes on the ER membrane . . . 73
9.4 Conclusion . . . 73

10 Discussion **77**
10.1 Cellular models of mitochondrial disease . . . 78
10.2 The mevalonate pathway is unaffected by a traditional retrograde signalling . . 79
10.3 Potential mechanisms . . . 81
10.4 Increased intracellular free cholesterol . . . 84
10.5 Source of the intracellular cholesterol . . . 85
10.6 Clinical relevance . . . 87

11 Conclusions **89**

12 Future perspectives **91**

13 Materials and Methods **93**
13.1 Reagents and chemicals . . . 93
13.2 Cyclodextrin loading . . . 93
13.3 Cell culture . . . 93
13.4 Transfections . . . 94
13.5 Growth rate and apoptosis assays . . . 94
13.6 Immunoblotting . . . 94
13.7 Real-time qPCR . . . 95
13.8 Seahorse XF analyser . . . 95
13.9 DNA sequencing . . . 95
13.10 3'RNAseq . . . 96
13.11 Metabolomics . . . 97
13.12 Gas chromatography . . . 98
13.13 Confocal microscopy . . . 99

14 Resource tables **101**
14.1 Chemicals . . . 101
14.2 Antibodies . . . 101
14.3 plasmids . . . 102
14.4 Primers . . . 102

Bibliography **103**

Curriculum Vitae **119**

List of Figures

1.1 The mitochondrial respiratory chain 2
1.2 Complex I schematic 3
1.3 Schematic of the mevalonate pathway 13
1.4 SREBP activation schematic 17

2.1 Inhibition of the respiratory chain complexes 29
2.2 Validation of mitochondrial dysfunction characteristics 31
2.3 Further characterisation of models of mitochondrial dysfunction 32

3.1 Inhibition of mitochondrial respiratory function activates a strong transcriptional response 35
3.2 Inhibition of mitochondrial respiratory function triggers activation of stress and inhibition of cholesterol biosynthesis 37
3.3 Inhibition of mitochondrial respiratory function decreases expression of cholesterol biosynthesis genes in a time dependent manner. 39
3.4 Cellular proliferation rates do not affect inhibition mevalonate pathway transcripts. 40

4.1 Inhibition of mitochondrial respiratory function affect abundance of mevalonate pathway metabolites. 42
4.2 Inhibition of mitochondrial respiratory function varyingly affects isoprenoid levels. 43
4.3 Inhibition of mitochondrial respiratory function varyingly affects ubiquinol levels. 44
4.4 Inhibition of mitochondrial respiratory function affects cholesterol precursor metabolites in similar fashion. 45

5.1 Knockout of complex I subunits impairs respiration. 48
5.2 Knockout of complex I subunits changes respiratory complex expression and growth rates. 50
5.3 Knockout of complex I subunits lowers expression of cholesterol biosynthesis genes. 51

6.1 Inhibiting the ISR has no effect on mevalonate pathway transcripts. 54
6.2 Downregulation of mevalonate pathway transcripts is not dependent on AMPK. 56

6.3 Downregulation of mevalonate pathway transcripts is not dependent on mTOR activation. 57

7.1 Rotenone impairs normal SREBP2 activation in low-lipid conditions. 60
7.2 Rotenone impairs normal mevalonate pathway gene expression in low-lipid conditions. 61
7.3 Complex I inhibition blunts maximal response of SREBP2 to lipid depletion. . . 62
7.4 Complex I impairment reduces induced SQLE accumulation. 63
7.5 Complex I impairment reduces induced HMGCR accumulation. 65

8.1 Complex I inhibition increases intracellular free cholesterol. 68
8.2 Complex I inhibition lowers mevalonate pathway transcripts independent of endosomal trafficking of cholesterol. 70

9.1 Complex I inhibition leads to a more severe phenotype in hepatocarcinoma cells. 72
9.2 Complex I inhibition has a strong effect on the levels of SREBP2 in in hepatocarcinoma cells. 74
9.3 Complex I inhibition has a strong depletion on the levels of ER-membrane cholesterol sensors in hepatocarcinoma cells. 75

10.1 Schematic representation of proposed sources of intracellular cholesterol transport. 86

11.1 Schematic representation of discovered adaptations 90

List of Tables

1.1 SREBP2 targets 18

2.1 IC50 values of respiratory inhibition 28

Abbreviations

ABCA1	ATP-binding cassette transporter A1
ACAT	Acetyl-CoA acetyltransferase
ACC	Acetyl-CoA carboxylase
ADP	Adenosine diphosphate
AMP	Adenosine monophosphate
AMPK	AMP-activated protein kinase (AMPK)
ANT	Adenine nucleotide translocase
ATF	Activating Transcription Factor
ATP	Adenosine triphosphate
CHOP	C/EBP homologous protein
CoQ	Coenzyme Q
DELE1	DAP3 Binding Cell Death Enhancer 1
DHCR7	7-Dehydrocholesterol reductase
ER	endoplasmic reticulum
ERAD	ER-associated protein degradation
GAPDH	Glyceraldehyde 3-phosphate dehydrogenase
GO	Gene Onthology
HMGCR	HMG-CoA reductase
HMGCS1	3-Hydroxy-3-Methylglutaryl-CoA Synthase 1
IMM	Inner mitochondrial membrane
INSIG	Insulin-induced gene protein
ISR	Integrated Stress Response
LDL	low-density lipoprotein
LXR	liver X receptor
mRNA	messenger ribonucleic acid
mTOR	mechanistic Target Of Rapamycin
NAD(H)	Nicotinamide adenine dinucleotide (reduced)
OMA1	OMA1 Zinc Metallopeptidase
OMM	Outer mitochondrial membrane
OSBP	Oxysterol-binding protein 1
ROS	Reactive oxygen species
SCAP	SREBP cleavage-activating protein
SOD	Superoxide dismutase

SQLE	Squalene epoxidase
SREBP	Sterol regulatory-element binding proteins
SSD	Sterol Sensing domain
StAR	steroidogenic acute regulatory protein
TSPO	Translocator protein
UPR	Unfolded protein response
VLDL	very low-density lipoprotein
WT	Wild Type

1 Introduction

Mitochondria are best known for their role of providing adenosine triphosphate (ATP) for the cell by oxidising highly energetic reduced molecules, which has earned them the honorary title "powerhouse of the cell". However, this description is an understatement of their significance in biological systems. Mitochondria are a highly versatile organelle that is central to many metabolic processes such as carbohydrate metabolism, fatty acid oxidation, calcium homeostasis and amino acid metabolism. More recently additional roles for mitochondria have been uncovered linking their function to several biological processes such as stress signalling, apoptosis and survival which suggests novel roles in the pathophysiology of diseases.

1.1 Mitochondrial function and oxidative phosphorylation

The most characteristic role of the mitochondria is the production of energy in the form of ATP. They do this by converting energy from reduced molecules into a form usable for biological systems: ATP (Mitchell, 1961). Energy rich molecules ingested from our diet are broken down by pathways such as glycolysis or fatty acid oxidation and the resulting metabolites converge on the Krebs' cycle to produce high energy reduced equivalents. The electrons released from the oxidation of these substrates are ultimately transferred to molecular oxygen to produce water. A set of highly specialised protein complexes on the mitochondrial inner membrane are the engines for this reaction and together are called the mitochondrial respiratory chain. According to the chemiosmotic theory the transport of electrons through the respiratory chain is tightly linked to the extrusion of protons out of the mitochondrial matrix, creating an energy rich electrochemical gradient. This proton gradient is the driving force for the phosphorylation of ADP into ATP by a protein complex (complex V). The energy stored in the membrane potential is used to fuel the transport of proteins, ions, metabolites and substrates across the mitochondrial membrane and acts as a quality control parameter to remove dysfunctional mitochondria (Zorova et al., 2018).

1.1.1 The respiratory chain complexes

The respiratory chain comprises of five protein complexes located on the inner mitochondrial membrane labelled complex I to V (Sousa et al., 2018). Collectively the first four complexes transport electrons derived from reducing equivalents NADH and succinate to molecular oxygen. Electrons enter the respiratory chain at complex I and II who accept electrons from molecules NADH and succinate. These electrons are transported down the respiratory chain by the electron carrier ubiquinone, called ubiquinol in its reduced form, to complex III. This complex then reduces cytochrome c which transfers the electrons to the complex IV, which reduces molecular oxygen to water. The free energy generated by this transfer of electrons is used by complex I, III and IV to pump protons from the matrix to the intermembrane space, creating an electrochemical gradient or proton motive force (PMF) across the mitochondrial membrane. The fifth complex in the respiratory chain, named ATP-synthase, consumes the energy stored in this electrochemical gradient to phosphorylate ADP into the energy rich ATP (Boyer, 1997). The resulting ATP is then transported to the cytosol by Adenine Nucleotide Translocases (ANTs, also known as SLC25A4) where the ATP can power energy demanding cellular processes. The complexes are inserted in the mitochondrial membrane in a semi-fluid state where they move around freely to interact with their substrates. To facilitate the transfer the electrons they show affinity among themselves and form multiprotein complexes called supercomplexes (Acin-Perez and Enriquez, 2014).

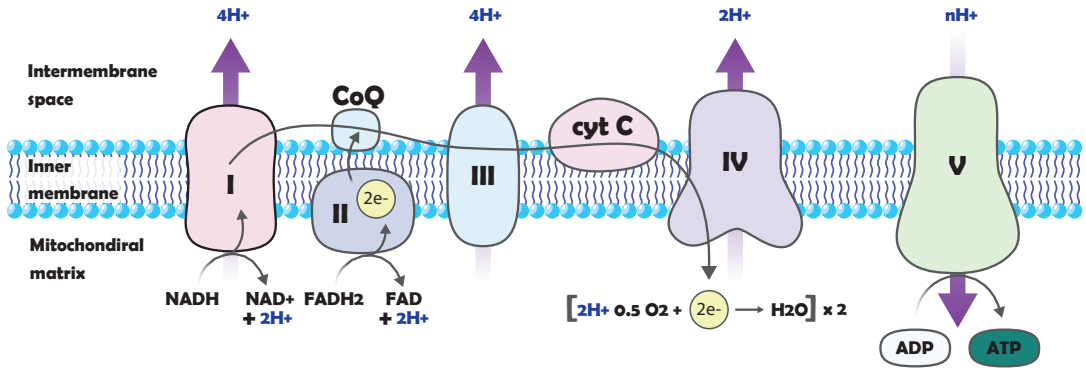

Figure 1.1 – **The mitochondrial respiratory chain**
A schematic of the mitochondrial respiratory chain complexes and the transfer of electrons and protons across the membrane.

The first complex in the respiratory chain is NADH:ubiquinone oxidoreductase (complex I, EC 7.1.1.2). This 1 MDa respiratory complex consists of 44 subunits of which 7 are encoded in the mitochondrial genome, making it the largest of all RC-complexes (Wirth et al., 2016). The biochemical functions of complex I consist of NADH binding, ubiquinone binding and pumping protons out of the mitochondrial matrix. These functions are taken care of by 14 central subunits, see figure 1.2. The electrons derived from the substrate of complex I (NADH), travel through iron sulphur-clusters embedded in the substrate binding region of the complex (Fassone and Rahman, 2012). The electrons of complex I are then passed onto the electron

carrier ubiquinone to be further transported along the respiratory chain. Complex I is also a main site of Reactive Oxygen Species generation (ROS) (Koopman et al., 2010).

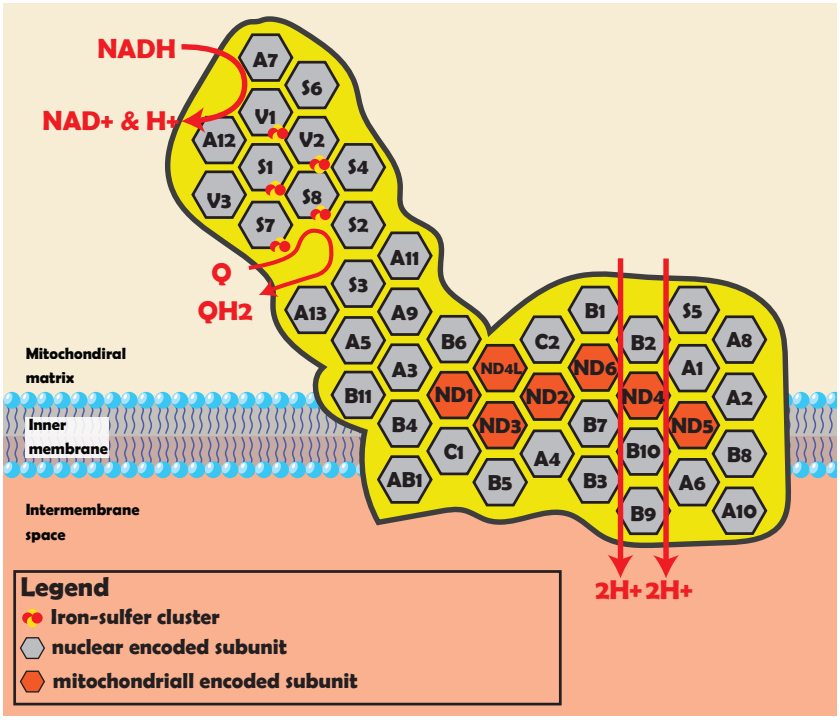

Figure 1.2 – **Schematic of complex I structure.** Schematic representation of the structure of complex I. The indiviual subunits are markerd. Nuclearly encoded subunits are indicated with a grey colour, mitochondrially encoded subunits are marked with an orange colour. The movement of biochemical subtrates and ions are marked with red arrows.

Electrons can enter the respiratory chain at a second protein complex called Succinate dehydrogenase (complex II, EC 1.3.5.1). This is a smaller protein complex of 124 kDa, consisting of only 4 subunits (Sousa et al., 2018). This complex oxidises succinate to fumarate as part of the TCA cycle. As with complex I, this enzyme transfers the released electrons to coenzyme Q.

Central in the respiratory chain is coenzyme Q: cytochrome c – oxidoreductase (complex III, EC 1.10.2.2). This dimeric enzyme complex consists of two identical monomers of 11 subunits (Sousa et al., 2018). This complex receives electrons from the reduced form of CoQ, ubiquinol and transfers them through iron-sulphur clusters to a protein called cytochrome c. Just as complex I, complex III contributes to forming the electrochemical gradient by pumping protons from the mitochondrial matrix into the intramembrane space. Also, complex III produces ROS, but in contrast to complex I, which produces ROS exclusively in the mitochondrial matrix, complex III produces ROS both in the matrix and into intramembrane space (Muller et al., 2004).

Complex IV is the last protein complex involved in shuttling electrons along the respiratory chain. This complex consists of 14 subunits of which three are encoded in the mitochondrial

genome (Sousa et al., 2018). This heme-copper oxidase enzyme receives the electrons from cyt c and transfers these electrons to oxygen, reducing it to water. The free energy released by this translocation of electrons is coupled to the extrusion of protons from the mitochondrial matrix to the intermembrane space, contributing to the generation of the proton electrochemical gradient across the IMM (Belevich et al., 2006).

The final protein complex in mitochondrial respiratory chain is ATP synthase (complex V). This large protein complex consists of two functional domains, F0 responsible for the proton translocation and F1 responsible for the ATP-synthesis. This unique enzyme functions as a molecular rotor, where the energy stored in the electrochemical gradient drives a confirmational change that phosphorylates ADP into ATP. Remarkable is that this protein complex can also perform the reaction in the opposite direction, consuming ATP to extrude protons (Boyer, 1997). This reversed action highlights the importance of maintaining the proton gradient over the mitochondrial membrane.

The remaining two components to complete the respiratory chain are the electron transporting molecules ubiquinone (Coenzyme Q, CoQ) and cytochrome c (cyt c). Coenzyme Q is an amphiphilic quinone with a tail of varying number of isoprenyl subunits, securely embedded in the mitochondrial membrane. This molecule very easily switches between the reduced and oxidised states, making it a highly efficient electron transfer molecule (Wang and Hekimi, 2016). There are various chain lengths ubiquinone, with ubiquinone-10 (CoQ10) being the most prevalent in humans. Cyt c is a nuclear encoded, positively charged protein that can receive electrons from complex III and transfers these to complex IV (Hüttemann et al., 2011). Cyt c electron transfer is considered the rate limiting step in the electron transport chain and is highly regulated through allosteric regulation and post-translational modifications (Hüttemann et al., 2007).

1.1.2 Beyond oxidative phosphorylation

Besides the essential role in oxidative phosphorylation which provides the cell with energy in the form of ATP, mitochondria have established themselves as a central metabolic regulator. Mitochondria are now recognised as a highly versatile organelle and sense many aspects of cellular health such as nutrient status, DNA damage and cellular stress (McBride et al., 2006). Mitochondria are also the main orchestrator of cellular apoptosis, releasing proapoptotic factors during cellular stress (Wang and Youle, 2009). Mitochondria serve as main biosynthetic hubs, being responsible for the synthesis of glucose, heme, amino acids whilst also providing substrates for cholesterol and fatty acid synthesis, and substrates for nucleotide synthesis (Spinelli and Haigis, 2018). Maintenance of mitochondrial activity is thus not just to maintain the levels of ATP, but essential to preserve cellular homeostasis.

1.2 Mitochondrial dysfunction

Due to the widespread integration of mitochondria into cellular metabolism, perturbation of mitochondrial function affects a broad range of cellular processes with possible pathological outcomes (Nunnari and Suomalainen, 2012; Vafai and Mootha, 2012). The inability of mitochondria to function properly however does not always lead to a mitochondrial disease. The pathological outcome depends on multiple factors ranging from cellular compensatory mechanisms to environmental influences (Ylikallio and Suomalainen, 2012). This multifactorial origin makes mitochondrial diseases a very heterogeneous group of pathologies where the underlying genetic defect is a poor predictor for disease outcome. Moreover, mitochondrial diseases are associated with largely varying symptoms and highly tissue specific phenotypes such as neurological defects, muscle weakness or liver disease (Suomalainen and Battersby, 2018). This suggests that the variations in disease outcome are linked to the intricate interaction of mitochondria with the cellular environment, instead of just energy availability. This heterogeneity reflects the tissue specificity mitochondrial function, as mitochondria in distinct tissues are highly specialised to the tissue requirements in terms of substrate preference and biosynthetic pathways (Kappler et al., 2019). Some symptoms of mitochondrial dysfunction also develop at specific stages in life, indicating influence of age-dependent signalling pathways. It is still not clear how the various influences on mitochondrial function affect tissues differently. Insights can be obtained from a proper understanding of the biochemical changes that follow respiratory chain dysfunction, and from the specific biochemical changes unique to impairments in the individual complexes and different tissues.

1.2.1 Clinical epidemiology of mitochondrial diseases

Although having a strong impact on cellular homeostasis, defects in the functioning of mitochondria are common. It is estimated that 1 in 7500 newborns will display some form of respiratory chain disorder at one point in their life (Skladal et al., 2003), however the incidence of severe mitochondrial diseases is much lower. The most common form of a severe mitochondrial disease is Leighs' syndrome which affects roughly 1 in 40'000 live births (Gerards et al., 2016). Mitochondrial disorders have a remarkable tissue specificity, showing specific symptoms in different tissues (Nunnari and Suomalainen, 2012; Vafai and Mootha, 2012). For example, neuronal defects are common as seen as the main clinical parameters of Leighs syndrome and Lebers Hereditary Optic Neuropathy (LHON), two major mitochondrial diseases. Overall tissues that are heavily dependent om mitochondria tend to have the most severe symptoms, however this does not fully explain the extent of heterogeneity. The discrepancy in incidences between mitochondrial defects and disease hints at a compensation at the cellular level which prevents exacerbations of cellular defects into diseases. This hypothesis is further strengthened by the observation that mitochondrial disease has such high tissue specificity, indicating the underlying mechanism is complex and dependent on the cellular metabolism or external influences. Dysfunctional mitochondria have also been associated with well known diseases such as cancer, Alzheimer's disease, Parkinson, diabetes and non-alcoholic fatty

liver disease (Koopman et al., 2012; Pessayre, 2007) and also with aging. Further research is needed to better understand the integration of mitochondrial function in the intracellular environment in the context of different tissues and pathologies. Treatment of mitochondrial diseases is lacking, with no treatment registered by the EMEA, FDA or other regulatory bodies worldwide (Weissig, 2020). The standard treatment of supplementation with coenzyme Q10 has not been proven significantly effective on clinical parameters (Pfeffer et al., 2012). A deeper understanding of the signalling events that follow mitochondrial diseases is needed for a complete picture of the cellular environment and will potentially lead to new targets for the treatment of mitochondrial diseases.

1.2.2 Biochemical consequences

Ultimately, a large majority of disturbances in mitochondrial function affect the electron transport chain directly or indirectly and are linked to partially dysfunctional oxidative phosphorylation. In general, this affects the cells capacity to produce ATP, the mitochondrial membrane potential, disrupts cellular redox balance and an increase in oxidative stress among others. This in turn can lead to secondary effects such as disrupted metabolite exchange between the mitochondria and the cytosol with metabolite accumulation as a consequence (Smeitink et al., 2006). Each of the respiratory complexes plays a unique role in mitochondrial respiration. Due to these specialised roles, each of the complex induces specific biochemical changes under conditions of malfunctioning. Complex I is an important complex involved in NADH metabolism using electrons to oxidise NADH to NAD+. Impairing the flow of electrons by inhibiting complex I or III thus affects redox metabolism by increasing NADH, more than blocking complex V.

Furthermore, complex I, II and III have been identified as the main sites of ROS production (Goncalves et al., 2015). There are site specific differences, complex I produces ROS exclusively in the mitochondrial matrix, complex III, in contrast, generates ROS both in the mitochondrial matrix and in the intramembrane space (al Maruf et al., 2014; Muller et al., 2004). The complex III inhibitor antimycin A was thus also shown to be more effective in inducing ROS and cellular death than the complex I inhibitor rotenone in primary hepatocytes (Siraki et al., 2002). All these biochemical signals are sensed by specialised quality control pathways which are activated to restore homeostatic balance in the cell. The resulting signalling is collectively called mitochondrial retrograde signalling (Butow and Avadhani, 2004; Liu and Butow, 2006), and mounting evidence supports the idea that it plays a significant role in the physiopathology of mitochondrial diseases.

1.3 Retrograde signalling

There have been numerous studies into the signals though which the mitochondrial communicate with the other compartments of the cell. Mitochondrial retrograde signalling has originally been defined as the communication from the mitochondria to the nucleus to ac-

tivate transcription of genes that to adapt mitochondrial function and cellular metabolism (Butow and Avadhani, 2004). The classical mitochondrial retrograde signals were discovered in yeast, where mitochondrial dysfunction has been shown to regulate the transcription of genes in response to mitochondrial dysfunction (Liu and Butow, 2006). In more recent years, the elaborate interaction between mitochondria and the intracellular environment has been studied in detail in mammalian model systems. The it became evident that mitochondria communicate with the cell through many different pathways on top of transcriptional programs. To have a more complete description the term retrograde signalling was expanded to include all metabolic signals that originate from the mitochondria that adapt organelle maintenance, quality control and fine-tune cellular metabolism (Suomalainen and Battersby, 2018).

1.3.1 Retrograde signalling in mitochondrial dysfunction

Integrated Stress Response (ISR) Perturbation of mitochondrial function causes a severe disturbance in the intracellular environment which generates stress signals. These stress signals are interpreted by a well-characterised stress signalling pathway called the integrated stress response (ISR). This pathway revolves around a central elongation-initiation factor called Eukaryotic Initiation Factor 2 (eIF2). When the α-subunit of the elongation factor is phosphorylated by one of four upstream kinases it creates a two-fold benefit for cellular homeostasis: both conserving energy by impeding the translation of proteins and activating pro-survival pathways by increasing the translation of transcriptional regulators involved in downstream stress management pathways.

The various signals that activate the integrated stress pathway are sensed by four kinases located on the ER membrane. Each of these kinases is activated by different stress signals, specific to the enzyme. The General Control Non-derepressible-2 (GCN2) kinase senses amino-acid starvation and thus provides an important link between nutrient levels and stress signalling. The Haem-Regulated Inhibitor (HRI) senses heam-deprivation, oxidative stress and heat stress. The RNA-dependent protein kinase (PKR) contains a domain able to bind double stranded DNA and plays an important role in the interferon-mediated anti-viral defence. The PKR like ER kinase (PERK) senses misfolded proteins in the ER and is thus an important link between protein homeostasis and the ISR pathway (Wek, 2018).

The phosphorylation of the α-subunit of eIF2 enables the bypass of an inhibitory ORF in the mRNA of the activating transcription factors 4 and 5 (ATF4, ATF5), leading to an increased translation of these proteins (Wek et al., 2006; Zhou et al., 2008). The main transcription factor ATF4 of this pathway induces the transcription of further downstream transcription factors such as ATF3, CHOP and GADD34. Together these transcription factors finely orchestrate a transcriptional response stimulating the cell for pro-survival or priming the cell for apoptosis, depending on the cofactors involved (Wek et al., 2006). Besides transcriptional regulation, certain factors are also preferentially translated by phosphorylated-eIF2α, such as ATF5, CHOP

and GADD34 (Lee et al., 2009; Palam et al., 2011).

Multiple studies have pointed towards a clear activation of the ISR by mitochondrial dysfunction. Exactly what signals activate the ISR is still an active area of research, but it is becoming evident that there are multiple metabolic signals involved. The activation has been shown to be tissue dependent and related to the metabolic state of the cell (Mick et al., 2020). One mechanism of activation is through a reduced asparagine synthesis, caused by a disrupted redox balance. The subsequent depletion in asparagine leads to the activation of GCN2 (Mick et al., 2020). Mitochondrial dysfunction also activates HRI through the cleavage the mitochondrial protein DAP3 Binding Cell Death Enhancer 1 (DELE1) by a protease in the inner mitochondrial membrane OMA1 zinc metallopeptidase (OMA1). The shorter fragments of DELE1 accumulate in the cytosol and activate HRI through directly binding to the protein (Fessler et al., 2020; Guo et al., 2020).

Mitochondrial unfolded protein response Besides activating the ISR, stress in the mitochondria disrupts the protein homeostasis and activates another stress pathway that shares similarities with the ISR, the mitochondrial unfolded protein response (UPRmt) (Jovaisaite and Auwerx, 2015; Pellegrino et al., 2013). The UPRmt is activated in response to an accumulation of mitochondrially targeted proteins in the cytosol, the direct result of impaired mitochondrial protein import following mitochondrial stress (Zhao and Hogenraad, 2002). In mammals it is proposed that ATF-5 is the main transcription factor central to the activation of the UPR following the protein disbalance (Fiorese et al., 2016). Similar to its ortholog in the Caenorhabditis elegans (Activating transcription factor associated with stress; ATFS-1), ATF-5 has both a mitochondrially targeted localisation signal and a nuclear localisation signal (Nargund et al., 2012). Under normal conditions this transcription factor is transported to the mitochondria where it is degraded. Impaired mitochondrial protein import causes this protein to localise to the nucleus where it activates the transcription of genes involved in restoring respiratory chain function and mitochondrial protein import. Many disturbances of mitochondrial function have been shown to activate the UPRmt such as respiratory chain dysfunction, impairments of the mitochondrial ribosome and protein import defects (Shpilka and Haynes, 2018). Both the ISR and the UPRmt pathways contribute to the important overall balance between cellular survival or apoptosis and are thus important pathways in deciding cellular fate after mitochondrial dysfunction.

AMPK When the capacity of mitochondria to produce ATP is impaired it creates a shift in the intracellular energy balance. In response to this, the energy sensing AMP-activated protein kinase (AMPK) is activated by a decrease in the ATP/AMP ratio (Hardie, 2007). AMPK tries to restore balance by inhibiting ATP consuming reactions such as protein synthesis while stimulating ATP producing processes such as promoting glycolysis, fatty-acid oxidation and stimulating mitochondrial biogenesis (Herzig and Shaw, 2018). Inhibition of mitochondrial respiratory chain complexes has been shown to activate AMPK, in a time and glucose depen-

dent manner. Inhibition induces an acute activation of AMPK that reduces over time and the activation can be supressed by high concentrations of glucose (Peng et al., 2015).

AMPK inhibits numerous ATP-consuming anabolic pathways such as sterol and lipid biosynthesis by phosphorylating ACC1, ACC2 and phosphorylating HMGCR (Carling et al., 1987). Under prolonged energy stress AMPK initiates rewiring of cellular metabolism through regulating the transcription of genes involved in biosynthetic pathways. The enzyme inhibits gluconeogenesis by phosphorylating CRTC2, a co-factor involved transcription of genes in gluconeogenesis (Koo et al., 2005). The transcriptional regulation is extended by AMPKs control over the key metabolic transcription factors SREBP1 (Li et al., 2011), chREBP (Kawaguchi et al., 2002) and HNF4a (Hong et al., 2003). AMPK is also able to reduce the cellular ATP consumption by slowing down energy-consuming processes such as protein translation and cellular growth. AMPK does this by inhibiting the mTOR pathway, a major regulator of intracellular anabolic pathways. AMPK does this in two ways, by activating the mTOR inhibiting factor tuberin (tuberous sclerosis complex 2 (TSC2)) (Inoki et al., 2003) and by directly inhibiting the mTOR subunit RAPTOR (Gwinn et al., 2008). AMPK also slows down protein synthesis directly by phosphorylating the elongation factor eEF2K (Leprivier et al., 2013). At the same time AMPK stimulates energy-producing processes such as increasing the glucose turnover of cells by increasing the transport of glucose (Chavez et al., 2008) and stimulating the glycolysis (Bando et al., 2005). Furhtermore, AMPK also increases lipolysis generating free fatty-acids which are transported to the mitochondria for B-oxidation producing ATP (Ahmadian et al., 2011).

The activation of AMPK directly affects mitochondrial function by stimulating biogenesis through the activation of PGC1α (Wu et al., 2014), promoting the fragmentation of mitochondria through the phosphorylation of the mitochondrial fission factor (MFF) (Wang and Youle, 2016) and stimulating the clean-up of dysfunctional mitochondria mitophagy through the phosphorylation of ULK1 (Egan et al., 2011). Additionally, AMPK also preserves cellular homeostasis by managing the response to mitochondrially produced ROS. The levels or mROS are non-canonical activators of AMPK which leads to a PGC1α mediated antioxidant response (Rabinovitch et al., 2017). Furthermore, AMPK promotes a metabolic shift to anaerobic glycolysis, thereby reducing the cellular dependency on the respiratory chain (Wu and Wei, 2012). By driving the energy metabolism away from energy consuming reactions and by increasing energy producing reactions, AMPK plays a key role in preserving the intracellular environment during energy stress following mitochondrial dysfunction. This is further exemplified by the observation that cells lacking AMPK are more prone to death upon inhibition of the respiratory chain (Distelmaier et al., 2015).

mTOR Another kinase that is closely tied to cellular homeostasis and mitochondrial function is the mechanistic Target Of Rapamycin (mTOR). This kinase is activated by growth factors, energy levels, the abundance of nutrients levels or oxygen levels and stimulates cellular growth and other anabolic processes (Laplante and Sabatini, 2009; Sarbassov et al., 2005; Wullschleger

et al., 2006). The activation of mTOR centres around the important GTP-ase activating protein complex called Tuberous Sclerosis Complex (TSC) or tuberin which integrates signals from the energy and oxygen sensing pathways (Long et al., 2005; Tee et al., 2003). The role of the mTOR pathway is in a ying-yang relationship with AMPK, as mTOR stimulates anabolic processes such as protein, lipid and organelle synthesis while inhibiting the catabolic process of autophagy (Liu and Sabatini, 2020). Activation of the mTOR pathway promotes mRNA synthesis and protein translation though activation of the eukaryotic initiation factor 4E binding protein 1 (4E-BP1) (Richter and Sonenberg, 2005) and the p70 ribosomal S6 kinase 1 (S6K1) (Ma and Blenis, 2009). These roles are executed by the pathways two central multiprotein complexes called mTOR complex 1 (mTORC1) and complex 2 (mTORC2).

The relation between mitochondrial dysfunction and the functional status of mTOR is controversial. Studies have reported an increase in mTOR activity in mouse models of mitochondrial disease and provided evidence that inhibition of mTOR improved health (Johnson et al., 2013; Peng et al., 2015). Supporting the hypothesis that mTOR might be a potential target for some types of mitochondrial diseases. Other studies however have shown a decreased mTOR activity after inducing mitochondrial dysfunction (Zhou et al., 2015). Activation of the mTOR pathway has a significant downstream effect on mitochondrial function. The mTOR pathway stimulates mitochondrial biogenesis through activation of PGC1α and the estrogen-related receptor-α (ERR-α) (Cunningham et al., 2007), the transcription factor A, mitochondrial (TFAM) (Picca and Lezza, 2015) and stimulates the transcription of mitochondrial proteins increasing the capacity of the cell to produce ATP (Morita et al., 2013). Inhibiting mTOR has been shown to increase aerobic glycolysis, decrease mitochondrial membrane potential, reduce oxidative respiration and lower ATP-producing capacity (Ramanathan and Schreiber, 2009; Schieke et al., 2006). However also the opposite has been shown that an inhibition of mTOR increases longevity by increasing membrane potential, reducing reactive oxygen species, and increasing expression of mitochondrially encoded genes in healthy fibroblasts (Lerner et al., 2013) and improves the phenotype in models of mitochondrial myopathy (Khan et al., 2017). There is a clear irregularity in the observed activation of mTOR by mitochondrial function and also in the downstream effects of mTOR on mitochondrial function. This likely depends on the cell type studied and extracellular influences on cell metabolism, suggesting a complex interaction between mitochondria, mTOR and other retrograde signalling pathways.

1.3.2 Targeting retrograde signalling

Targeting retrograde signaling components to enhance the restoration of cellular homeostasis constitutes a rational mechanism to prevent or treat mitochondrial disease. Successful targets to restore mitochondrial function have been found in retrograde signalling pathways activated by mitochondrial dysfunction as described above, such as the inhibition of mTOR improving viability in a mouse model of Leighs disease (Johnson et al., 2013) and in cells derived from mice suffering from CoQ mediated respiratory chain dysfunction (Peng et al., 2015). Also, activation of Sirtuin 1 (Sirt1) has been shown effective in a mouse model of impaired Cyt c

synthesis (Cerutti et al., 2014).

Additionally, through unbiased screening of factors that influence mitochondrial dysfunction, other pathways have been identified that when targeted have a positive effect on mitochondrial function or disease progression. The activation of the HIF pathway has been shown to increase survival in mouse models of mitochondrial dysfunction (Ferrari et al., 2017; Jain et al., 2016). Inhibition of the Bromodomain-containing protein 4 (BRD4), has been shown to upregulate oxphos proteins and rescue cellular bioenergetics following complex I dysfunction (Barrow et al., 2016). Successful strategies have also been found in the form of specific nutrient supplementation which protects patient derived fibroblasts from galactose induced death (Iannetti et al., 2018) and inhibition of translation (Peng et al., 2015).

What adds to the complexity of targeting mitochondrial retrograde signalling is that many pathways intercommunicate to orchestrate adaptations depending on the state of the cell. For instance, the phosphorylation of Raptor by AMPK can inhibit mTOR under conditions of energy depletion (Gwinn et al., 2008) and the integrated stress response is under direct regulation of both AMPK (Gwinn et al., 2008) and mTOR (Khan et al., 2017) and plays are role in cholesterol metabolism (Fusakio et al., 2016). This interaction between retrograde signalling pathways underlines the complexity of these metabolic responses and calls for further research to uncover the exact mechanisms.

1.4 Cholesterol metabolism

Cholesterol is an essential constituent of living cells contributing to rigidity and permeability of cellular membranes. Both excessive and insufficient amounts of cholesterol are detrimental for cellular functioning thus it is imperative that the levels are tightly controlled (Simons and Ikonen, 2000). Intracellular levels of sterols are tightly controlled by regulating the rate of biosynthesis, fine-tuning the transport in and out of the cells and by adapting the metabolic processing of sterols. When sterol levels in the cell increase, pathways are activated that reduce the uptake and increase the excretion of sterols. At the same time excess cholesterol is metabolised through esterification or conversion into bile acids.

1.4.1 Cholesterol distribution

The vast majority (65%-90%) of all intracellular cholesterol is located at the plasma membrane (Lange et al., 1989). The remaining fraction is distributed mostly between the endosomes, Golgi and intracellular lipid droplets. The ER and mitochondrial membranes are very cholesterol poor and contain only a fraction of the total cellular cholesterol (Horvath and Daum, 2013). This large amount of cholesterol located in the plasma membrane is not randomly distributed but organised into clusters called lipid rafts (Simons and Ikonen, 1997). More recently three specific subtypes of these rafts have been identified with specific signalling functions, suggesting a more specialised contribution to maintain intracellular cholesterol

homeostasis (Das et al., 2014).

Intracellular cholesterol can undergo many modifications which affect its signalling properties such as methylation, oxidation or esterification. When the intracellular cholesterol levels become too high, a specialised family of enzymes, Acyl coenzyme A:cholesterol acyltransferases (ACATs), bind a fatty acyl-CoA molecule to the hydroxyl group of the steroid backbone (Chang et al., 2009). These esterified cholesterol molecules are metabolically inactive and are either excreted in lipoprotein vesicles or stored in intracellular lipid droplets (Luo et al., 2020). Lipid droplets are intracellular vesicles consisting of a protein rich phospholipid monolayer and a hydrophobic core consisting of sterol esters and triglycerides (Walther and Farese, 2012). They resemble lipoproteins for circulating cholesterol, however lipid droplets are much larger. Lipid droplets serve the role of lipid reservoirs, providing building blocks for membranes and substrates for energy metabolism. Lipid droplets also interact with other organelles and the plasma membrane through proteins called caveolins (Martin and Parton, 2006). Disruption of this interaction has been shown to disrupt cellular cholesterol homeostasis and increase intracellular cholesterol (Pol et al., 2001).

1.4.2 The mevalonate pathway

In mammalian cells cholesterol is synthesised from acetyl-CoA into cholesterol through a series of enzymatic reactions that take place in the ER and peroxisomes. A series of 11 different enzymes convert acetyl-CoA into long non-sterol carbon chains called isoprenoids after which these are converted into cholesterol. The reactions in the cholesterol biosynthesis pathway are highly compartmentalised between the ER and peroxisomes, because many of the intermediates are highly hydrophobic molecules that have low solubility in the ER-matrix.

The first step in cholesterol biosynthesis is the conversion of Acetyl-CoA is into acetoacetyl-CoA by the enzyme Acetyl-CoA Acetyltransferase 2 (ACAT2). This molecule is then converted into 3-hydroxy-3-methylglutaryl-CoA (HMG-CoA) by the enzyme HMG-CoA Synthase (HMGCS). This reaction takes place in either the ER, mitochondria, or the peroxisomes. Higher eukaryotes have two forms of HMGCS, the difference being their location, either in the ER and peroxisome or in the mitochondria. The HMGCS-1 isoform mainly resides in the ER and peroxisome and contributes to the synthesis of cholesterol, producing HMG-CoA as a substrate to produce cholesterol. The mitochondrial form HMGCS-2 mainly plays a role in the synthesis of ketone bodies, where HMG-CoA is converted into acetoacetate and further into the ketone bodies D-3-hydroxybutarate and acetone. The next enzyme in the cholesterol biosynthesis pathway is 3-Hydroxy-3-methyl-glutarylCoA reductase or HMG-CoA reductase (HMGCR). The enzyme is responsible for the conversion of HMG-CoA into mevalonate. This enzyme is an important enzyme in the mevalonate pathway as it is the rate limiting reaction and the target of many regulatory pathways. HMGCR is also the target of an important class of lipid-lowering drugs called statins. Due to this high importance of this enzyme in the mevalonate pathway, HMGCR is tightly controlled at the levels of transcription, translation

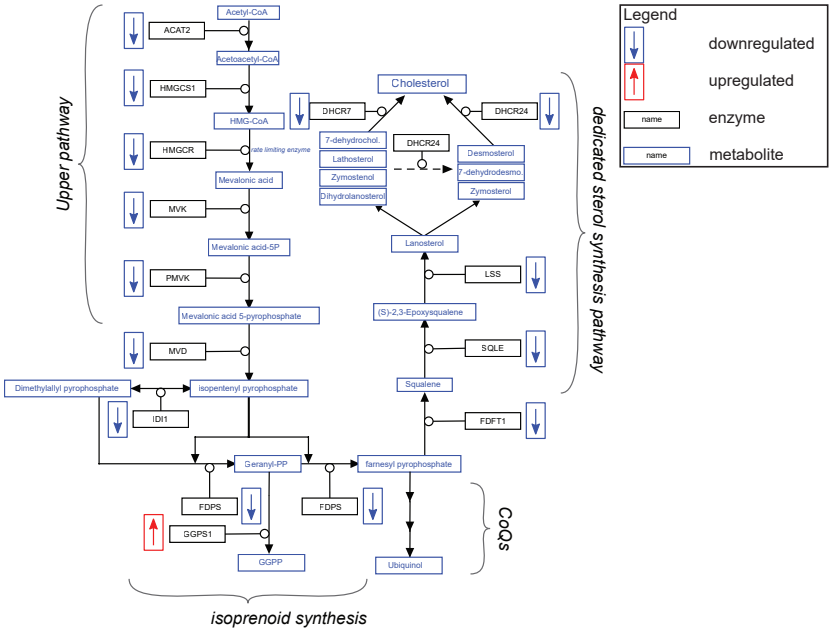

Figure 1.3 – Schematic representation of the mevalonate pathway reactions and metabolites

and post-translation see paragraph 1.4.4.

The next enzymes in the mevalonate pathway are a group of ATP consuming enzymes. A series of three enzymes convert mevalonate into isopentenyl -pyrophosphate, the first isoprenoid metabolite produced in the cholesterol biosynthesis pathway. The fist enzyme in this cascade is mevalonate kinase (MVK). This enzyme transfers a phosphate group from ATP onto mevalonate, generating mevalonate-5-phosphate. Following this reaction, the enzyme phosphomevalonate kinase (PMVK) performs a similar reaction, adding another phospho-group to the metabolite, generating mevalonate-5-pyrophosphate. A final decarboxylation step is provided by mevalonate-diphosphate-decarboxylase (MVD) which generates isopentenyl pyrophophate (IPP), the first isoprenoid metabolite in the pathway. The resulting IPP isoprenoid is subject to isomerisation due to a chiral centre in the molecule. The enzyme Isopentenyl diphosphate δ-isomerase (IDI1) can convert the relatively unreactive IPP into a more reactive form dimethylallyl pyrophosphate (DMAPP). In the next steps the isoprenoid chain is elongated by Farnesyl Diphosphate Synthase (FPPS), where a molecule of IPP is combined with a molecule of DMAPP to form geranyl-pyrophosphate. The same enzyme then combines a molecule of GPP and IPP to produce farnesyl pyrophosphate, a water-soluble 15-carbon isoprenoid. These reactions mainly take place in the peroxisomes due to the hydrophobic nature of the metabolites.

The following reaction is the synthesis of squalene by Squalene Synthase (SQS). This reaction combines two long isoprenoid carbon chains of FPP to produce squalene. This reaction takes place on the ER-membrane, with a part of the enzyme open to the cytosol to receive the soluble FPP substrate, the other end creating a hydrophobic pocket for the squalene

product to be released. This enzyme is responsible for a pivotal reaction in the mevalonate pathway as it is the first reaction that dedicates the metabolite for the synthesis of cholesterol. The resulting squalene metabolite then undergoes an epoxidation reaction catalysed by the enzyme squalene epoxidase (SQLE), also called squalene monooxygenase, resulting in the production of 2,3-oxidosqualene. The next enzyme Lanosterol Synthase (LSS) catalyses the transformation of oxidosqualene into lanosterol. Both these last two metabolites are very hydrophobic hydrocarbon chains. For this reason, these steps take place in the peroxisomes.

The final steps in the mevalonate pathway are slightly different from earlier steps others, as this part is split into two parallel pathways: the Bloch and Kandutsch-Russel pathways. The pathways follow the same steps, a reduction, a series of demethylations, a desaturation, and a reduction, with the only difference that the Bloch pathway processes sterol intermediates with an unsaturated bond at the Δ-24 position and as a last step the enzyme 24-dehydrocholesterol reductase (DHCR24) reduces this bond to produce cholesterol. The Kandutsch-Russel pathway in contrast, processes sterols that have already been reduced at the Δ-24 position by DHCR24. At any point in the Bloch pathway, the metabolites can be subject to reduction by DHCR24 and enter the Kandutsch-Russel pathway, however the metabolites have different affinities for DHCR24. This reaction is irreversible and thus the balance of reactions will shift towards the Kandutsch-Russel pathway.

1.4.3 The biological relevance of mevalonate pathway metabolites

Besides being the source of endogenous cholesterol synthesis, the mevalonate pathway produces many other metabolites that are biologically active and play an important role in various aspects of cellular metabolism. Considering the pathway from mevalonate, the first dedicated metabolite, there are over 26 metabolites directly produced in the mevalonate pathway. The isoprenoids, various length ubiquinol intermediates and the cholesterol precursors themselves have a biologically active role in addition to being a metabolic intermediate in the synthesis of cholesterol. Mevalonate itself has a regulatory role in direct feedback to the producing enzyme HMGCR. Mevalonic acid, or its complementary base mevalonate or mevalonolactone stimulates the phosphorylation of HMGCR and consequently inhibiting its function (Beg et al., 1984).

Isoprenoids Isoprenoids are another group of metabolites produced by the mevalonate pathway that have a significant biological role. These carbon chains consist of multiple blocks of 5 carbon IPP units, generating the 15 carbon FPP and 20 carbon GGPP (Kellogg and Poulter, 1997). These isoprenoids can be covalently bound to proteins, a process called prenylation, by specific enzymes that binds the isoprenoid carbon chain to the C-terminus of the protein. This prenylation facilitates the anchoring of proteins to membranes, which is necessary for their proper functioning (Wang and Casey, 2016). For example, the family of Rho GTPases need to be prenylated to properly fulfil their function in cells which in turn activates the

YAP/TAZ mediators of the Hippo pathway (Sorrentino et al., 2014) and stimulates cellular proliferation among others (Zanconato et al., 2015). The YAP/TAZ pathway has been linked to mitochondrial function, by affecting the fusion (Deng et al., 2016) structure (Huang et al., 2018) and function (Nagaraj et al., 2012) of mitochondria, highlighting an important connection between mitochondria and the mevalonate pathway.

Ubiquinone The isoprenoid FPP can also be used to initiate the synthesis of another metabolite that is crucial for mitochondrial function, CoQ10. This molecule consists of a quinone ring with a polyisoprenoid tail. At least 12 enzymes are involved in the synthesis, however the exact reactions are yet unknown (Acosta et al., 2016). The final product of this synthesis pathway is an electron carrying molecule that directly participates in the transport of electrons along the mitochondrial respiratory chain. Impairments in the synthesis of ubiquinone have directly been associated with a decrease in mitochondrial function and the cause of disease (Quinzii and Hirano, 2010; Trevisson et al., 2011). Finally, the pathway produces many cholesterol intermediates that serve as feedback signals to regulate the mevalonate pathway, but also some serve as cofactors for other reactions such as 7-dehyrocholesterol which is a substrate for the biosynthesis of vitamin D. Even the role of cholesterol, the final product of the pathway serves not only as a physical addition to membranes regulating the fluidity but plays important roles as a substrate in downstream processes. Cholesterol can be transformed into bile acids which have an important role in the digestion of food passing the stomach and play a role as gut hormones signalling back to the central nervous system (Mertens et al., 2017; Thomas et al., 2008). Steroid hormones are another highly relevant class of signalling molecules that are derived from cholesterol, which includes the synthesis of progestogens, glucocorticoids, mineralocorticoids, androgens, and estrogens. Synthesis of these hormones starts with the conversion of cholesterol to the precursor pregnenolone on the mitochondrial membrane. Cholesterol can also be converted into oxysterols which have an important feedback role in cholesterol metabolism (Radhakrishnan et al., 2007), see paragraph 1.4.4.

1.4.4 Regulation of the mevalonate pathway activity

The importance of the mevalonate pathway can be inferred from its multiple points of regulation. Various rate limiting reactions of the mevalonate pathway are controlled transcriptionally, translationally, and post-translationally by multiple mechanisms at multiple points in the pathway. Notably the enzyme HMGCR is the main target for the regulation of the mevalonate pathway, which becomes evident when we consider the HMGCR is regulated by multiple sterols and metabolites that affects its transcription, translation, stability, and activity.

Transcriptional regulation of the mevalonate pathway is mediated by SREBP2

Several of the enzymes of the cholesterol biosynthesis pathway are under transcriptional control of the Sterol regulatory element-binding proteins family of transcription factors (see

table 1.1, adapted from (Sharpe and Brown, 2013)). These basic-helix-loop-helix leucine zipper (bHLH-Zip) family of transcription factors consist of multiple isoforms, SREBP1a, SREBP1c and SREBP2. The SREBP1a and SREBP1c isoforms are more involved in the transcriptional control of lipid synthesis pathways and the SREBP2 transcription factor more with sterols (Brown and Goldstein, 1997). The SREBP2 protein is a 124 kDa transmembrane protein consisting of 7 transmembrane helices which anchor this protein tightly to the ER membrane, see figure 1.4.

Under normal physiological conditions SREBP2 is tightly associated with the Sterol Cleavage Activation Protein (SCAP). This transmembrane protein regulates SREBP2 activation in response to changing sterol levels in the ER (Hua et al., 1996). When sterol levels are depleted, SCAP binds to coat protein complex II (COPII) proteins which facilitate the vesicular transport of the SCAP/SREBP2 complex to the Golgi network. Here SREBP2 is cleaved sequentially by a series of proteases called S1p and S2p that cleave SREBP2 to release a 60 kDa N-terminal fragment. This part is the active transcription factor which is translocated to the nucleus to initiate transcription of genes involved in cholesterol synthesis and uptake.

When sterol levels in the ER are high, cholesterol binds to SCAP inducing a conformational change and stimulating the binding of the SREBP2/SCAP complex to a third protein Insulin induced gene (INSIG) (Sun et al., 2005). Two different isoforms of this protein exist: INSIG1 and INSIG2. INSIG1 is a 30 kDa protein is expressed in all tissues and is highly expressed in the liver (Yang et al., 2002). Its expression predominantly depends on the transcriptional activation by SREBP2. INSIG2 is a smaller 25 kDa protein and less abundant than INSIG1, however its expression is constitutive and not dependent on SREBP2 activation (Yabe et al., 2002). However, INSIG2 expression has been shown to be induced by the HIF1α transcription factor, providing a link between oxygen levels and the cholesterol biosynthesis pathway (Hwang et al., 2017). INSIG proteins themselves don't have any binding affinity for cholesterol, but instead bind the oxidised derivatives, oxysterols (Radhakrishnan et al., 2007). The binding of oxysterols to INSIG stabilises and retains the SREBP/SCAP/INSIG complex in the ER independently of cholesterol (Sun et al., 2007).

The sensitivity of the SREBP2/SCAP/INISG complex to the cholesterol content on the ER-membrane is very precise and behaves in an ultrasensitive manner around a set concentration of cholesterol, 3%-5% in Chinese hamster ovarian cells (Radhakrishnan et al., 2008). Below the threshold SREBP2 is rapidly transported to the Golgi and processed and above the threshold SREBP2 is almost entirely inactivated. The concentration limit depends on the ratio of INSIG to SCAP, where higher INSIG/SCAP ratio leads to a lower cholesterol concentration set point below which SREBP2 is inactivated.

The translational regulation of mevalonate pathway enzymes

Besides the regulation of gene expression, the rate-limiting enzyme HMGCR is also under translational control by sterols. Although not much is known about the exact mechanisms,

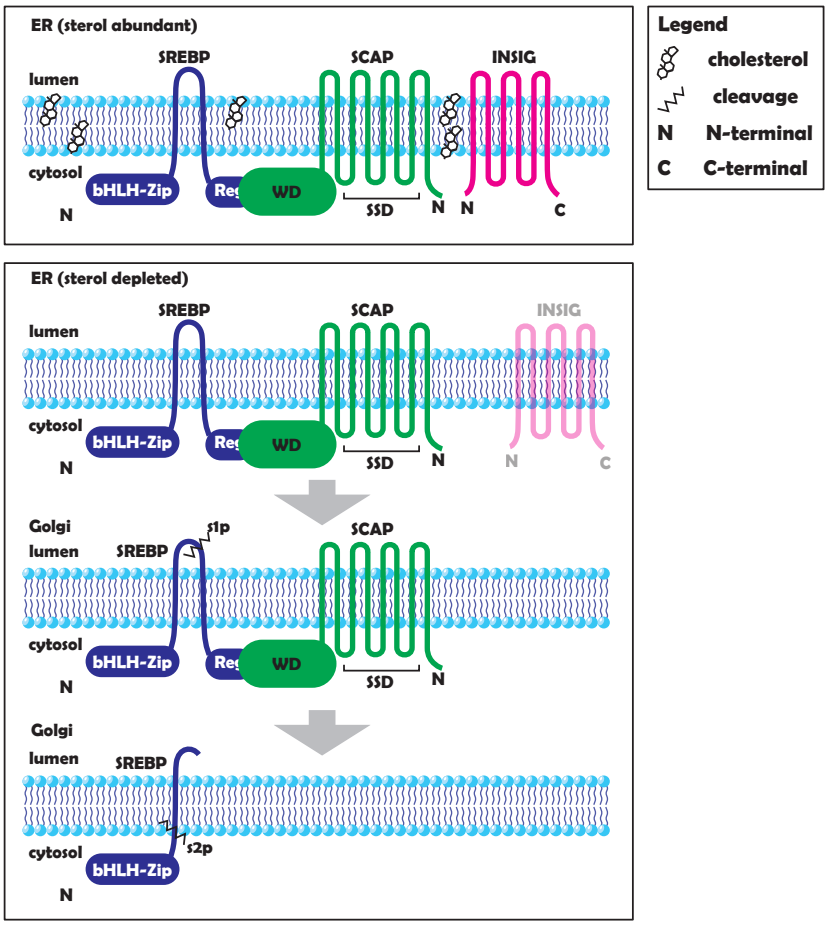

Figure 1.4 – **Schematic of SREBP activation.** Schematic representation of the activation of SREBP2. Activation begins in the ER-membrane in conditions of low cholesterol, when release of INSIG stimulated translocation to the Golgi. Here SREBP2 is cleaved to release the N-terminal transcriptionnaly active fragment. (INSIG: Insulin induced gene protein ; bHLH-zip: bacis-helix-loop-helix leucine zipper transcription factor; SREBP: Sterol regulatory-element binding protein; SCAP: SREBP-cleavage-activating protein; s1p: Site-1 protease; s2p: Site-2 protease; WD: WD40 repeat domain; Reg: regulatory domain.)

there is evidence that oxysterols and oxylanosterols are able to interfere with the translation of HMGCR mRNA. These sterol derivatives were shown to reduce the amount of HMGCR independent of the amount of RNA present, adding another layer of regulation to the mevalonate pathway (Chambers and Ness, 1998; Ness, 2015).

The post-translational regulation of mevalonate pathway enzymes

Besides tight transcriptional control of genes encoding key mevalonate pathway proteins, cholesterol biosynthesis is carefully regulated by post-translational mechanisms. These enzymes are regulated post-translationally by cholesterol itself or by metabolites produced in

Table 1.1 – SREBP2 targets

HGNC gene name	**Gene symbol**
Acetyl-CoA acetyltransferase, cytosolic	ACAT2
3-Hydroxy-3-methylglutaryl-CoA synthase 1 (soluble)	HMGCS1
3-Hydroxy-3-methylglutaryl-CoA reductase	HMGCR
Mevalonate kinase	MVK
Phosphomevalonate kinase	PMVK
Mevalonate decarboxylase	MVD
Isopentenyl-pyrophosphate δ-isomerase 1/2	IDI1/IDI2
Farnesyl-pyrophosphate synthase	FDPS
Geranylgeranyl-pyrophosphate synthase 1	GGPS1
Farnesyl-pyrophosphate farnesyltransferase 1	FDFT1
Squalene epoxidase	SQLE
Lanosterol synthase	LSS
Cytochrome P450. family 51, subfamily A, polypeptide 1	CYP51A1
Transmembrane 7 superfamily member 2	TM7SF2
Lamin B receptor	LBR
Methylsterol monooxygenase 1	SC4MOL
NAD(P)-dependent steroid dehydrogenase-like	NSDHL
Hydroxysteroid 17β-dehydrogenase 7	HSD17B7
Emopamil-binding protein (sterol isomerase)	EBP
Sterol C5-desaturase	SC5D
7-Dehydrocholesterol reductase	DHCR7

the mevalonate pathway. Most enzymes contain a Sterol Sensitive Domain (SSD) which allows them to directly interact with sterols (Goldstein et al., 2006). These domains enable sterols to bind and affect the function or stability of the enzymes, mostly through sterol mediated degradation pathways. The cholesterol induced degradation of several enzymes in the mevalonate pathway is facilitated by the recruitment of specific ubiquitin ligases on the ER membrane which prime the enzymes for degradation by the proteasome. This pathway, called the ER-associated protein degradation pathway (ERAD) has been extensively studied in its role to eliminate misfolded ER-proteins (Meusser et al., 2005). However, the factors that recognise misfolded proteins are not the same factors responsible for the degradation of the mevalonate pathway enzymes.

HMGCR The rate-limiting enzyme HMGCR is under control of the ERAD pathway (Burg and Espenshade, 2011). Excessive amounts of certain sterols stimulate the binding of HMGCR to an INSIG protein (Sever et al., 2003). As described above, the INSIG proteins are also involved in the stabilisation of the SREBP/SCAP complex and thus contribute to both transcriptional and post-translational regulation of the mevalonate pathway. INSIG proteins are essential for the sterol mediated degradation of HMGCR. After associating with an INSIG protein, at least 3 E3 ubiquitin ligases have been identified which target the mevalonate pathway enzymes

specifically: Gp78 (Song et al., 2005), Trc8 (Lee et al., 2010) and RNF145 (Jiang et al., 2018). These ligases ubiquitinate and prime HMGCR for dislocation by hexameric ATPases to the cytoplasm where it is degraded by the 26S proteasome (Bodnar et al., 2018).

The degradation of HMGCR by ERAD is not under the control of cholesterol, but under a more fine-tuned control by other less abundant sterols. The interaction of HMGCR and INSIG is mediated by lanosterol and its derivatives, a key difference with the interactions of INSIG and SCAP which are mediated by cholesterol. Various reduced or oxidised forms of lanosterol have increased potencies for the degradation of HMGCR, such as 24,25-dehydrolanosterol and oxylanosterol (Song et al., 2005; Trzaskos, 1995). Cholesterol itself has no effect on the half-life of HMGCR. Oxidised forms of cholesterol however, such as 25-hydroxycholesterol and 27-hydrocholesterol also affect the abundance of HMGCR though their interaction with INSIG proteins. Other nonsterol mevalonate pathway intermediates have also been shown to play a role, where the isoprenoid GGPP amplified the sterol mediated ERAD in a post-ubiquination step of membrane dislocation of the enzyme (Garza et al., 2009; Sever et al., 2003). Besides degradation, HMGCR is also target for phosphorylation by AMPK on serine 872 which impairs its activity (Beg et al., 1984).

SQLE SQLE is another enzyme which is under strict post-translational control. However, in contrast to HMGCR this enzyme is not under control by derivatives of cholesterol, but by cholesterol itself (Gill et al., 2011). Upon the binding of cholesterol to SQLE, this induces a conformational change which primes the enzyme for interaction with ubiquitin ligases. The enzyme SQLE does not contain an SSD but recognises cholesterol through a N-terminal regulatory domain. This interaction with cholesterol is independent of INSIG and SCAP as in contrast to HMGCR. The exact mechanism of this binding in still unknown, there is strong evidence suggesting a conformational change initiated by high levels of cholesterol in the surrounding membrane (Chua et al., 2017; Howe et al., 2017). This confirmational change is the signal for binding with the ubiquitin ligase membrane-associated RING finger 6 (MARCH6 also known as Teb4) in mammalian cells (Foresti et al., 2013; Zelcer et al., 2014) which ubiquitinate the protein priming it for degradation by the proteasome. This stimulated degradation of SQLE is prevented by accumulation of its downstream metabolite squalene, which has been shown to increase abundance of SQLE by stabilising the N-terminal region and prevent ubiquitination and degradation (Nathan, 2020).

DHCR7 The enzyme 7-dehydrocholesterol reductase (DHCR7) is another enzyme of the mevalonate pathway that is post-translationally controlled by ER-membrane sterol levels. This protein catalyses the NADPH fuelled conversion of 7-dehydrocholesterol into cholesterol in the final step of the Kandutsch-Russell arm of the cholesterol biosynthesis pathway. This protein also contains an SSD, which is the main site of its regulation. Both cholesterol and the downstream metabolite desmosterol have been shown to bind to this protein and induce its degradation (Prabhu et al., 2016).

Phosphorylations Additionally, several components of the mevalonate pathway are subject to phosphorylation by kinases which alter their function. As mentioned above, the activity of HMGCR is controlled by AMPK, where phosphorylation reduces the kinetic activity of the enzyme. Additionally, SREBP can be phosphorylated by AMPK which inhibits its functioning (Li et al., 2011). The list of enzymes subject to phosphorylation is extensive and includes HMGCS, MVK, MVD, DHCR7 and DHCR24 (Luu et al., 2014; Sharpe and Brown, 2013). SREBP2 can be phosphorylated by Glycogen synthase kinase 3, which induces its ubiquitination and degradation (Sundqvist et al., 2005). Other pathways indirectly regulate the activity of the mevalonate pathway by affecting the function of regulatory proteins. Such as the mTORC1 complex, which phosphorylates and inhibits the protein Lipin1. Normally the nuclear factor Lipin1 inhibits the transcriptional function of SREBP, thus activity of the mTOR pathway indirectly stimulates the transcription of cholesterol synthesis genes (Peterson et al., 2011).

1.4.5 Intracellular cholesterol trafficking

Systemic cholesterol transport Dietary Cholesterol is taken up from the ingested food in the intestine where enterocytes convert the free fatty acids into chylomicrons (CM) (Lim, 2007). These chylomicrons facilitate the transport of dietary lipids directly to the tissues. After releasing their lipid load, the chylomicron remnants are transported back to the liver to be degraded. The endogenous transport of lipids and sterols between tissues and cells is mediated by specialised vesicles called lipoproteins. These vesicular transporters consist of a lipid monolayer containing apolipoproteins and a lipid-rich hydrophobic core. Different lipoproteins are synthesised in the liver with each a specific role and are classified by density. Very Low-Density Lipoprotein (VLDL) is responsible for the transport of lipids from the liver to the peripheral tissues. As lipids are gradually moved from VLDL to the tissues by lipoprotein lipase, the particle becomes Intermediate-density Lipoprotein (IDL) and ultimately Low-Density Lipoprotein (LDL). LDL can be taken up through receptor mediated endocytosis and release its lipids and cholesterol to the intracellular environment. High-Density Lipoprotein (HDL) is responsible for the reversed transport of lipids and cholesterol. It takes up lipids and cholesterol from tissues and circulating lipoproteins and either transfers them back to VLDL or transports them back to the liver for excretion (Gropper et al., 2016). LDL and HDL are the most widely known lipoproteins, due to their contribution to cardiovascular diseases. Increased circulating LDL has been associated with an increase of risk for atherosclerosis and HDL with a decrease.

Intracellular cholesterol distribution Once cholesterol reaches the intracellular space, many systems are in place to ensure the cholesterol is transported to the sites where it is needed or exported from the cells in situations of an excess. After LDL enters the cell through the receptor mediated endocytosis, the lipoprotein vesicle enters the sorting endosomes, where it is released from the bound receptor. The LDL-receptor is then recycled back to the cell membrane or degraded (see below). The LDL particle releases its esterified cholesterol in

the endocytic recycling compartment where the sterols are hydrolysed by Acid Lipase into free cholesterol (Sugii et al., 2003). This free cholesterol is then recycled back to the plasma membrane or transported to the ER, the peroxisomes, the Trans-Golgi Network or the mitochondria. The release of sterols from the late endosomes is facilitated by a coordinated cholesterol binding of the proteins NPC1, NPC2 and lysosomal membrane glycoproteins (Li and Pfeffer, 2016).

Once transported to the intracellular membranes, cholesterol can rapidly redistribute between intracellular compartments, with half-times in the order of minutes (DeGrella and Simoni, 1982). In cases of excess, free cholesterol is transported back to the ER where it can again be esterified on the ER surface by Acyl-CoA:cholesterol acyltransferase (ACAT) enzymes (Chang et al., 2009). These esterified sterols are then stored in intracellular lipid droplets or exported (Simons and Ikonen, 2000). Two pathways have been identified to transport the free sterols to the ER-surface, one though the Golgi network, and the other independent of the Golgi (Soccio and Breslow, 2004). Vesicular transport from the Golgi to the plasma membrane is only responsible for a small part of the anterograde cholesterol transport, as experiments have shown that blocking Golgi trafficking only reduces cholesterol transport to the membrane by 20

Intracellular non-vesicular transport A large part of intracellular cholesterol is transported by non-vesicular manner, through sterol transfer proteins (STPs). There are two major families of STPs: the steroidogenic acute regulatory protein (StAR)-related lipid transfer domain containing (STARD) proteins and the oxysterol-binding proteins (OSBP)-related proteins (ORPs). So far 15 different STARD proteins have been identified divided into 6 subfamilies (Iaea et al., 2014). They transport various sterol or lipid ligands through the intracellular space. The first discovered and best known is the steroidogenic acute regulatory protein (StAR, later renamed to STARD1) (Clark et al., 1994). This protein facilitates the transfer of cholesterol from the outer mitochondrial membrane to the inner mitochondrial membrane (Elustondo et al., 2017). Closely related to this is the more recently discovered STARD3 protein, which has been shown to stimulate transport of cholesterol to late endosomes and to the mitochondrial membrane (Voilquin et al., 2019). Both these proteins have an ER-protein binding motif and a membrane spanning domain. Other STARD proteins that have been known to interact with cholesterol are STARD4/5/6. STARD4 plays an important role shuttling cholesterol between the plasma membrane and the ERC (Iaea et al., 2017) and has been shown to have a direct link with SCAP/SREBP2 cholesterol sensing (Mesmin et al., 2011). STARD5 has been shown to respond to ER stress signals and manipulates the levels of plasma membrane cholesterol accordingly (Rodriguez-Agudo et al., 2019). STARD6 also been shown to transport cholesterol, but its exact role is unknown. Besides binding cholesterol as a ligand STARD4/5/6 also have affinity for 25-hydroxycholesterol (Rodriguez-Agudo et al., 2005). Other STARD proteins are involved in the transport of various lipids between the intracellular compartments and do not transport cholesterol (Alpy and Tomasetto, 2005).

Another family of non-vesicular transport proteins that is still shrouded in mystery are the Oxysterol-binding protein (OSBP)-related proteins (ORPs) (Ridgway, 2010). The name of this family of STPs is derived from the first identified protein OSBP and as the name suggests, this protein was identified because of its affinity to bind oxysterols. The human OSBP family consists of 12 proteins, subdivided into 6 classes I to VI. Characteristic of this family of proteins is that all contain an OSBP-homology domain (OSH), which binds sterols or oxysterols with high affinity (Lehto et al., 2001). The roles of the ORPs are not yet fully understood but include cell signalling, lipid transport and sterol trafficking (Nakatsu and Kawasaki, 2021; Raychaudhuri and Prinz, 2010). Most ORPs also contain motifs targeted to organelle membranes which suggests that these proteins are involved in the intra-organelle trafficking of cholesterol. The exact mechanisms through which OSBPs regulate cholesterol metabolism remain to be elucidated. For some ORPs there is evidence that they affect cholesterol homeostasis, such as the overexpression of OSBP leads to increased cholesterol synthesis and decreased esterification (Lagace et al., 1997). Studies show that OSBP and ORP8 negatively regulate ABCA1 functioning, through post-translational modifications and LXR promoter activity respectively (Bowden and Ridgway, 2008; Yan et al., 2008).

Cholesterol export through LXR signalling In the situation of an excess of intracellular cholesterol an intricate system of cholesterol export is activated alongside the esterification of excess free cholesterol described above. Export of cholesterol is facilitated by the ATP-cassette binding protein (ABC) family of exporters. Specifically, the ABC subfamily A protein 1 (ABCA1) and the ABC subfamily G proteins 1,5 and 8 (ABCG1, ABCG5 and ABCG8) are responsible for the export of cholesterol (Li et al., 2013). The expression of which is dependent on the cell type. These exporters are under the transcriptional control of the Liver-X-receptor (LXR) pathway. The LXR is a family of nuclear transcription factors that are bind metabolic substrates and activate the transcription of genes involved in the regulation of cholesterol metabolism. There are two isoforms of LXR, α and β. LXR executes its activity by forming a heterodimeric complex with a second type of nuclear receptor retenoid-X-receptror (RXR). More recently it has also been shown that the targets of the LXR pathway are more widely involved in metabolism, such as fatty acid and glucose metabolism (Calkin and Tontonoz, 2012). Both nuclear receptors are activated by substrates that are derived from intracellular cholesterol metabolism. The LXR receptors are activated by oxidised sterol derivatives known as oxysterols (Janowski et al., 1996) and the RXR receptors are activated by bile acids (Parks et al., 1999). Besides stimulating the export of cholesterol, this pathway simultaneously inhibits the endocytosis of cholesterol. Two LXR target genes include proprotein convertase subtilisin/kexin type 9 (PCSK9) and the Inducible Degrader of the LDL-receptor (IDOL) which both reduce the expression of the LDLR on the plasma membrane surface. PCSK9 binds to LDLR in the endocytic compartment and prevents the recycling of the LDLR back to the plasma membrane (Zhang et al., 2007). IDOL directly binds to LDLR on the plasma membrane, leading to the polyubiquitination of the protein and its clathrin independent endocytosis and lysosomal degradation (Zelcer et al., 2009).

1.4.6 Mitochondrial cholesterol

Role of mitochondria in cholesterol metabolism The mitochondria are very sensitive to changes in cholesterol homeostasis, having one of the lowest concentrations of membrane cholesterol of all cellular membranes. The outer mitochondrial membrane contains roughly 40 times less cholesterol than the plasma membrane and the inner mitochondrial membrane has nearly unmeasurable amounts of cholesterol present (Horvath and Daum, 2013). In line with this low concentration of cholesterol, mitochondria are very sensitive to increases in membrane cholesterol. Mitochondria actively contribute to various aspects of cholesterol metabolism, synthesising downstream metabolites such as oxysterols, steroid hormones and bile acids.An important protein in the transport of cholesterol to the mitochondrial is the Steroidogenic Acute Regulatory protein (StAR or StarD1), which facilitates the transport of cholesterol from the OMM to the IMM (see paragraph 1.4.5). However, StAR does not act alone. The capacity of StAR to transport cholesterol is enabled by the Translocator Protein (TSPO), an 18 kDa protein located on the OMM (Gatliff and Campanella, 2016). TSPO enables the cleavage of StAR to its active form and together with VDAC forms a protein complex that recruits the StAR to the IMM (Rone et al., 2009). Another protein associated with mitochondrial cholesterol transport is the sterol-carrier protein 2. This protein has been shown to increase the trafficking of cholesterol from lysosomes to the mitochondrial membrane (Gallegos et al., 2000).

An important role of mitochondria is the synthesis of steroid hormones from cholesterol by steroidogenic cells. In these cells, cholesterol is transported to the inner mitochondrial membrane and is converted into pregnenolone by the enzyme CYP11A1 in the mitochondrial matrix, which is further converted to steroid hormones by other enzymes (Soccio and Breslow, 2004). Furthermore, mitochondria covert sterols into bile acids through the enzyme CYP27A1 which is present on the outer mitochondrial membrane. This enzyme hydroxylates cholesterol to produce 27-hydroxycholesterol, which is the first step in the “acidic” pathway of bile acid synthesis (Hall et al., 2005). The resulting oxysterols also directly affect cholesterol metabolism by inhibiting the processing of SREBP2 on the ER membrane and thus slowing down cholesterol biosynthesis (see above).

Cholesterol metabolism and mitochondrial function Excess cholesterol on the mitochondrial membranes directly impacts mitochondrial functioning. Artificially overloading the mitochondria with cholesterol reduces the respiratory capacity (Martin et al., 2016; Solsona-Vilarrasa et al., 2019; Yu et al., 2005) and impairs the transport of GSH over the mitochondrial membrane, due to a reduction in the activity of the 2-oxoglutarate carrier following the reduced membrane fluidity (Martin et al., 2016). Excess of cholesterol on the mitochondrial membrane also leads to an increase of oxysterols, as cholesterol concentration is the rate limiting step in the reaction. The oxysterols produced by excess mitochondrial cholesterol inhibit the processing of SREBP2 on the ER membrane and thus hinder cholesterol biosynthesis.

The proper functioning of mitochondria is also tied to the cholesterol biosynthesis pathway

as one of the outputs of the cholesterol biosynthesis pathway is CoQ10, or ubiquinol, which directly participates in the transport of electrons along the mitochondrial respiratory chain. Excess mitochondrial cholesterol may thus indirectly impact mitochondrial respiratory chain function. Other impairments of the cholesterol biosynthesis pathway also have been reported to induce mitochondrial dysfunction. Most notably, the use of statins, an important family of cholesterol lowering drugs, have been suspected to cause mitochondrially mediated side-effects in patients (Golomb and Evans, 2008) and through reduced production of ubiquinol (Littarru and Langsjoen, 2007) or reduced protein prenylation (Rauthan et al., 2013).

Thus, it is evident that intracellular cholesterol distribution and the proper functioning of the mevalonate pathway are essential for the proper functioning of mitochondria. Furthermore, recent discoveries have associated mitochondrial cholesterol to well known pathologies such as Alzheimers disease (Torres et al., 2019). This makes studying the interplay between mitochondrial function and cholesterol metabolism a worthwhile area of research possibly leading to new therapies for well known diseases.

Mitochondrial dysfunction affects cholesterol metabolism However, there are very few studies that have directly looked at the influence of mitochondrial dysfunction on cholesterol metabolism. One study discovered that a primary defect in mitochondrial dynamics caused mitochondrial respiratory chain dysfunction by inhibitory effects on the cholesterol biosynthesis pathway (Mourier et al., 2015). Indirectly there is evidence which connects mitochondrial dysfunction to cholesterol metabolism, such as how mTORC1 activates SREBP2 by reducing cholesterol trafficking from lysosomes (Eid et al., 2017; Peterson et al., 2011). Finally, mitochondrial dysfunction induces ER-stress (Lim et al., 2009), which in turn has been shown to activate SREBP2 (Colgan et al., 2007) and regulate ATF4-mediated transcriptional modulation of transcripts involved in cholesterol metabolism (Fusakio et al., 2016; Röhrl et al., 2014). All this highlights the intersection between mitochondrial function and mevalonate pathway functioning, suggesting the inverse direction of communication may also be plausible.

1.5 Outline of the thesis project

The activation of retrograde signalling by mitochondrial dysfunction can make the difference between the recovering of homeostasis or the deterioration into disease. However, the exact transcriptional programs that are activated as a consequence of mitochondrial dysfunction are not yet fully uncovered. Through comparing the transcriptional programs activated, we can learn about potential new mechanisms of disease for mitochondrial dysfunction. In addition, the initial results pointed in the direction of cholesterol metabolism. The delicate control over cholesterol metabolism is affected in conditions of respiratory chain dysfunction such as those taking place mitochondrial disease patient cells, and whether these mechanisms contribute to the pathology have been barely explored in the literature.

Therefore, the main objectives of this PhD thesis were to discover a new cellular adaptation to

mitochondrial dysfunction and to characterise the mechanism behind this adaptation. These objectives can be subdivided in the following aims: - To characterise the chemical models of mitochondrial dysfunction - To study the transcriptional responses to three inhibitors and identify potential novel adaptations to mitochondrial respiratory chain dysfunction - To follow up on the observed phenotype of mevalonate pathway transcripts suppression - To investigate the mechanism of downregulation of cholesterol sensors - Translate the findings into a physiologically relevant model

Here, taking advantage of an unbiased transcriptomic investigation, we demonstrate that impairment of mitochondrial respiratory chain interacts with intracellular cholesterol signalling. Complex I dysfunction negatively impacts the expression of cholesterol sensors on the ER and the processing of SREBP2. This has a consequence of the abundance of mevalonate pathway functioning and leads to a decrease in mevalonate pathway metabolites. Further research is needed to study the consequence of the altered metabolite levels on cell health and mitochondrial function.

2 Pharmacological models of respiratory chain dysfunction

Ultimately all mitochondrial defects affect the expression of the respiratory complexes and lead to a decrease in the respiratory function of mitochondria. For this reason, focussing on the intracellular signalling caused by respiratory chain dysfunction is an effective approach to discover new retrograde signalling pathways. There are various strategies for inducing mitochondrial respiratory chain dysfunction, each with its own advantages and pitfalls. Generally available are chemical interventions, genetic mouse models or samples from patients. The potentials and pitfalls of these models have been reviewed in detail elsewhere (Breuer et al., 2013; Lee and O'Brien, 2010; Valsecchi et al., 2012).

In our work we focussed on chemically induced mitochondrial respiratory chain dysfunction, for the ability to fine-tune the degree of respiratory impairment, the abundance of literature available and to avoid possible clonal or inter-patient bias in the initial discovery phase of the project. Multiple protein complexes of respiratory chain can be targeted with compounds that specifically impair their function. The biochemical changes following use of these inhibitors had been well documented, see chapter 10.1 of the introduction. Targeting multiple individual sites is especially interesting because, even though the protein complexes of the respiratory chain all contribute to cellular respiration, there are molecular differences between the complexes that could be used in the interpretation of the retrograde signalling. The comparison of the site-specific biochemical changes and the retrograde signals originating from different sites of inhibition provide clues into the potential mechanisms.

Following this rationale, we decided to treat human primary fibroblasts with either rotenone, antimycin A or oligomycin A which inhibit the respiratory chain at complex I (NADH:ubiquinone oxidoreductase), complex III (CoQH2-cytochrome c reductase), and complex V (ATP-Synthase) respectively (figure 2.1-A). Fibroblasts are a good model of choice as the contribution of the mitochondria to their metabolism has been well studied (Pereira et al., 2018). Furthermore, skin fibroblasts are often isolated from skin biopsies taken from patients suspected to suffer from mitochondrial disease and are used for studies of mitochondrial disease, allowing comparison to our findings.

2.1 Dose finding

To optimise the model for our research question we wanted to strongly inhibit respiration while still maintaining cellular viability. In this balance, the cells suffer from a severe respiratory impairment, but cellular homeostatic mechanisms adapt to the defect and the cells are able to survive. The severity of the respiratory defect will also make it more likely that retrograde signalling mechanisms will be activated, increasing the likelihood of discovery. To study the effect of the inhibitors on cellular respiration, we treated human primary fibroblasts with rotenone, antimycin A or oligomycin A and measured the acute effects on cellular respiration. To find the optimal conditions, we titrated the compounds over a wide range of concentrations and calculated the residual respiration compared to control fibroblasts. From this data the IC50 were calculated by fitting a logistic model. The compounds all effectively reduced the respiratory function of the cells with IC50 values of 12.39 nM, 9.33 nM and 405.6 nM respectively (figure 2.1-B,table 2.1).

Table 2.1 – IC50 values of respiratory inhibition

	IC50 (nM)	95% CI
Rotenone	12.39	8.425 to 18.33
Antimycin A	9.33	6.598 to 13.16
Oligomycin A	405.6	211 to 772.4

To find a concentration that maintained cellular viability while strongly inhibiting oxygen consumption, we measured the degree of apoptosis on our cellular models over a series of concentrations with proven strong respiratory inhibition. We found that concentrations of 100 nM rotenone, up to 5 μM antimycin A and up to 10 μM oligomycin A did not significantly induce apoptosis over a treatment duration of 5 days , suggesting that the cells are indeed able to adapt to the respiratory impairment (figure 2.2-A). A concentration of 1 μM rotenone significantly induced apoptosis. Interestingly, rotenone was the only mitochondrial inhibitor that had any effect on the degree of apoptosis in our models at the concentrations tested. Mitochondrial stress slows down proliferation in a response to the respiratory chain dysfunction as has been shown in detail in earlier studies of mitochondrial dysfunction models (García-Bartolomé et al., 2017; Peng et al., 2015; Stöckl et al., 2006).

To assess the effect of our inhibitors on cellular proliferation we cultured human fibroblasts for 5 days in the presence of a range of inhibitor concentrations. From the resulting growth curves, we extrapolated the maximal growth rate and plotted this to the concentrations used (figure 2.2-B). Rotenone and antimycin A lowered maximal proliferation rates to a similar degree in low concentrations, however rotenone had a more pronounced effect at concentrations over 10 nM. At the highest concentrations rotenone almost completely arrested cellular proliferation, correlating with the observed increase of apoptosis. Oligomycin A had a pronounced effect at low concentrations (< 1nM), however at higher concentrations only had a modest effect on proliferation. At a concentration of 500 nM antimycin A had a similar

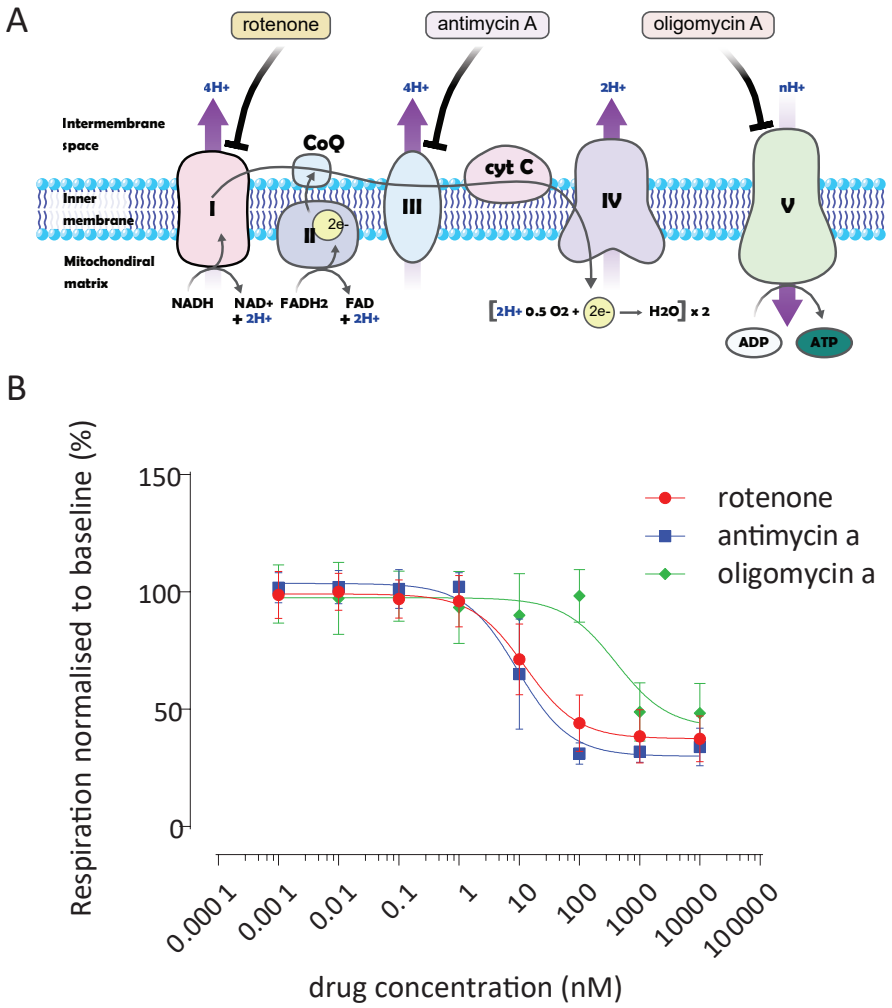

Figure 2.1 – **Inhibition of the respiratory chain complexes**
(A) A schematic of the mitochondrial respiratory chain complexes with indicated the compounds used to inhibit the protein complexes rotenone (complex I), antimycin A (complex III), oligomycin A (complex V). (B) Dose dependent inhibition of oxygen consumption by respiratory chain inhibitors. Inhibitors were added acutely at increasing concentrations as indicated for rotenone (red circles), antimycin A (blue squares) or oligomycin (green diamonds). Respiration was measured in a Seahorse XF96 oxygraph (see Materials and Methods). Oxygen consumption per unit of protein was calculated for each well and expressed as percentage of basal respiration in fibroblasts in the absence of the inhibitors. Shown is the average of 3 independent experiments ± standard deviation. Each independent experiment comprises 6 separate wells pooled. The IC50 values are given in the results section.

effect on proliferation as 1 µM oligomycin A (figure 2.2-C). For the remainder of this work, we continued with models of 100 nM rotenone, 500 nM antimycin A and 1 µM oligomycin A as these concentrations best fulfilled our predefined criteria of strong respiratory impairment, non-significant increase in apoptosis and comparable effect on cellular proliferation rates.

2.2 Further phenotyping of the models

Mitochondrial dysfunction can induce cellular senescence depending on the type of impairment and the metabolic state of the cell (Stöckl et al., 2006; Wiley et al., 2016). To investigate if the observed reduction in proliferation was paired with a concurrent switch to a senescent phenotype, we measured the senescence marker β-galactosidase (BGAL) in our models of mitochondrial dysfunction and compared this to control and very high passage fibroblasts (figure 2.3-A). We observed a low abundance of BGAL in the exponentially dividing control fibroblasts and a significant increase of the BGAL staining in very late passage fibroblasts, suggesting a transition into a senescent phenotype following extensive passaging of cells. In our models of mitochondrial dysfunction, we do not observe an increase in BGAL staining, implying that the mitochondrial inhibitors do not induce a senescent phenotype in the concentrations used for the duration of the measured treatment.

Respiratory chain dysfunction leads to impairments in energy balance and an increase in oxidative stress. To characterise the effect of our inhibitors on the energy stress and oxidative stress we measured the energy sensor AMP-activated protein kinase (AMPK) and the reactive oxygen species (ROS) scavenger protein Superoxide Dismutase 2 (SOD2). We observed that rotenone and antimycin A do not have a significant effect on the phosphorylation of AMPK and its downstream target ACC (figure 2.3-B). Rotenone shows a slight increase of phosphorylation of these enzymes after 5 days. Strikingly, oligomycin A shows a dramatic increase in phosphorylation after 5 days indicative of severe energy stress. Increased levels of intracellular ROS induce the abundance of SOD2 through translocation of the FOXO3 transcription factor to the nucleus (Kops et al., 2002). Antimycin A and oligomycin A show a slight increase of SOD2 after one day of treatment, but during longer incubations show levels comparable to control.

2.3 Conclusion

We conclude that inhibition of human primary fibroblasts with rotenone, antimycin A or oligomycin A at concentrations of 100 nM, 500 nM, and 1 µM respectively is a reliable system to study cellular adaptations to respiratory chain dysfunction. These concentrations induce a severe reduction in cellular respiration, without inducing severe apoptosis or senescence. Furthermore, these concentrations do not activate AMPK after 1 day of treatment, whereas rotenone and oligomycin A show an increase in phosphorylation after 5 days, suggesting a shift in metabolic adaptation during this timeframe. The levels of SOD2 are slightly induced after 1 day of treatment with antimycin A and oligomycin A, but show levels comparable to control at longer treatment durations.

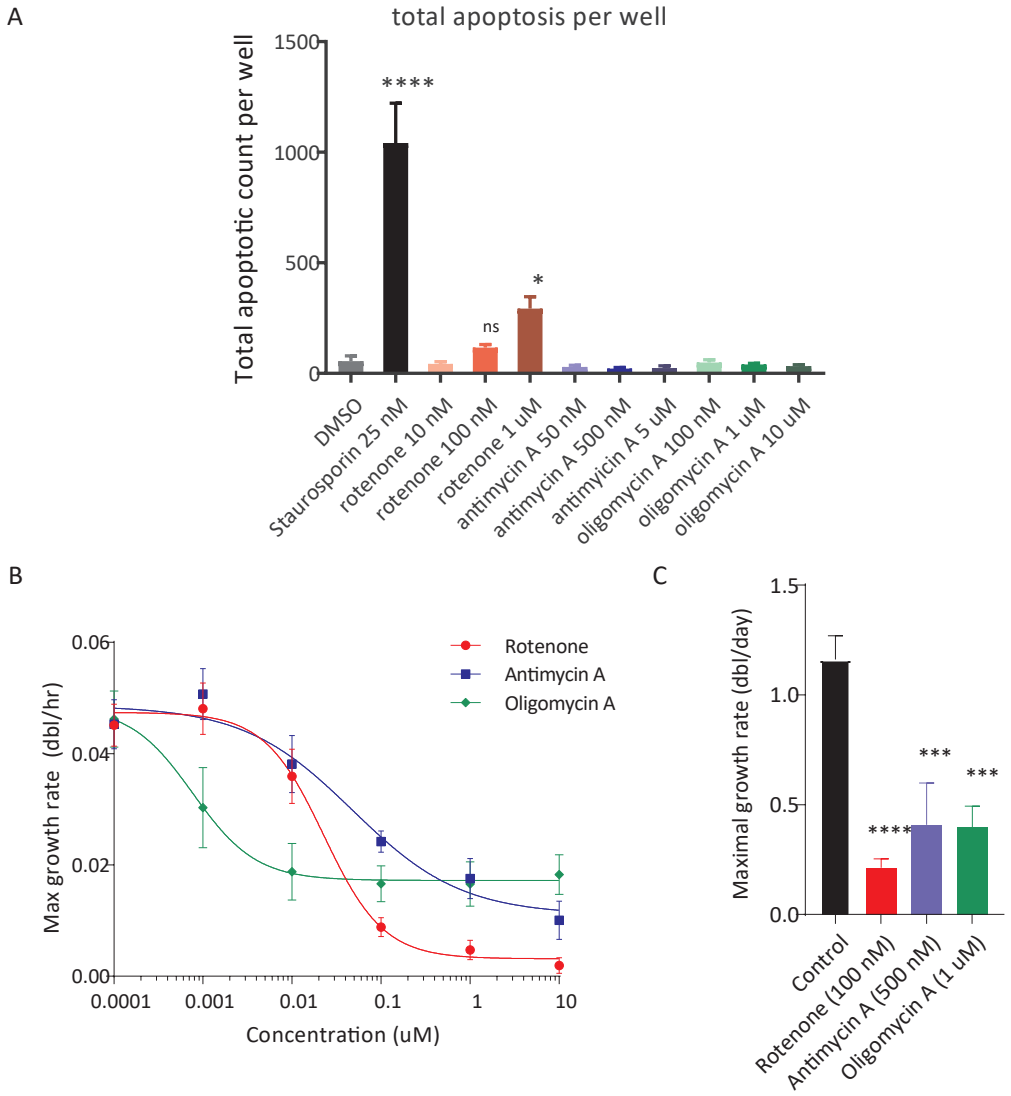

Figure 2.2 – **Validation of mitochondrial dysfunction characteristics**
(A) Bar graph representing the induction of apoptosis by various concentrations of respiratory chain inhibitors. Apoptosis of human fibroblasts was measured with Annexin V Green marker in a ZOOM Live-Cell analysis system (see Materials and Methods). Apoptosis is expressed as total counts after growth for 5 days in the absence or presence of respiratory chain inhibitors. The compound staurosporin (25nM; grey bar) was used to induce apoptosis as positive control. Shown are means calculated from 3 independent experiments ± standard deviation. (B) Dose dependent reduction of proliferation by treatment with respiratory chain inhibitors. Shown is the maximal growth rate of cells in the exponential phase. Maximal growth rate was calculated by fitting a sigmoidal curve to the datapoints and extracting the slope values in the exponential phase. Markers indicate mean of three independent experiments ± standard deviation (C) Bar graph showing maximal growth rates of selected concentrations of inhibitors. Bars indicate mean of three individual experiments ± standard deviation. (A,C) Significance was calculated by ANOVA with Dunnett's multiple-comparisons post-hoc test. Stars indicate significance compared to DMSO control. ns not significant,* p<0.05, ** p<0.01, *** p<0.001.

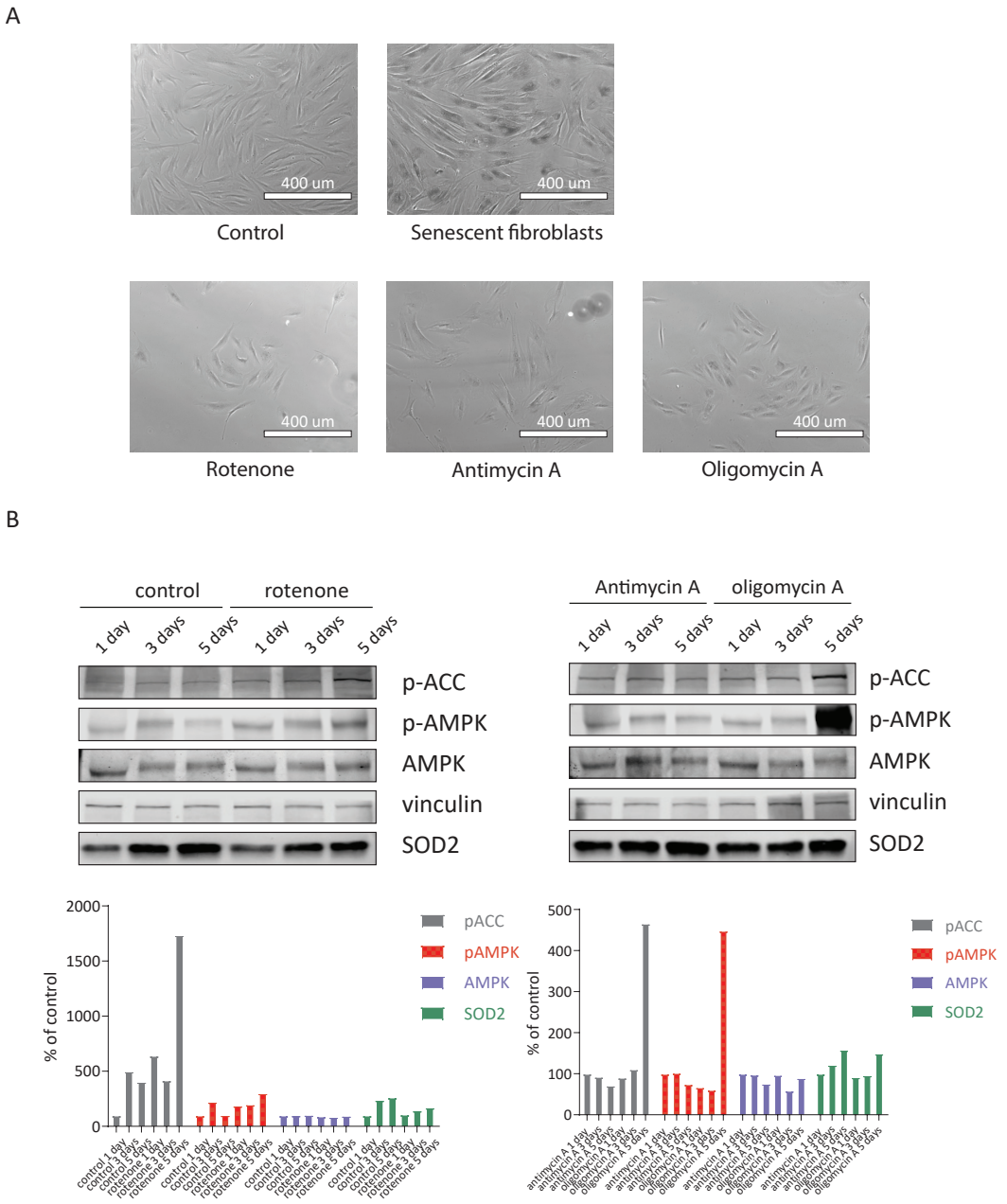

Figure 2.3 – **Further characterisation of models of mitochondrial dysfunction**
(A) Representative bright field images of cells stained for senescence markers. Cells were fixed and stained for β-galactosidase. Cells were grown for 5 days in the presence of inhibitors. Senescent cells were grown for more than 40 passages. Dark areas in the images indicate expression of senescence markers. Scale bars indicate 400um length. (B) Western blot of proteins involved in mitochondrial retrograde signalling. Cells were treated with 100 nM rotenone, 500 nM antimycin A or 1 µM oligomycin A for 1,3 or 5 days before protein lysate was collected. (p)AMPK, (phosphorylated)-AMP-activated kinase; (p)ACC, (phosphorylated)-Acetyl-CoA carboxylase; SOD2, Superoxide Dismutase 2.

3 Transcriptional profile of mitochondrial respiratory chain dysfunction

To study the mitochondrial retrograde signalling response, we took advantage of an unbiased transcriptomics approach on our multiple models of RC deficiency. We measured the transcriptome of the three independent cellular models of mitochondrial respiratory chain dysfunction with QuantSeq 3'RNA sequencing and compared this to untreated cells. In our experiment we treated the cells for two different durations, namely 1 and 5 days, to discover retrograde signalling that is activated rapidly and persists over multiple days. For each timepoint we included 5 individual replicates for each of the treatments.

3.1 Exploratory data analysis

To visualise if there were differences gene expression patterns in the data, we performed a Principal Component Analysis (figure 3.1-A). This shows a separation of the samples when the data is plotted on the first two principal components, showing that treatment with mitochondrial inhibitors changes the gene expression profiles of the cells. The treatment groups are separated from the control samples in both the first and second principal component. Oligomycin A shows the most modest separation from the cluster of control samples. The first two principal components only explain 35.8% percent of the total variation, thus a lot of the variation in the data are not visualised in this plot. The clusters of the two timepoints are visible in this plot and are separated on both the first and second principal component.

In total, 32041 unique genes were identified in the sequencing experiment. Of these features 10881 genes were kept in the analysis after filtering for low expressed genes. Only genes with at least 16 counts on a minimum of 6 samples were included. Of these included genes, 1250 (11.48%) were related to mitochondria, as categorised by the MitoCarta database (Calvo et al., 2016). For the statistical comparison of expression changes, we fit a Negative Binomial generalized linear model, estimated the dispersion across all genes and constructed a contrast matrix to assess differential expression between inhibitors, holding all other variables constant. A value of 0.05 for the False Discovery Rate (FDR) was used as cut-off for significance testing compared to control.

The total number of significantly differentially expressed genes (DEG) was roughly similar for both rotenone and antimycin A at around 3000 total genes (figure 3.1-B). Oligomycin A shows a somewhat milder transcriptional response, with only 499 genes significantly changed. All treatments show a roughly 10% fraction of genes are that are related to mitochondria, in accordance to earlier published work (Quirós et al., 2017). This is similar to the fraction of total included genes, suggesting there is no enrichment in the fraction of mitochondrially related genes.

The distribution of genes seems to be roughly equally divided between the up- and down-regulated genes for rotenone and antimycin A with a slight tendency for more significant genes to be upregulated, as shown in the volcano plots (figure 3.1-C). Oligomycin A seems to have a slightly higher proportion of upregulated genes. Our main interest was to discover possible synergies and contrasts between the different treatment groups.

To visualise these similarities and differences between the treatment groups we plotted the significant differentially expressed genes in a Venn diagram, including both up and downregulated genes (figure 3.1-D). This diagram shows there is a lot of similarity in the transcriptional response between rotenone and antimycin A with 2529 (63.0%) of all genes shared. Antimycin A treatment also induced a large fraction of genes that were unique to this compound (977 genes or 24.4% of total). Most interestingly, there is an almost 10% group of genes (387 genes, 9.6% of total) that is shared by all treatments. Almost all these genes (384/ 99%) were changed in the same direction for the three mitochondrial inhibitors. In this subset of genes, 283 genes were upregulated, and 101 genes were downregulated. One gene had varying directionality depending on the treatment. Such coherent regulation in this gene set suggests the presence of a general adaptive response to respiratory dysfunction that is activated independent of the site of inhibition. We further investigated this pool of shared genes, as these might be characteristic of a general adaptation to mitochondrial respiratory chain dysfunction.

3.2 The mevalonate pathway

To put the subset of genes in a biologically context, we calculated the enrichment in Gene Ontology (GO) – biological process pathways (figure 3.2-A). The enrichment was calculated for the upregulated and downregulated subsets separately. This clustered enrichment analysis shows that in the upregulated shared genes there is a strong enrichment in genes associated with cellular stress, apoptosis, and negative regulation of metabolic processes. This is in line with earlier studies on the transcriptional response to mitochondrial dysfunction and are have been studied in detail elsewhere (Guo et al., 2020; Mick et al., 2020; Quirós et al., 2017). In the subset of shared downregulated genes, we discovered a strong enrichment in cholesterol biosynthetic processes, an observation also made earlier but was never studied in depth (Kühl et al., 2017; Mick et al., 2020).

A deeper investigation of the genes included in this ontology indeed showed an overall downregulation of transcripts that are linked to the mevalonate pathway, which is the main

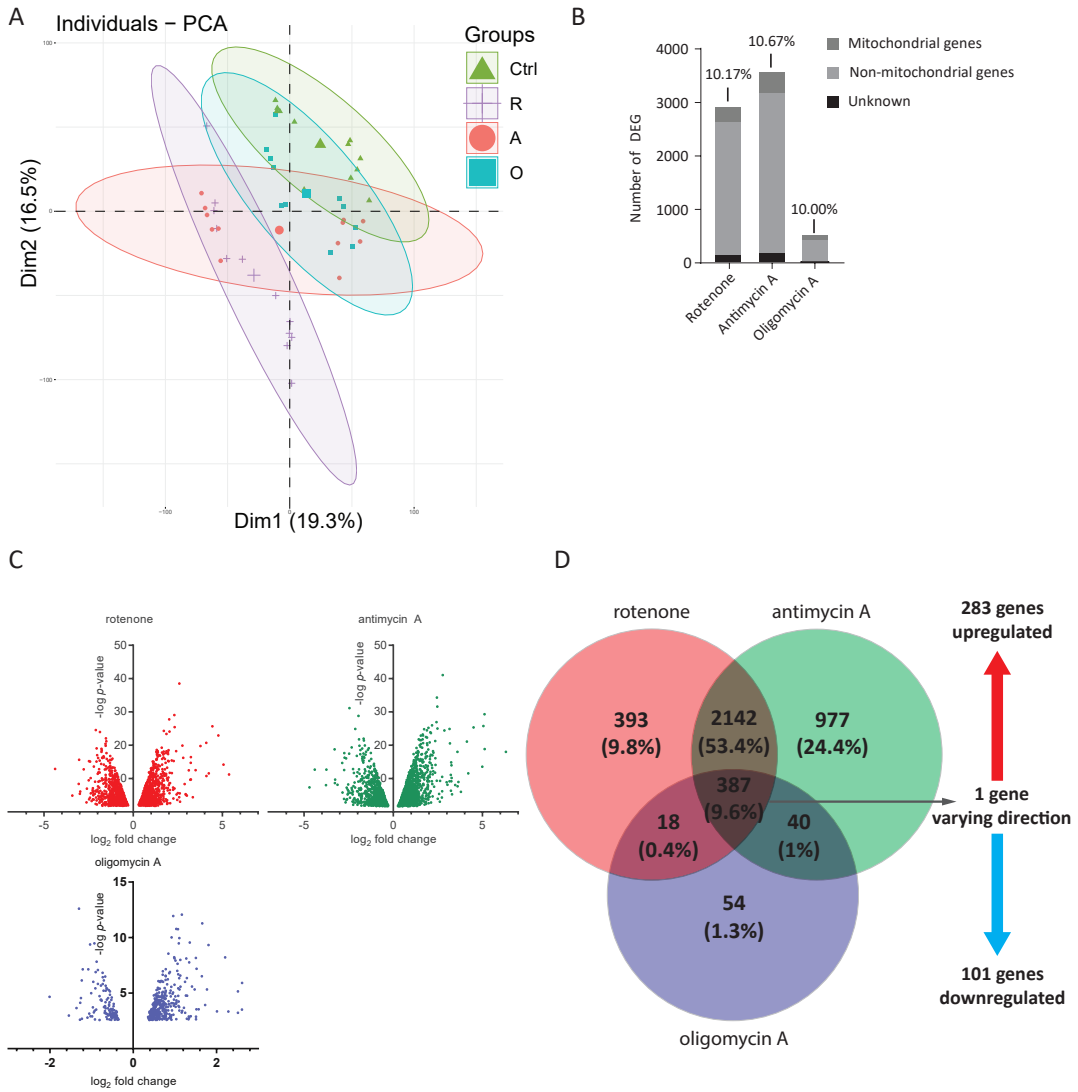

Figure 3.1 – **Inhibition of mitochondrial respiratory function activates a strong transcriptional response**
(A) Principal Component Analysis of gene expression levels derived from QuantSeq of fibroblasts treated with respiratory chain inhibitors for either 1 or 5 days. N=5 for each condition. Ctrl, control; R, rotenone; A, antimycin A; O, oligomycin A. Circles indicate 95% confidence ellipses. Large icon in centre of ellipse indicates mean of effect. The first two principal components PC1 and PC2 are shown. (B) Bar graph showing the total number of significantly Differentially Expressed Genes and fraction of mitochondrially related genes as assessed by the MitoProfiler database. (C) Volcano plots representing the fraction of down- and upregulated genes of all inhibitors. Each point represents a single gene. (D) Venn diagram showing overlap and differences of DEGs between treatment groups.

pathway for endogenous cholesterol synthesis (figure 3.2-B). The mevalonate pathway can de divided into three parts, the upper pathway responsible for the synthesis of mevalonate, the lower pathway that converts mevalonate into squalene and other metabolites, and finally

the cholesterol synthesis pathway which transforms squalene into cholesterol (figure 1.3). Transcripts for all 8 enzymes in the upper and lower mevalonate pathway were downregulated in all three models of respiratory chain dysfunction. The following part of the pathway converts squalene to cholesterol. This pathway is more complex with multiple enzymes and two different pathways involved. In general, also the transcripts involved in this final part of the mevalonate pathway were downregulated. The only the expression of sterol-C5-desaturase-like protein (SC5DL) was upregulated after inhibition of the different respiratory chain complexes.

3.3 Validation

To confirm the observed differential expression in the 3'QuantSeq experiment, we measured the time dependent change in a subset of mevalonate pathway genes. The selected transcripts ACAT2, HMGCS1, HMGCR, SQLE and DHCR7 all encode key enzymes of the mevalonate pathway and showed strong differential expression in the QuantSeq data. We measured the levels of the transcripts over a period from 30 minutes to 24 hours. The relative fold change of these transcripts compared to control decreases in a time dependent manner up to the maximum measured time for all genes (figure 3.3-A), validating the observations made in the QuantSeq experiment that complex I inhibition reduces the levels of mevalonate pathway transcripts.

Cholesterol homeostasis is regulated by several mechanisms such as endogenous synthesis in the mevalonate pathway and the transport of lipoproteins in and out of the cell. The low-density-lipoprotein receptor (LDLR) and very-low-density-lipoprotein receptor (VLDLR) are responsible for the cellular import of respectively cholesterol rich and lipid rich lipoprotein vesicles. After observing that transcripts of cholesterol biosynthesis were affected by respiratory chain dysfunction, we questioned whether transcripts of cholesterol transport were similarly affected. To study this, we measured transcripts of the main lipoprotein receptors responsible for the endocytosis and excretion of cholesterol containing lipid vesicles. We observed a downregulation of LDLR transcripts after 24 hours of treatment with rotenone (figure 3.3-B). Earlier timepoints showed a lot of variability and no conclusions can be drawn from this. We also observed a concurrent increase in the gene for VLDLR after 4 hours, with maximal levels reached after 8 hours and consistent up to 24 hours. This shows that the cells are limiting the import of sterol rich lipoprotein vesicles, while stimulating the import of triglyceride rich vesicles.

The effects of respiratory chain dysfunction on the mevalonate pathway may be an indirect consequence of a reduced proliferation rate which may lower the cellular demand for cholesterol. To validate our hypothesis that the lowering of mevalonate pathway transcripts is a direct consequence of respiratory chain dysfunction, we measured the effect of complex I inhibition on gene expression in cells at low proliferation rates. Fibroblasts that are cultured in high density slow their proliferation rates naturally by contact inhibition. We measured the

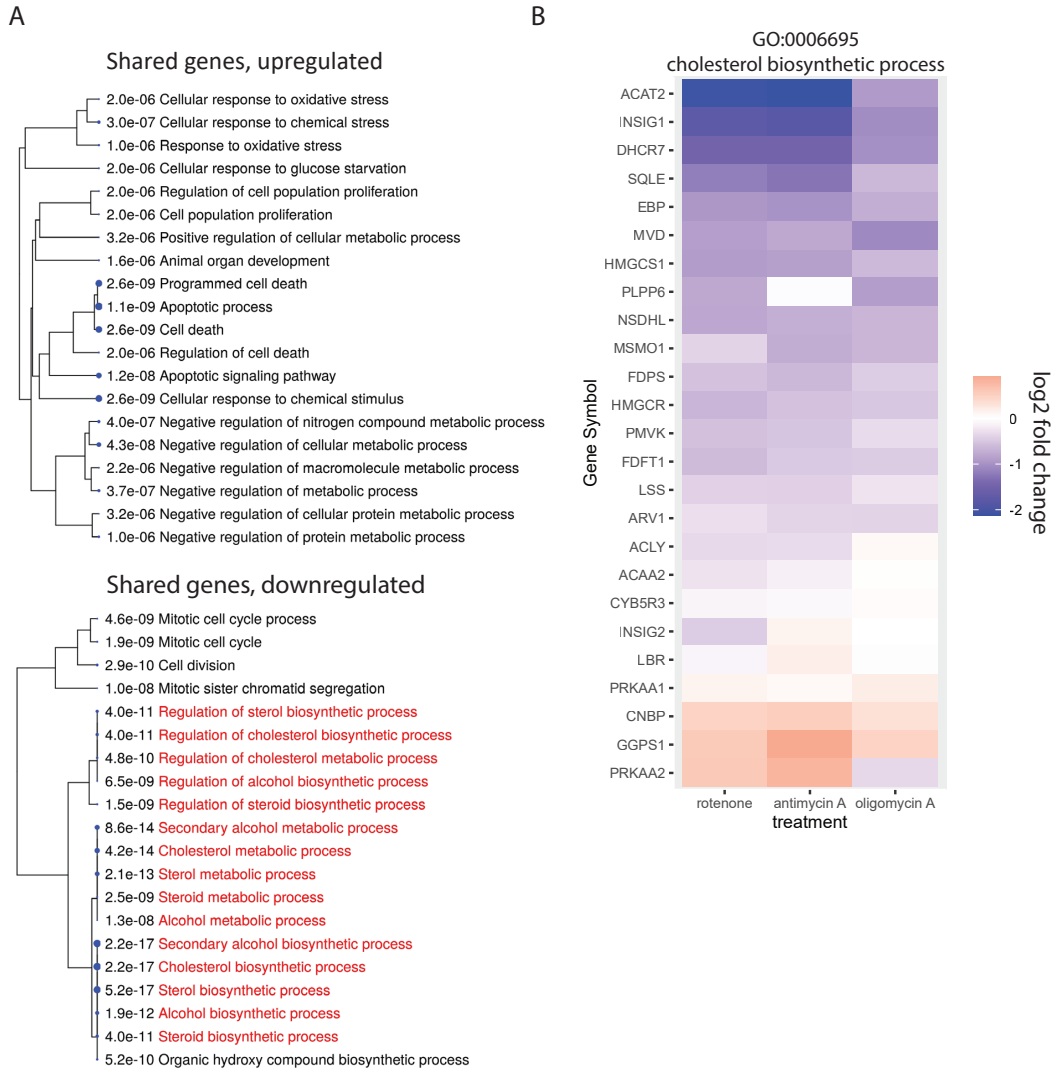

Figure 3.2 – **Inhibition of mitochondrial respiratory function triggers activation of stress and inhibition of cholesterol biosynthesis**
(A) Clustered Gene Onthology analysis of significant differentially expressed genes. Enrichments were calculated separately for the upregulated and downregulated fractions of the shared genes. Onthologies relating to cholesterol metabolism are highlighted in red. (B) Heatmap showing expression levels of genes in the GO cholesterol biosynthetic process pathway.

expression of key mevalonate pathway genes after rotenone treatment in cells grown in high confluence and compared this to normally proliferating cells (figure 3.4-A). We observed that rotenone lowers the expression of genes in both normally proliferating and contact-inhibited fibroblasts to a similar degree. This finding supports our hypothesis that the transcriptional activity of the mevalonate pathway is under the influence of signals originating from mitochondria following perturbation of respiratory chain function and rejects the possibility that suppression of mevalonate pathway transcripts is a secondary consequence of the lower

demand for cholesterol associated to the lower proliferation rates observed in our models.

3.4 Conclusion

Taken together we observed that in multiple models of respiratory chain dysfunction, cholesterol biosynthesis is concurrently downregulated. This downregulation affected almost without exception all the transcripts of the mevalonate pathway enzymes. Measuring these genes by qPCR showed a time dependent decrease in these transcripts, and a strong reduction after 24 hours. Importantly, this reduction in mevalonate pathway genes occurred in cells growing at normal and at reduced proliferation rates, thus proving the effect is not secondary to reduced cell growth. The downregulation in mevalonate pathway transcripts is thus likely a response to mitochondrial respiratory chain dysfunction.

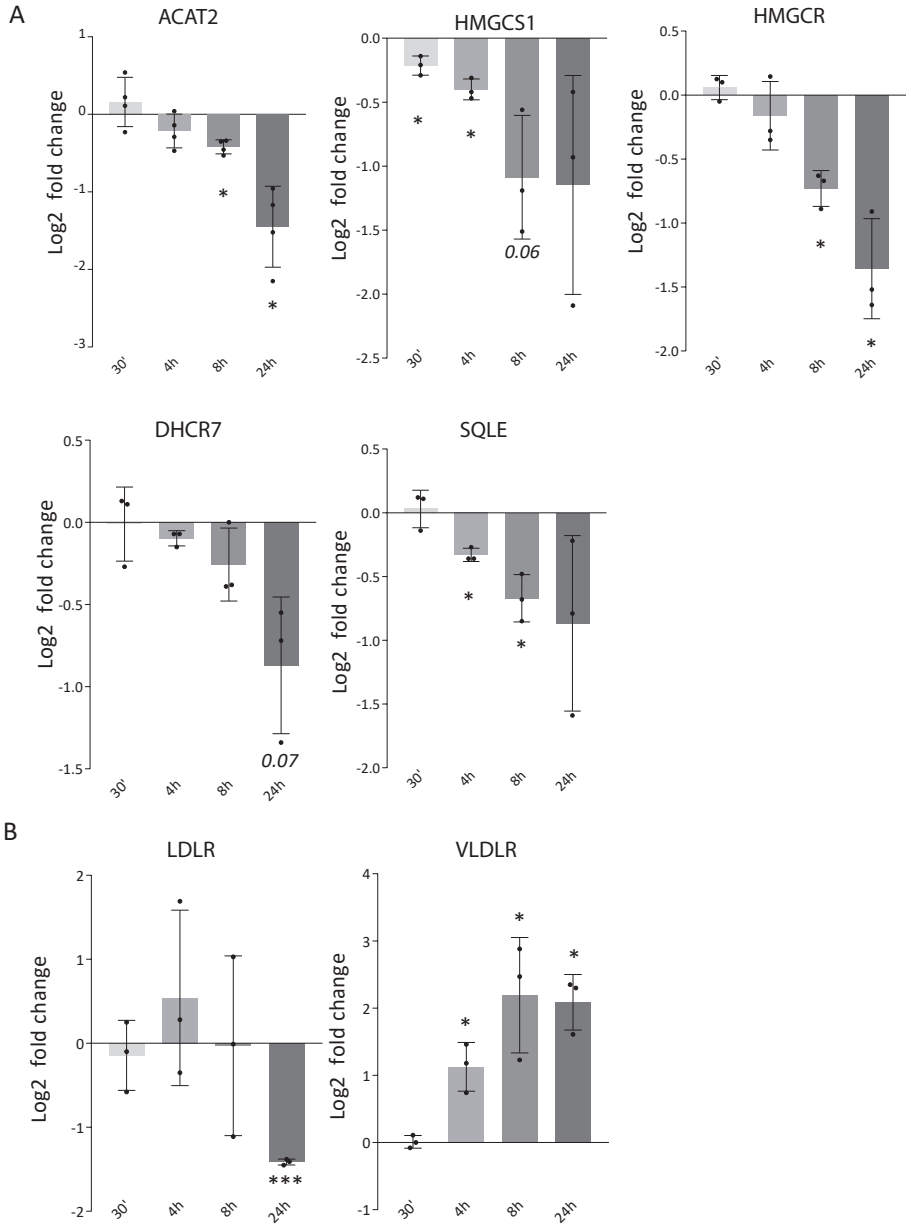

Figure 3.3 – **Inhibition of mitochondrial respiratory function decreases expression of cholesterol biosynthesis genes in a time dependent manner.** (A) Gene expression changes of key mevalonate pathway genes measured by qPCR. Cells were treated with 100 nM rotenone for the times indicated. Bars represent mean of three independent experiments ± standard deviation. Significance of difference was calculated by one-sample t-test compared to baseline. (B) Gene expression changes of lipoprotein receptors. Data acquired as in (A). ns not significant,* p<0.05, ** p<0.01, *** p<0.001. (ACAT2, Acetyl-CoA Acetyltransferase 2; HMGCS1, 3-Hydroxy-3-Methylglutaryl-CoA Synthase 1; HMGCR, 3-Hydroxy-3-Methylglutaryl-CoA Reductase; SQLE, Squalene Epoxidase; DHCR7, 7-Dehydrocholesterol Reductase; LDLR, Low Density Lipoprotein Receptor; VLDLR, Very Low Density Lipoprotein Receptor.)

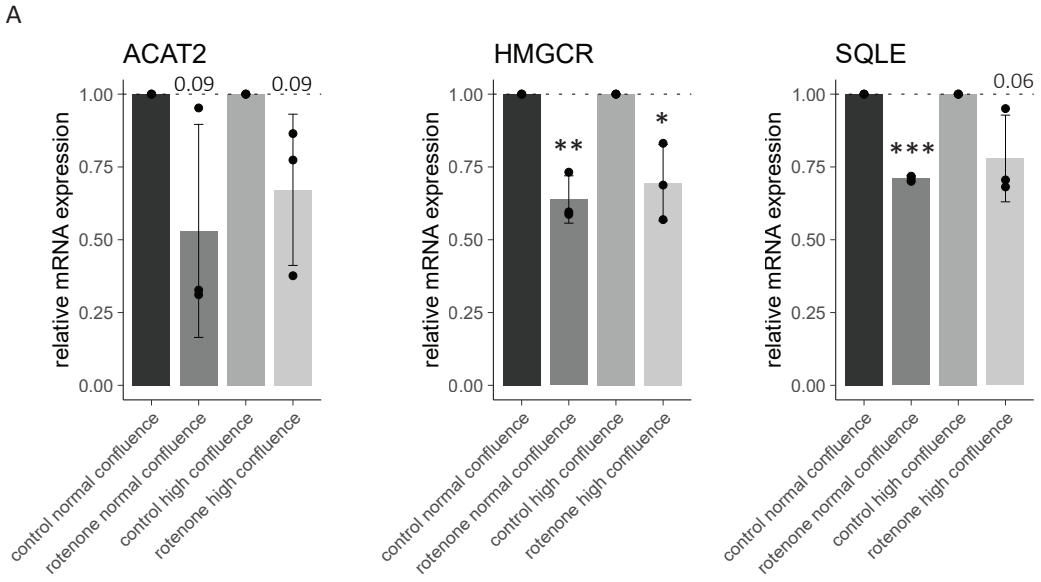

Figure 3.4 – **Cellular proliferation rate do not inhibition affect mevalonate pathway transcripts.** (A) Gene expression of key mevalonate pathway genes measured by qPCR following rotenone treatment in either normal confluent or fully confluent cells. Genes were normalised to housekeeping genes. Bars indicate mean of here independent experiments ± standard deviation. Points indicate individual replicates. Significance was calulated with students two-sided t-test. * p<0.05, ** p<0.01, *** p<0.001. (ACAT2, Acetyl-CoA Acetyltransferase 2; HMGCR, 3-Hydroxy-3-Methylglutaryl-CoA Reductase; SQLE, Squalene Epoxidase)

4 Metabolic profile of mitochondrial respiratory chain dysfunction

The mevalonate pathway is an important endogenous biosynthetic pathway that produces many biologically active metabolites, among which cholesterol. The metabolites produced include isoprenoids, ubiquinone (coenzyme Q; CoQ) and sterol intermediates. Impairment of this pathway and the consequent changes in metabolite concentrations can have severe consequences and lead to disease (Buhaescu and Izzedine, 2007). We thus questioned if the transcriptional downregulation of mevalonate pathway transcripts has a functional consequence on the levels of mevalonate pathway metabolites. To study this, we performed untargeted metabolomics on the three mitochondrial disease models. We measured the absolute amounts of the metabolites. This allowed us to compare the various inhibitors and identify general and complex specific adaptations.

4.1 Exploratory data analysis and validation

We measured the absolute quantity of 22 metabolites of the mevalonate pathway. The metabolites covered all the regions of the pathway: the upper, lower, CoQ synthesis, isoprenoid and sterol-synthesis regions. All metabolite levels were normalised to total protein levels. From the heatmap we observed that respiratory chain inhibition has a clear effect on the levels of mevalonate pathway metabolites (figure 4.1-A). It also becomes evident that in cells treated with rotenone the various regions of the mevalonate pathway were affected differently. Furthermore, a clear difference between the three inhibitors was evident, suggestive of target specific retrograde signalling pathways. Treatment with the HMG-CoA reductase inhibitor atorvastatin overall lowered the levels of mevalonate pathway metabolites. The levels the HMG-CoA metabolite however were increased, proving the well-functioning of the drug and our ability to detect metabolite changes in response to defects of the mevalonate pathway.

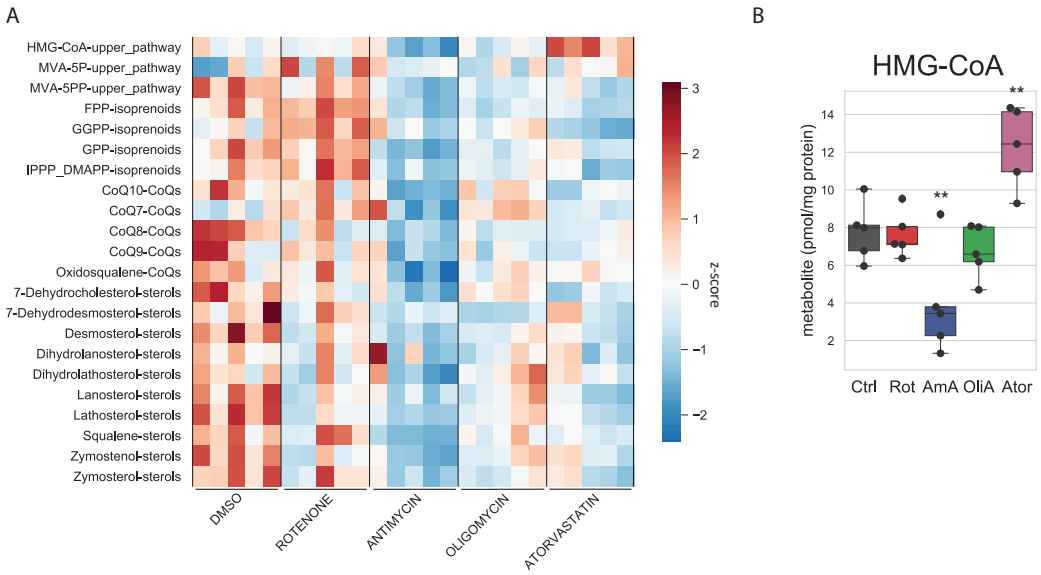

Figure 4.1 – **Inhibition of mitochondrial respiratory function affect abundance of mevalonate pathway metabolites.** (A) Heatmap showing abundance of mevalonate pathway metabolites following treatment of respiratory chain inhibitors for 48 hours in primary fibroblasts. Concentrations of 100 nM rotenone, 500 nM antimycin A and 1 µM oligomycin A were used. The z-scaled absolute values of 22 metabolites measured are shown. Each sample was individually normalised to total protein content. All 5 separate measured replicates are shown. (B) Boxplot showing absolute abundance of HMG-CoA metabolite following treatment with respiratory chain inhibitors or atorvastatin as indicated. Significance calculated by fitting variables into a linear model and calculating influence of variable on outcome. * p<0.05, ** p<0.01, *** p<0.001. (HMG-CoA, 3-hydroxy-3-methylglutaryl-coenzyme A; Ctrl, control conditions DMSO; Rot, 100 nM rotenone, AmA, 500 nM antimycin A; OliA, 1 µM oligomycin A)

4.2 Isoprenoids

Isoprenoids are an important biomolecule that is covalently linked to proteins, facilitating their anchoring to membranes often necessary for their function. We measured the quantities of the isoprenoids isopentenyl pyrophosphate (IPP) and its stereoisomer dimethylallyl pyrophosphate (DMAPP), geranyl pyrophosphate (GPP) and geranylgeranyl pyrophosphate (GGPP) following treatment with the respiratory chain inhibitors (figure 4.2). A strong target specific effect was observed comparing the levels of the isoprenoids in each group. Overall inhibition of complex I affected the levels of isoprenoids differently than inhibition of the other respiratory chain complexes III and V. Inhibition of complexes III and V reduced the levels of IPP/DMAPP, GPP and FPP to levels comparable with atorvastatin or below, whereas complex I impairment either has no effect as seen for GPP and FPP, or even shows an increase such as IPP/DMAPP and GGPP. Interestingly, the gene encoding Geranylgeranyl Diphosphate Synthase 1, the enzyme that synthesises GGPP is upregulated in all models of mitochondrial dysfunction. This disconnection between the transcriptional regulation and the changes in

metabolite levels hinted at a possible translational or post translational regulation of GGPP synthase following inhibition of complexes III and V.

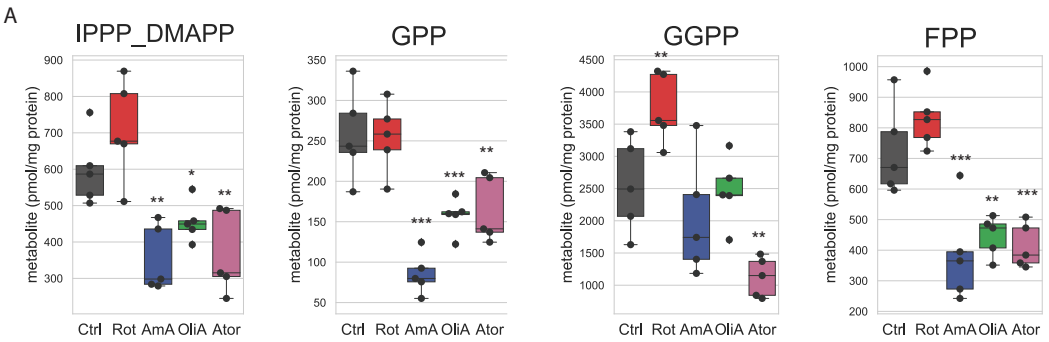

Figure 4.2 – **Inhibition of mitochondrial respiratory function varyingly affects isoprenoid levels.** (A) Boxplot showing absolute abundance isoprenoid metabolites following treatment with respiratory chain inhibitors or atorvastatin as indicated. Absolute amounts were normalised to total protein content for each sample individually. Significance calculated by fitting variables into a linear model and calculating influence of variable on outcome. * p<0.05, ** p<0.01, *** p<0.001. (IPPP, Isopentenyl pyrophosphate; DMAPP, Dimethylallyl pyrophosphate; GPP, geranylpyrophosphate; GGPP, geranylgeranylpyrophosphate; FPP, farnesylpyrophosphate; Ctrl, control conditions DMSO; Rot, 100 nM rotenone, AmA, 500 nM antimycin A; OliA, 1 µM oligomycin)

4.3 Ubiquinone

Another important family of metabolites produced in the mevalonate pathway are the ubiquinone (coenzyme Q; CoQ) metabolites. These enzymatic cofactors shuttle electrons along the electron transport chain and thus have an essential role in the functioning of mitochondria. To study the effect of RC dusfunction we measured the abundance of ubiquinones of length 7 to 10 carbon units following treatment with RC-inhibitors (figure 4.3). The most abundant ubiquinone in humans is CoQ10, which is represented by its 400x higher concentration than the 7 and 8 carbon length molecules and 40x higher than CoQ9. The levels of CoQ10 were reduced when the mevalonate pathway was inhibited with atorvastatin and even further two-fold reduced in cells with impaired complex III. Interestingly the levels of CoQ10 were not changed following complex I or V inhibition, suggesting that the specific function of complex III plays a role in the abundance of CoQ10. The precursors CoQ7-9were also reduced following complex III impairment, showing that both supply and catabolism of ubiquinol were affected. Both complex I and complex V inhibited cells showed a similar pattern of changes, where CoQ7 was slightly elevated, CoQ8 slightly was reduced and CoQ9 was minorly affected.

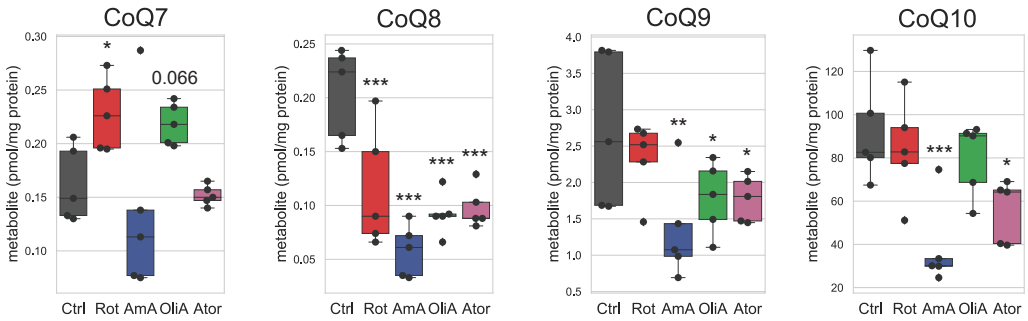

Figure 4.3 – **Inhibition of mitochondrial respiratory function varyingly affects ubiquinol levels.** (A) Boxplot showing absolute abundance various chain length ubiquinone metabolites following treatment with respiratory chain inhibitors or atorvastatin as indicated. Absolute amounts were normalised to total protein content for each sample individually. Significance calculated by fitting variables into a linear model and calculating influence of variable on outcome. * p<0.05, ** p<0.01, *** p<0.001. (CoQ; coenzyme Q; Ctrl, control conditions DMSO; Rot, 100 nM rotenone, AmA, 500 nM antimycin A; OliA, 1 µM oligomycin)

4.4 Sterol intermediates

The final part of the mevalonate pathway starts with the synthesis of squalene. This part, also called the sterol synthesis or post-squalene pathway, produces many sterol intermediates from two parallel pathways. Some sterol intermediates have a biological role beyond being a precursor in the synthesis of cholesterol, such as regulating the activity of upstream mevalonate pathway enzymes. In our models, the overall abundance of the cholesterol intermediates was lowered when the respiratory chain function was impaired (figure 4.4). The metabolites were lowered to comparable levels as atorvastatin, suggesting that the reduction was due to the impairment of the mevalonate pathway activity. The changes in the sterol intermediate abundance were not complex specific, as a similar reduction was observed in all models of respiratory chain dysfunction. Cells that had impaired complex III activity seemed to show a slightly more severe reduction in sterol precursor metabolite levels. This stronger effect observed after complex III inhibition is comparable to the transcriptional phenotype observed earlier (figure 3.1-D) hinting at a possible mechanistic connection between the degree of transcriptional responses and the severity of the effect on the sterol intermediates.

4.5 Conclusion

Overall, we observed altered levels of mevalonate pathway metabolites following the inhibition of respiratory chain complexes. Sterol precursors were downregulated in a general manner by respiratory chain inhibition. All affected complexes reduced sterol precursors to a similar level as the HMGCR-inhibitor atorvastatin. Complex III inhibition had a stronger reduction on

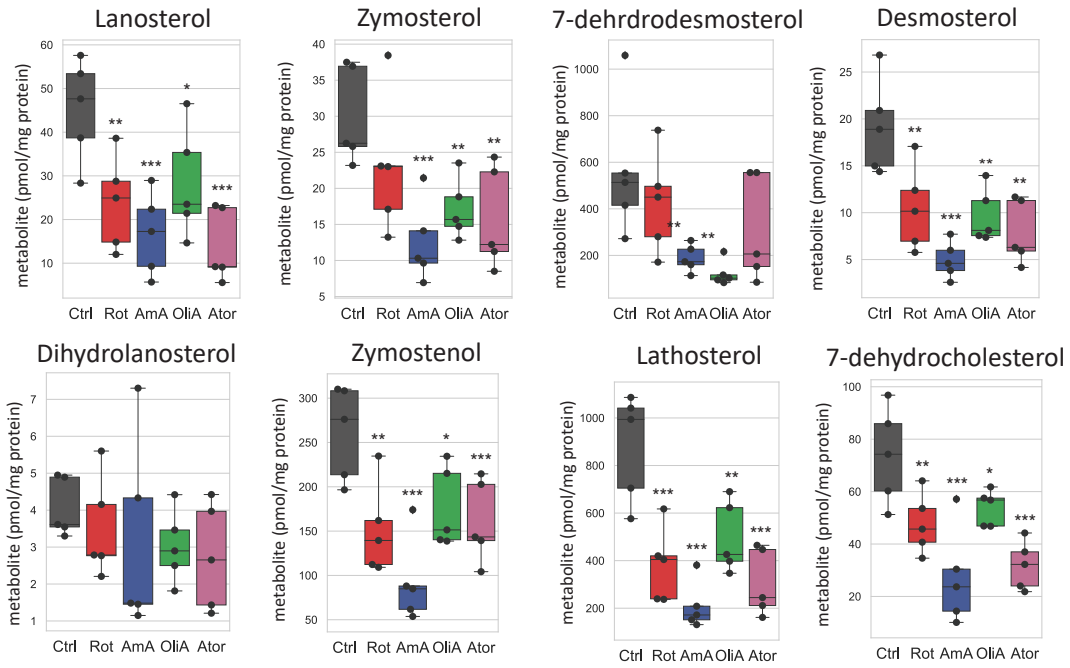

Figure 4.4 – **Inhibition of mitochondrial respiratory function affects cholesterol precursor metabolites in similar fashion.** (A) Boxplot showing absolute abundance cholesterol precursor metabolites following treatment with respiratory chain inhibitors or atorvastatin as indicated. Absolute amounts were normalised to total protein content for each sample individually. Significance calculated by fitting variables into a linear model and calculating the influence of the variable. * p<0.05, ** p<0.01, *** p<0.001. (Ctrl, control conditions DMSO; Rot, 100 nM rotenone, AmA, 500 nM antimycin A; OliA, 1 µM oligomycin)

the sterol precursors overall. The changes in the isoprenoid metabolite levels were differently affected depending on the complex affected, where complex III and V impairment lowered metabolite concentrations to levels comparable with atorvastatin. Complex I impairment behaved differently, overall showing no change or an increase. The most biologically relevant ubiquinone, CoQ10 was unaffected following complex I or V inhibition. Cells with impaired complex III showed a reduction of both CoQ10 and at the shorter chain precursors, suggesting both supply and catabolism of these metabolites was affected.

5 Genetic models of mitochondrial respiratory chain dysfunction

Pharmacological models of mitochondrial respiratory chain dysfunction have the advantage that the effect is reproducible due to the low inter-clonal or inter-patient variability often seen with other strategies of modelling mitochondria disease. However chemical impairment of respiratory chain complexes comes with its own dangers of not exactly mimicking the pathological mechanism of the in-vivo situation, due to the abrupt nature of the induced dysfunction. To validate the changes observed in the pharmacological model, we generated genetic models of mitochondrial dysfunction that more closely reflect the pathophysiological condition of mitochondrial disease patients. The respiratory dysfunction in these cellular models was created by knocking out individual subunits of complex I, impairing its function. We targeted two genes that encode different subunits of complex I: NADH:Ubiquinone Oxidoreductase Subunit S4 (NDUFS4) and subunit S6 (NDUFS6). Double stranded breaks were induced in three separate regions of the coding gene with the help of CRISPR-Cas9 technology. Successful edits were uncovered by sequencing the targeted regions of selected single cell derived clones and confirming deleterious mutations in the DNA (see Materials and Methods).

5.1 Validation of knockout models

For each targeted gene, 2 different monoclonal cell lines were selected with mutations in the targeted region, labelled A and B. Both cell lines failed to express the NDUFS4 or NDUFS6 protein subunit as demonstrated by Western blotting (figure 5.1-A), confirming a successful knockout. In cells lacking NDUFS4 expression, NDUFS6 was also reduced compared to the WT fibroblasts indicating that the maintenance of physiological levels of NDUFS6 requires the presence of NDUFS4. Disruption of the NDUFS6, however, did not affect protein levels of NDUFS4 compared to the control. To confirm that the absence of the protein subunit of complex I affected mitochondrial function we measured respiration in a Seahorse XF96 respirometer. Basal respiration was significantly reduced in all four knockout clones (figure 5.1-B, C). Cells lacking the NDUFS6 subunit suffered a stronger reduction of basal respiration. Acute addition of rotenone (100nM) caused a decrease of respiration in both control cells and knockout clones. This sensitivity to rotenone demonstrated that complex I remained partially

functional in agreement with earlier reports of a truncated form of complex I after loss of subunits (Iommarini et al., 2015). We calculated the complex I dependent respiration from the decrease in respiration after rotenone addition compared to baseline (figure 5.1-D). All clones retained residual complex I respiration, but it's contribution to the total respiration was significantly reduced. The NDUFS4 knockout clone B showed the least residual complex I respiration.

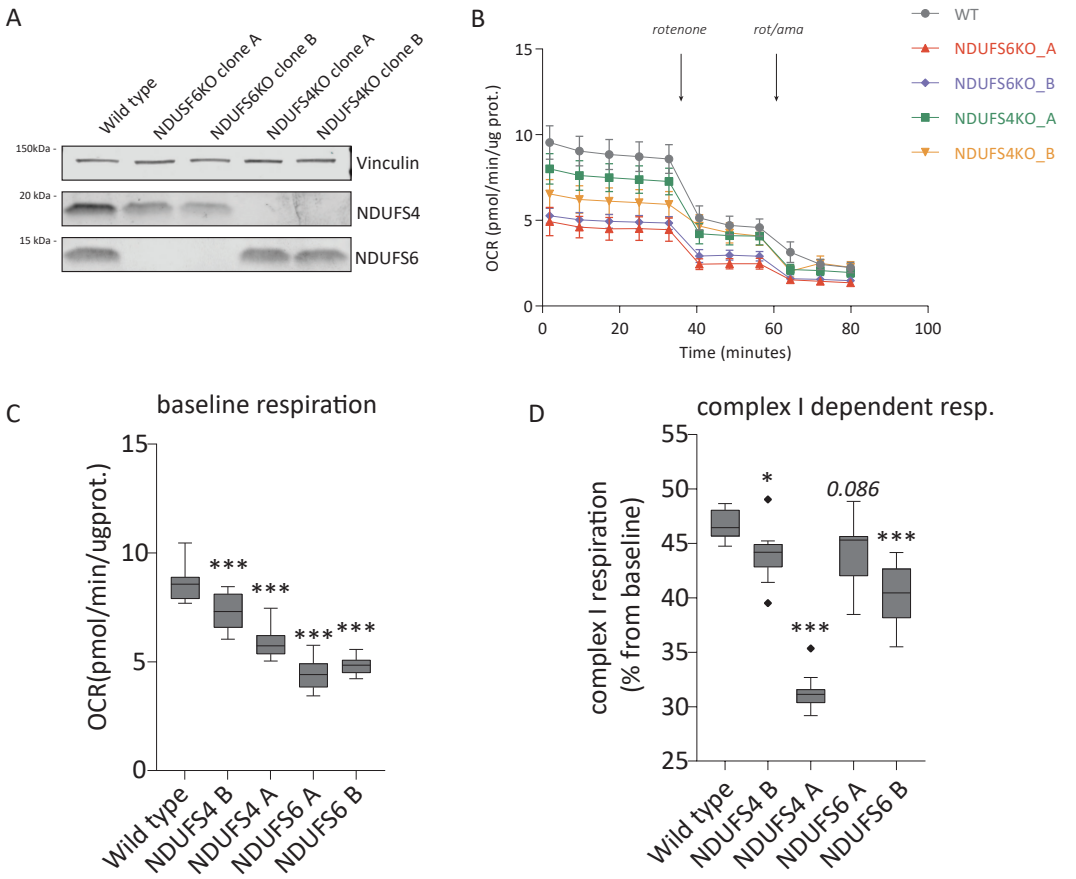

Figure 5.1 – **Knockout of complex I subunits impairs respiration.** (A) Westernblot of complex I subunits in cell lines genetically modified with CRISPR-Cas9 targeted to the subunits NDUFS4 or NDUFS6. (B) Cellular respiration of knockout cell lines measured by Seahorse XF96 oxygraph. Oxygen consumption expressed per unit of protein was calculated for each well. Rotenone to a concentration of 100 nM final or rotenone and antimycin A to al final concentration of 50 µM (rot/ama) were injected as indicated. Points indicate average measurement of 6-wells pooled. (C) Baseline respiration of complex I knockout-clones or control cell lines from (A). (D) Complex I dependent respiration of complex I knockout-clones or control cell lines from (A). Complex I dependent respiration was calculated as percentage difference between baseline and complex I inhibited respiration. Significance calculated by Dunnett's multiple comparisons test. * p<0.05, ** p<0.01, *** p<0.001.

5.2 Further characterisation of the genetic models

The differences in complex I subunit expression prompted the question if the other respiratory chain complexes were also differentially affected between the knockout clones. To study this, we measured the protein expression of key mitochondrial respiratory chain subunits I, II, III and V (figure 5.2-A). Complex IV was undetectable. The measured subunits are liable when not associated in a protein complex, thus the readout can be interpreted as a proxy for total complex levels. We observed the knockout clone NDUFS6-A had a much higher expression of complex II and I compared to the other clones. Clones NDUFS4-A and NDUFS4-B also showed a slight increase of complex I compared to control, however no increase of complex II could be observed. None of the clones showed an increase in the levels of complex III or V. These changes in complex I and II levels suggest that the knockout of a subunit of complex I activates retrograde signalling pathways that induce synthesis of specific complexes to compensate for the respiratory impairment. The differences between clones however showed there is clonal specific variation in the responses.

To further investigate the phenotypical consequences of the complex I impairment, we measured the maximal growth rate of the clones and compared this to control (figure 5.2-B). We observed that the knockout of a complex I subunit lowers cellular proliferation rates compared to the control cell line in all the affected clones. Overall, the knockout clones all show a similar reduction in proliferation rates, with the exception of the knockout clone NDUFS4 B, which has a slightly lower rate than the other clones. This same clone showed the lowest residual complex I activity of all knockout clones, making it tempting to associate the lower proliferation rate of the NDUFS4 clone B to the lowered complex I activity.

5.3 Expression of mevalonate pathway genes

Having characterised the effect of knocking out a complex I subunit on mitochondrial function, we questioned if the mevalonate pathway transcripts were affected similarly as the pharmacological models of mitochondrial dysfunction (figure 3.2). To answer this, we tested the expression of key mevalonate pathway genes by qPCR and compared these to control (figure 5.3). The expression of ACAT2, HMGC, HMGCS1, SQLE and DHCR7 tended to be lower in the complex I knockout clones but due to the slight amplitude of the effect and the large variation in expression most changes did not reach significance. The transcripts of ACAT2 were significantly reduced all the knockout clones, where the clone NDUFS4-B showed the most pronounced effect. In both the expression levels of HMGCR and HMGCS1 only the NDUFS4 clone B reached significance, due to the larger effect observed. The expression of SQLE was only significantly lower in NDUFS6-B. Ongoing additional experiments will verify this with statistical significance.

Interestingly, we observed a correlation between the severity of the complex I dysfunction, growth rate and expression of mevalonate pathway genes. The clone NDUFS4-B showed

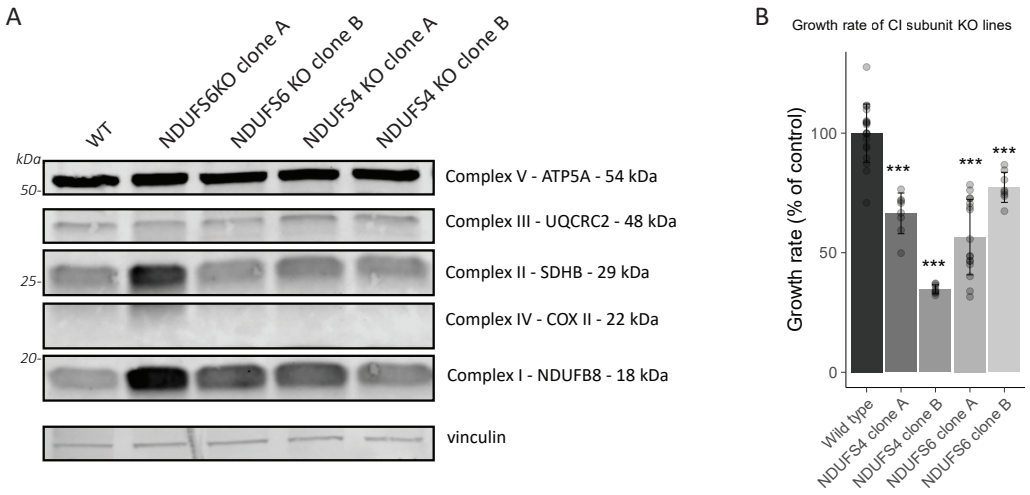

Figure 5.2 – **Knockout of complex I subunits changes respiratory complex expression and growth rates.** (A) Western blot of mitochondrial respiratory chain complexes in complex I knockout clones. Cells were cultured in normal media for 48 hours before protein lysate was collected. (B) Maximal growth rate of complex I knockout clones. Growth rates were measured in an Incucyte ZOOM live-cell analysis system. Maximal growth rates in the exponential phase were calculated with the Growthcurver package in R and expression as % of control. Bars indicate means ± standard deviation, individual points indicate individual wells. N = 12 from 2 individual experiments. Significance calculated with ANOVA followed by a Tukey's HSD post-hoc test. (WT, wild-type; ATP5A, ATP synthase lipid-binding protein; UQCRC2, Ubiquinol-Cytochrome C Reductase Core Protein 2; SDHB, Succinate Dehydrogenase Complex Iron Sulfur Subunit B; COXII, Cytochrome c oxidase subunit 2; NDUFB8, NADH:Ubiquinone Oxidoreductase Subunit B8)

the lowest residual complex I activity (figure 5.1-C), alongside the lowest amount of complex I protein (figure 5.2-A). This clone also showed the lowest proliferation rate and the most pronounced effects on transcripts involved in cholesterol biosynthesis (figure 5.3-A). The baseline respiration of this clone however, was not markedly different from the other clones. This suggests that not just impairing mitochondrial respiration, but specifically residual complex activity is involved in the transcriptional responses to cholesterol management.

5.4 Conclusion

Overall, there is a trend for reduced expression of mevalonate pathway genes in cells lacking the subunit of complex I, however this only reached significance in clones with the most severe impairment on complex I activity. The downregulation of mevalonate pathway transcripts thus occurs in both chemical and genetic models of mitochondrial dysfunction, providing evidence that this effect is in fact an adaptive response to mitochondrial respiratory chain dysfunction. A correlation could be observed between the residual complex I activity, a reduction in proliferation rates and the reduction in gene expression of mevalonate pathway

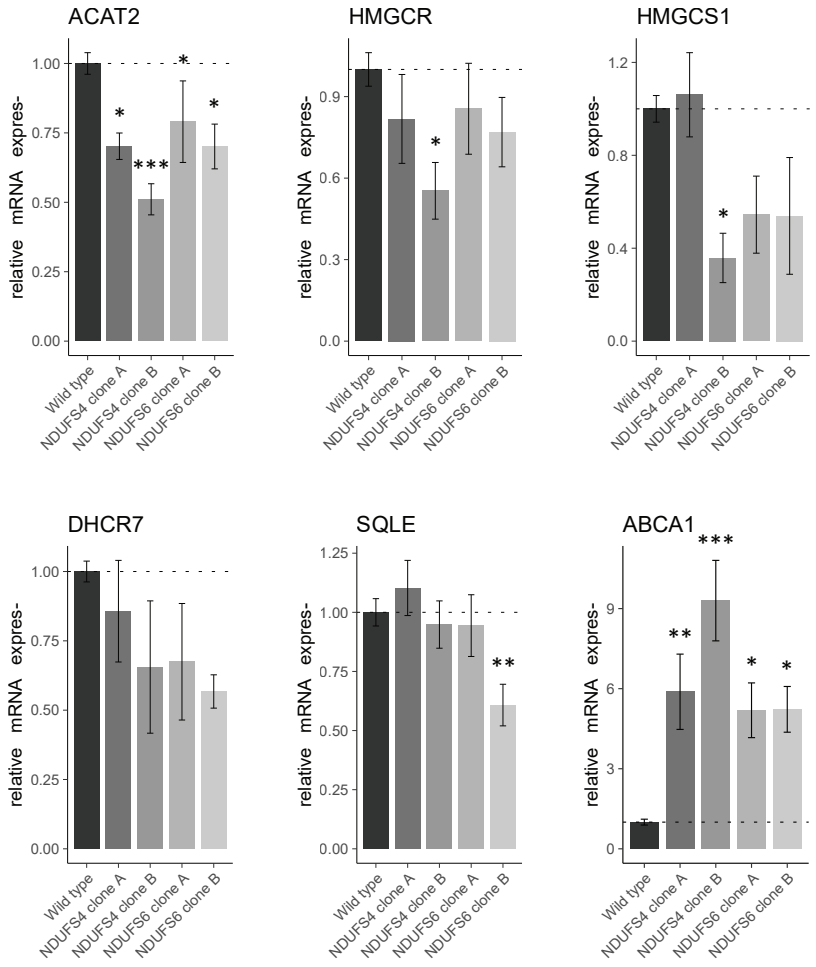

Figure 5.3 – **Knockout of complex I subunits lowers expression of cholesterol biosynthesis genes.** (A) Relative mRNA expression of mevalonate pathway transcripts in complex I knockout clones measured by qPCR. Expressed as relative expression compared to control. Expression levels were normalised to housekeeping genes (see materials and methods). Bars indicated mean of three independent experiments ± standard deviation. Significant differences were calculated by multiple t-tests with bonferonni multiple testing correction. * p<0.05, ** p<0.01, *** p<0.001.

transcripts, suggesting a mechanistic link. The difference between the genetic models and pharmacological models can be attributed to differences in residual complex activity between the two models. Pharmacologically inhibiting complex I near-completely impairs the functioning of the complex, while the knockout of a subunit has been proven to still leave a rotenone-sensitive form of complex I intact that retains metabolic capabilities. This difference in residual complex activity again reflects the degree of reduction of mevalonate pathway transcripts.

6 Investigation of upstream signalling pathways

Inhibition of the respiratory chain complexes leads to a pronounced downregulation of mevalonate pathway transcripts and leads to a change in mevalonate pathway metabolite levels. Following this discovery, we were interested in uncovering the main factors originating from the respiratory chain defect and triggering the observed transcriptional downregulation of mevalonate pathway genes. To investigate this, we studied a selection of pathways that are well-known to be activated by mitochondrial retrograde signals and play a vital role in cellular metabolism. Specifically, we will focus on dissecting the mechanism following complex I deficiency as this is the most common form of respiratory chain disease in humans.

6.1 Integrated stress response

A well-known pathway that is activated by mitochondrial dysfunction is the Integrated Stress Response (ISR). This pathway has been shown to orchestrate pro-survival pathways in response to mitochondrial dysfunction (see introduction 1.3.1). In the transcriptomic analysis of the pharmacological models of mitochondrial dysfunction we observed an enrichment of stress pathways (figure 3.2-A). We hypothesised that the ISR could be involved in the observed downregulation of the mevalonate pathway transcripts as a response to cellular stress as earlier studies identified a link between activation of this pathway and the regulation of cholesterol homeostasis (Fusakio et al., 2016).

To investigate this, we treated primary human fibroblasts with rotenone and measured the expression of key downstream transcripts of the ISR pathway (figure 6.1-A). Inhibiting of complex I induced a marked increase in all transcripts, confirming the activation of the ISR in our models of mitochondrial RC dysfunction. To interfere with the ISR signalling we treated cells with an ISR-inhibitor (ISRIB), which blocks the ISR at the level of the eukaryotic Initiation Factor 2 impairing expression of all downstream targets. Treatment with this inhibitor alone supressed levels of ATF4, ATF3 and CHOP transcripts to below baseline levels (figure 6.1-A). Cells that were treated with both compounds showed a decrease in ATF4 transcripts to near baseline, confirming the ISR is near completely inhibited. The other stress markers ATF3

and CHOP were also reduced, however residual expression remained as these transcripts are also activated by other stress pathways such as the mitochondrial unfolded protein response (UPRmito). The ISRIB compound alone did not significantly affect the transcript levels of the mevalonate pathway enzymes ACAT2, HMGCR or SQLE (figure 6.1-B). A minor trend is visible for HMGCR, albeit not significant. As observed earlier rotenone decreased the levels of mevalonate pathway the transcripts. When cells were treated with a combination of rotenone and ISRIB there was no change in the decrease of mevalonate pathway transcripts. This demonstrated that the induction of the ISR is not responsible for the observed transcriptional suppression of the mevalonate pathway.

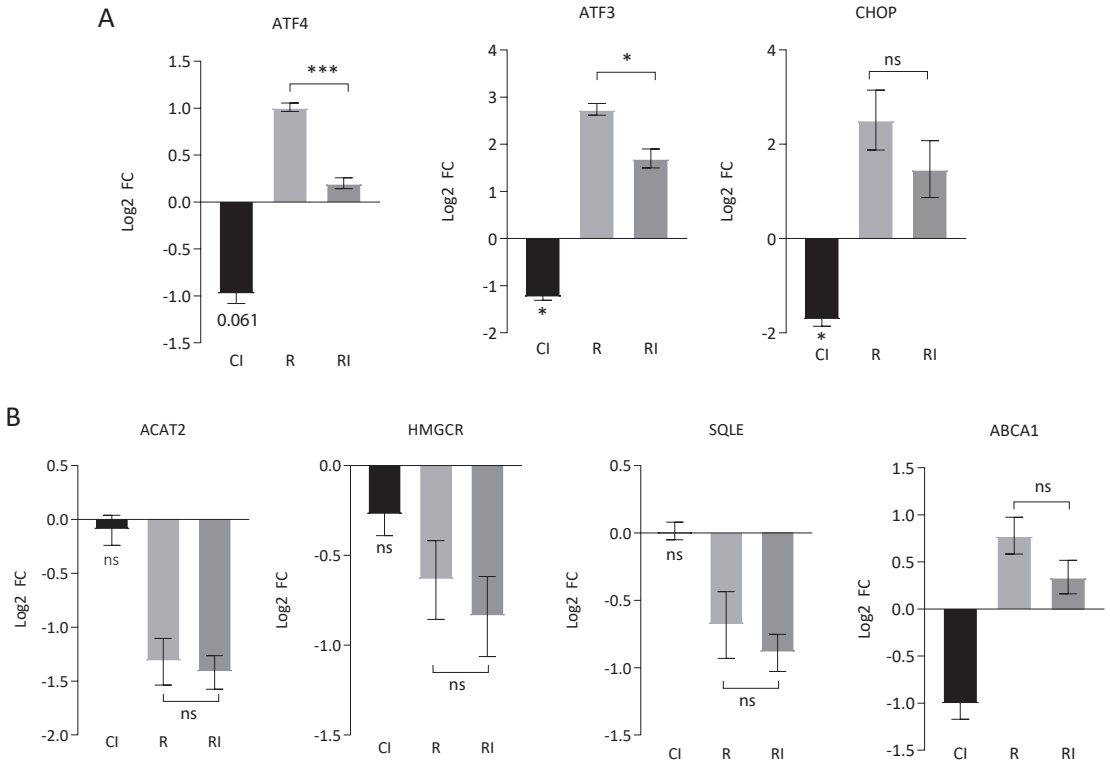

Figure 6.1 – **Inhibiting the ISR has no effect on mevalonate pathway transcripts.** (A) Relative mRNA expression of stress related genes following treatment with 500 nM ISRIB (CI, black bars), 100 nM rotenone (R, light grey bars) or both (RI, dark grey bars) in primary fibroblasts as measured by qPCR. Data shown are log2 fold-change from DMSO, normalised to housekeeping genes. Bars indicate mean of three independent experiments ± standard deviation. (B) Relative mRNA expression of mevalonate pathway genes in cells treated as in A. Bars indicate mean of three independent experiments ± standard deviation. Significance calculated by unpaired t-test. * p<0.05, ** p<0.01, *** p<0.001. (ATF4, Activating Transcription Factor 4; ATF3, Activating Transcription Factor 3; CHOP, C/EBP Homologous Protein; ACAT2, Acetyl-CoA Acetyltransferase 2; HMGCR, 3-Hydroxy-3-Methylglutaryl-CoA Reductase; SQLE, Squalene Epoxidase; ABCA1, ATP Binding Cassette Subfamily A Member 1)

6.2 AMPK

Another well-described retrograde signalling pathway is the activation of AMP-activated protein kinase (AMPK) by the reduced capacity of the mitochondria to produce ATP. AMPK functions to correct energy balance by supressing energy consuming reactions, while stimulating ATP producing processes. To investigate the role of AMPK in the suppression of mevalonate pathway transcripts, we treated primary human fibroblasts with compounds that prevent (compound C) or stimulate (991) the activation of AMPK. These compounds successfully increased or decreased the levels of phosphorylation of AMPK and it's downstream substrate acetyl-CoA carboxylase (ACC) (figure 6.2-A). Cells treated with rotenone showed a slight increase in ACC phosphorylation, indicative of energy stress. When compound C or 991 are added in combination with rotenone, the phosphorylation of AMPK and ACC proteins was relatively decreased or increased.

We then measured the effect of these activation levels on the expression of the mevalonate pathway transcripts ACAT2, HMGCR and SQLE. Inhibition of AMPK by compound C strongly induced the expression of ACAT2, HMGCR and SQLE (figure 6.2-D) which is in line with earlier reports (Li et al., 2011). Activation of AMPK with 991 however did not lower the levels of these transcripts compared to control, suggesting AMPK activation alone is not sufficient to decrease expression of these transcripts. Inhibiting complex I with rotenone reduced the expression of mevalonate pathway transcripts as expected. Cotreatment with rotenone and compound C produced an intermediate phenotype, lowering the expression compared to compound C alone, even though there was a no activation of AMPK visible. This suggests that the lowering of transcripts was not due to a significant increase of AMPK activation. When the activation of AMPK was further stimulated by coincubation with rotenone and 991, there was no significant effects on the expression of transcripts. It seems that inhibition of AMPK by compound C has an inducive effect on the transcripts measured and addition of rotenone attenuates this induction, however independently of AMPK phosphorylation levels.

To strengthen the hypothesis that the mechanism is AMPK independent, we measured the effect of rotenone treatment on mouse embryonic fibroblasts (MEFs) lacking both isoforms of the AMPK-α subunit (AMPK-null). This cell line lacks functional AMPK and shows an incomplete ability to activate AMPK and phosphorylate the downstream substrate ACC (figure 6.2-C). The control MEFs displayed a similar reduction in mevalonate pathway transcripts following rotenone treatment (figure 6.2-C), suggesting the mechanism is conserved in other mammals . Furthermore, rotenone showed a similar reduction in transcripts in absence of AMPK, confirming the mechanism of suppression is AMPK independent in both human and mouse fibroblasts.

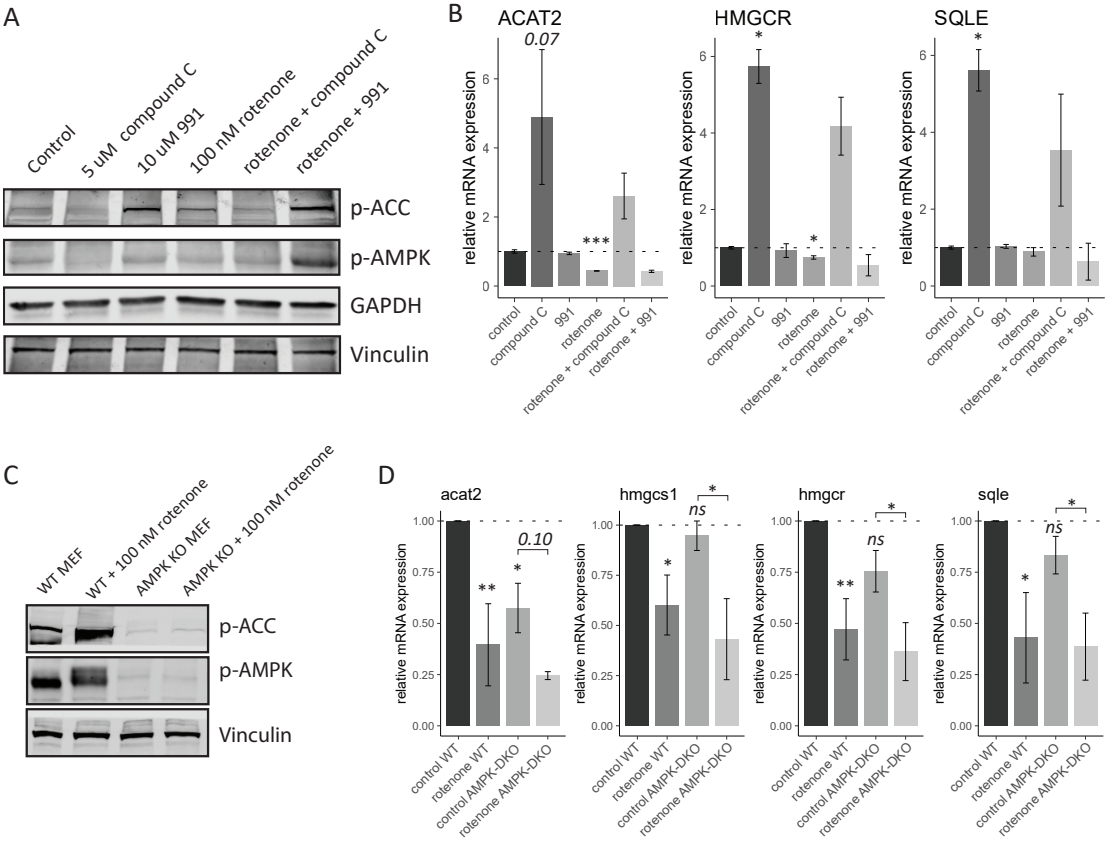

Figure 6.2 – **Downregulation of mevalonate pathway transcripts is not dependent on AMPK.** (A) Western blot showing AMPK activation and it's downstream target ACC following treatment with 5 µM compound C, 10 µM 991, 100 nM rotenone or a combination for 24 hours in primary human fibroblasts. (B) Relative mRNA expression of mevalonate pathway genes following treatment as in A measured by qPCR. Data shown as relative mRNA expression from DMSO, normalised to housekeeping genes. (C) Western blot showing AMPK activation and it's downstream target ACC following treatment with 100 nM rotenone or empty vehicle for 24 hours in wild-type (WT) or AMPK-α double knockout (AMPK KO) mouse embryonal fibroblasts (MEFs). (D) Relative mRNA expression of mevalonate pathway genes following treatment as in C. Data shown as relative mRNA expression from DMSO, normalised to housekeeping genes. (B,D) Bars indicate mean of three independent experiments ± standard deviation. Significance was calculated with a students t-test, followed by Benjamini-Hochberg correction. * p<0.05, ** p<0.01, *** p<0.001. (ACAT2, Acetyl-CoA Acetyltransferase 2; HMGCS1, 3-Hydroxy-3-Methylglutaryl-CoA Synthase 1; HMGCR, 3-Hydroxy-3-Methylglutaryl-CoA Reductase; SQLE, Squalene Epoxidase)

6.3 mTOR

Another highly conserved pathway which has been suggested to play a role in mitochondrial dysfunction is the mechanistic target of rapamycin (mTOR). Activation of this pathway by an abundance of nutrients stimulates anabolic pathways and the biogenesis of intracellular

components. Treatment of primary human fibroblasts with rotenone slightly increased the phosphorylation of mTOR and its downstream targets: ribosomal protein S6 (S6) and p70 S6 kinase (p70S6K) (figure 6.3-A). The drug rapamycin is an effective inhibitor of the mTOR pathway and even concentrations in the nM range fully supressed the activation observed with rotenone. To investigate if the activation of mTOR is linked to the expression mevalonate pathway transcripts, we measured the effects of inhibiting mTOR in control and in rotenone treated conditions. Inhibition of mTOR cells had a slight tendency to decrease the expression ACAT2 and HMGCR, however these changes were not significant (figure 6.3-B). Treatment with rotenone, again suppressed the mevalonate pathway transcripts as observed earlier. Cotreatment with rotenone and rapamycin did not affect the suppression following complex I inhibition, clearly demonstrating that activation of mTOR is not the driving mechanism supressing mevalonate pathway transcripts during complex I impairment.

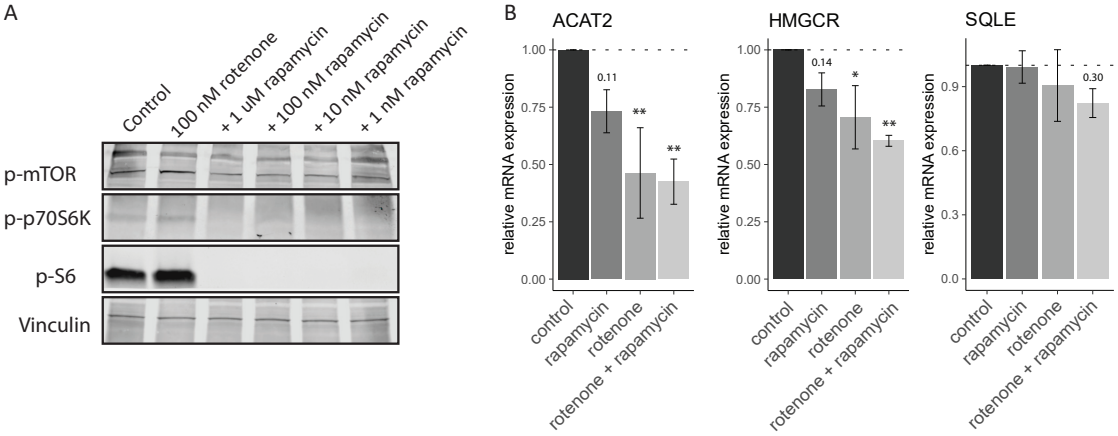

Figure 6.3 – **Downregulation of mevalonate pathway transcripts is not dependent on mTOR activation.** (A) Western blot showing mTOR activation and its downstream targets p70S6K and S6 following treatment with empty vehicle (DMSO), 100 nM rotenone or indicated concentrations of rapamycin for 24 hours in primary human fibroblasts. (B) Relative mRNA expression of mevalonate pathway genes following treatment with empty vehicle (DMSO), 1 nM rapamycin, 100 nM rotenone or both in primary human fibroblasts. Data shown as relative mRNA expression from DMSO, normalised to housekeeping genes. Bars indicate mean of three independent experiments ± standard deviation. Significance was calculated with a students t-test, followed by Benjamini-Hochberg correction. * p<0.05, ** p<0.01, *** p<0.001. (ACAT2, Acetyl-CoA Acetyltransferase 2; HMGCR, 3-Hydroxy-3-Methylglutaryl-CoA Reductase; SQLE, Squalene Epoxidase)

6.4 Conclusion

Although the whole extent of mitochondrial retrograde signalling is still not completely uncovered, the activation of the ISR, AMPK and mTOR pathways have been well documented to affect cellular homeostasis in response to mitochondrial dysfunction. In the above chapter we investigated if these well-known pathways were related to our phenotype of mevalonate

pathway suppression after mitochondrial respiratory chain dysfunction. Here we provided evidence that the ISR, AMPK and mTOR pathway are activated in our models of mitochondrial dysfunction. Interrupting the signalling of these pathways under conditions of complex I dysfunction did not affect the observed downregulation of mevalonate pathway transcripts providing evidence that the transcriptional suppression is due to a yet unknown mechanism.

7 Characterisation of cholesterol signalling

For the remainder of this study, we focused uncovering the molecular mechanisms that instigated the coordinated transcriptional downregulation of mevalonate pathway genes. In the earlier work we focussed on investigating the signals that have been known to arise from mitochondrial dysfunction. Studies of the well-known pathways of mitochondrial retrograde signalling did not provide mechanistic answers on the signals that originate from the mitochondria to downregulate the mevalonate pathway transcripts. To continue the investigation, we changed perspective and instead focussed on the how the transcripts themselves are transcriptionally regulated and attempted to dissect the mechanism from this angle.

7.1 Changes in SREBP2 activation

The expression of mevalonate pathway genes is under the control of a family of transcription factors called Sterol regulatory-element binding proteins (SREBPs) (see introduction 1.4.4). These ER-bound transcription factors sense the concentration of ER-membrane cholesterol and under conditions of depleted cholesterol are activated and initiate transcription of transcripts regulating cholesterol biosynthesis. We questioned whether the difference in transcripts was due to dysregulation in SREBP2 signalling. To study this, we measured the degree of cleavage of the SREBP2 protein by western blot. To stimulate the cleavage of SREBP2 we cultured cells in media that was devoid of lipoproteins and sterols that was supplemented with 1 μM atorvastatin (see 13). We measured the degree of activation over a period ranging from 8 hours to 2 days to see if there was any time dependent effect on SREBP2 proteolytic activation.

Cells that were cultured in these lipid deficient conditions showed a strong increase in the cleaved fragment of SREBP2 (figure 7.1-A, B), showing our culture conditions truly depleted intracellular cholesterol and our cells were able to normally respond to low levels of intracellular sterols. Placing cells in sterol-free culture conditions slightly induced SREBP2 cleavage after 8 hours and gradually increased the cleavage as the intracellular cholesterol pools were depleted. Inhibition of complex I with rotenone clearly reduced the amount of cleaved SREBP2 in the

low lipid conditions. We suspected rotenone also reduces the amount of cleaved SREBP2 in normal lipid conditions, but the baseline expression of the proteins was too low to accurately measure this. It can be observed that rotenone supressed SREBP2 cleavage from the earliest timepoint and the cells were unable to induce SREBP2 cleavage over time in response to the low lipid culture conditions.

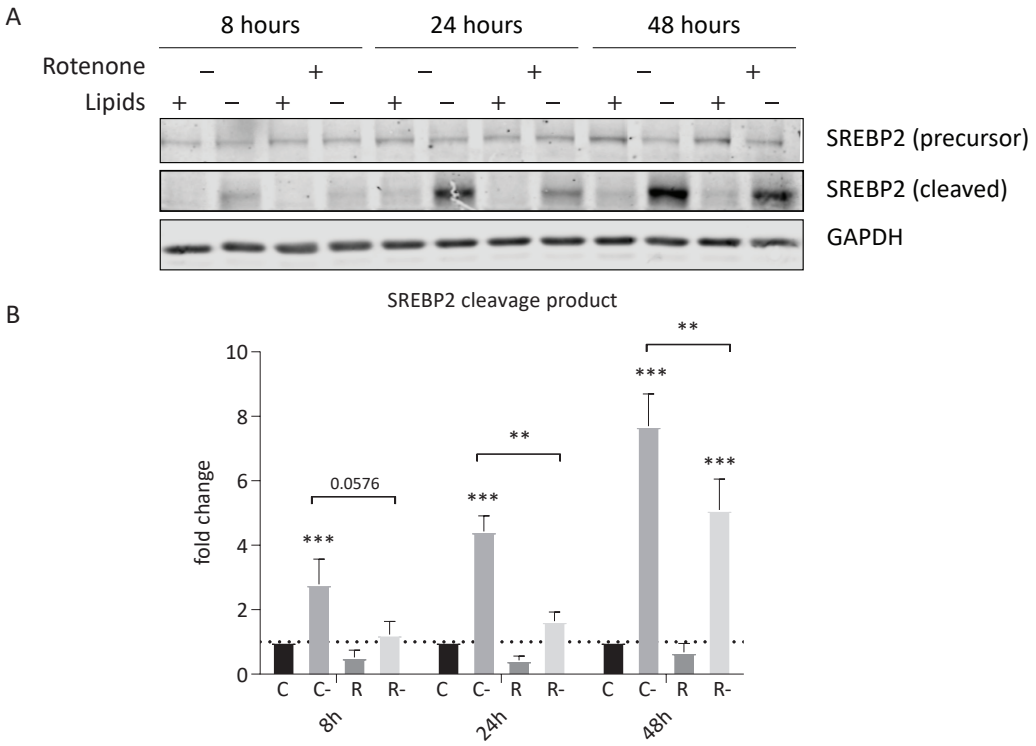

Figure 7.1 – **Rotenone impairs normal SREBP2 activation in low-lipid conditions.** (A) Western blot showing SREBP2 precursor and activated SREBP2 cleavage product following culture in normal or lipid free conditions (see materials and methods) supplemented with empty vehicle (DMSO) or 100 nM rotenone in primary human fibroblasts. Cells were treated for the times indicated. (B) Quantification of A. Data shown as fold change from control. Bars indicate mean of three independent experiments ± standard deviation. Bars indicate mean of three independent experiments ± standard deviation. Significance was calculated with a students t-test, followed by Benjamini-Hochberg correction. * p<0.05, ** p<0.01, *** p<0.001. (SREBP2; Sterol Regulatory Element-Binding Protein 2)

To put the degree of SREBP2 activation in lipid deficient culture conditions into context of our earlier findings, we measured the expression of mevalonate pathway transcripts regulated by SREBP2 in the various lipid conditions (figure 7.2). We observed that in low-lipid conditions the cleavage of SREBP2 activated the transcription of the downstream targets, as expected. Treatment with rotenone again lowered the expression of transcripts, as shown previously. Inhibiting complex I in cells cultured in low-lipid conditions showed an increased expression of the measured transcripts compared to normal lipid conditions, albeit lower than the low-lipid conditions without complex I inhibition. This degree of expression is identical to the

degree of SREBP2 protein cleavage shown earlier, linking the levels of SREBP2 cleavage product to the expression of transcripts. This also shows that complex I inhibition reduces mevalonate pathway transcripts through the suppression of SREBP2 processing and that the residual cleaved SREBP2 protein can normally translocate to the nucleus to initiate transcription of target genes.

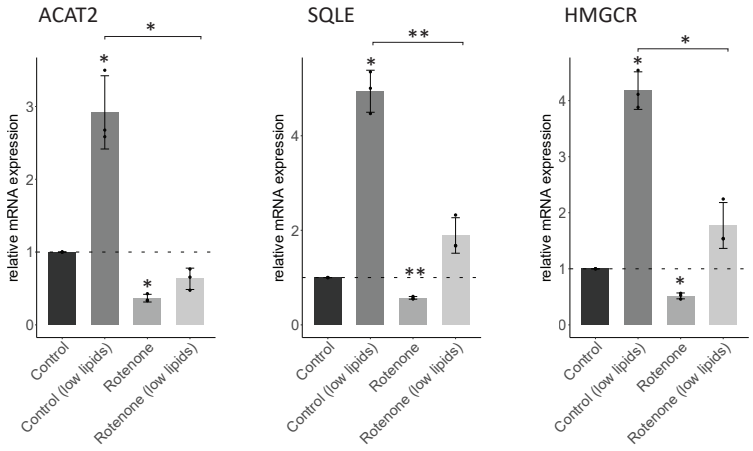

Figure 7.2 – **Rotenone impairs normal mevalonate pathway gene expression in low-lipid conditions.** Relative mRNA expression of mevalonate pathway genes following treatment as in A for 24 hours in primary human fibroblasts measured by qPCR. Data shown as relative mRNA expression from DMSO, normalised to housekeeping genes. Bars indicate mean of three independent experiments ± standard deviation. Significance was calculated with a students t-test, followed by Benjamini-Hochberg correction. * p<0.05, ** p<0.01, *** p<0.001. (ACAT2, Acetyl-CoA Acetyltransferase 2; HMGCR, 3-Hydroxy-3-Methylglutaryl-CoA Reductase; SQLE, Squalene Epoxidase)

7.2 Adaptations to rapid cholesterol changes

The activation of SREBP2 is a complex process with many proteins involved that closely regulate its activation in response to changes in sterol levels. To determine if the cholesterol sensing capabilities of SREBP2 were still intact in conditions of complex I inhibition, we manipulated the levels of intracellular cholesterol with cyclodextrins. Empty cyclodextrins rapidly deplete cellular cholesterol and inversely when these molecules are pre-loaded with cholesterol, they rapidly increase the levels of intracellular cholesterol. To see these rapid effects on SREBP2 processing, we treated cells with a combination of either rotenone or vehicle control together with a short duration of empty or loaded cyclodextrins.

Manipulating cellular cholesterol with cyclodextrins rapidly supressed or induced the levels of SREBP2 cleavage for the loaded or empty cyclodextrins, respectively (figure 7.3-A). In cells treated with loaded cyclodextrins, all SREBP2 was in its precursor form. The protein abundance of the precursor is in such conditions thus an indication of total SREBP2. Inhibiting

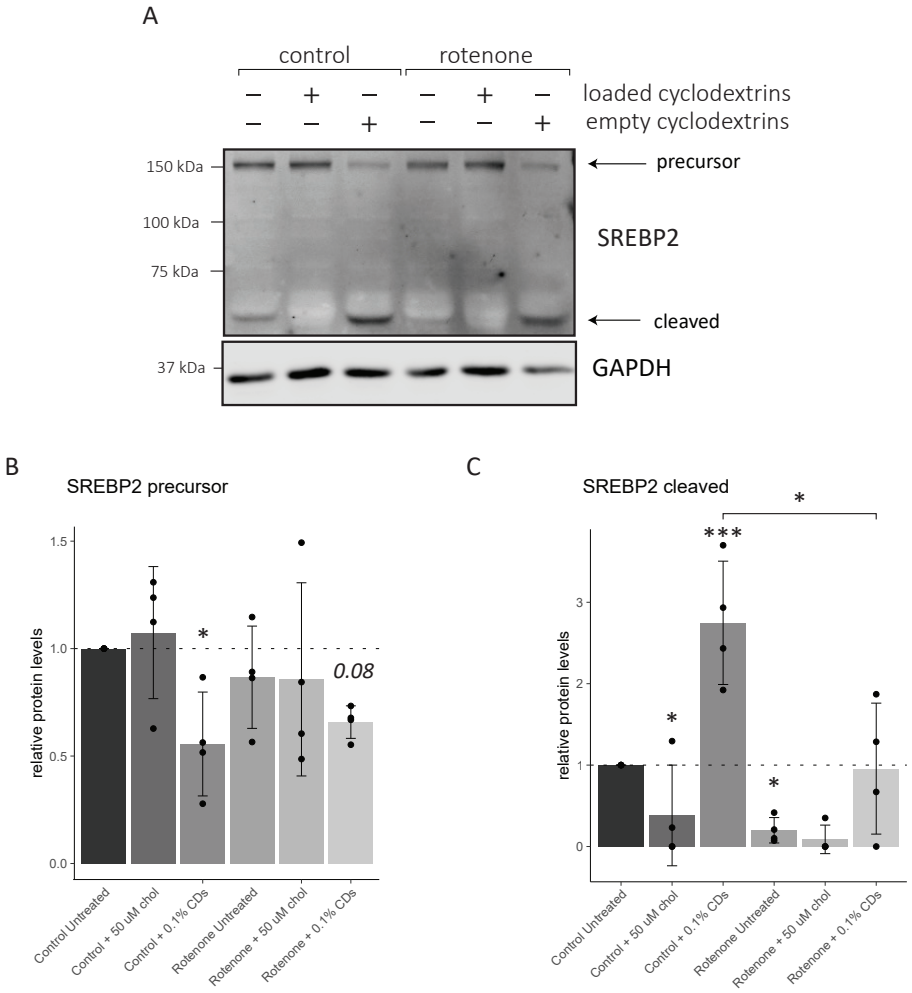

Figure 7.3 – **Complex I inhibition blunts maximal response of SREBP2 to lipid depletion.** (A) Western blot showing SREBP2 precursor and activated SREBP2 cleavage product following culture in lipid free conditions (see materials and methods) for 48 hours supplemented with empty cyclodextrins or loaded cyclodextrins for 30 mins before collection of protein lysate in primary human fibroblasts. GAPDH was used as loading control. (B) Quantification of the SREBP2 precursor protein in A. Data shown as relative protein levels from DMSO treated control. Bars indicate mean of 4 independent experiments ± standard deviation. Significance was calculated with a students t-test, followed by Benjamini-Hochberg correction. * p<0.05, ** p<0.01, *** p<0.001. (C) Quantification of the SREBP2 cleaved protein in A. Data as in B.

complex I had no marked effect on the levels of precursor protein in cells treated with loaded cyclodextrins, suggesting that the amount of total SREBP2 was unchanged (figure 7.3-B). However, technical limitations and biological variability make the determination difficult. In cells treated with empty cyclodextrins, the protein abundance of the cleaved fraction is a marker for the maximal activation. Cells that had impaired complex I function could not reach

the same maximal level of activation (figure 7.3-C). This difference could either be due to an insensitivity to the depletion of cholesterol or a local increase of ER-cholesterol due to the mitochondrial respiratory chain dysfunction. This indicates that the response of SREBP2 to increased levels of cholesterol remains unchanged, but the response to lowering of cholesterol is somehow blunted.

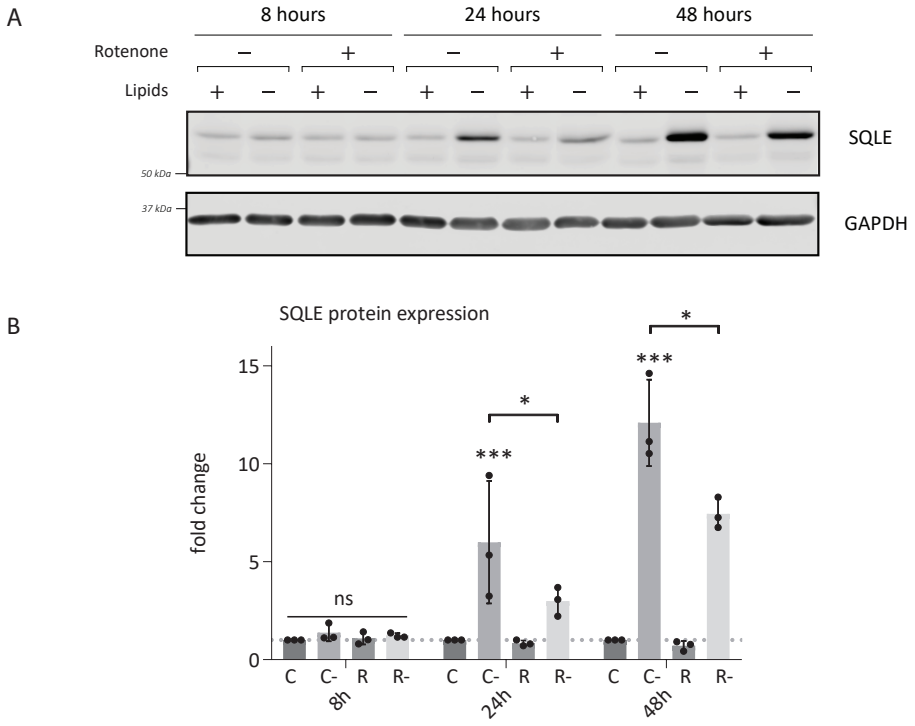

Figure 7.4 – **Complex I impairment reduces induced SQLE accumulation.** (A) Western blot showing SQLE protein following culture in normal or lipid free conditions (see materials and methods) supplemented with empty vehicle (DMSO) or 100 nM rotenone in primary human fibroblasts. Cells were treated for the times indicated. (B) Quantification of A. Data shown as fold change from control. Bars indicate mean of three independent experiments ± standard deviation, black points indicate individual replicates. Significance was calculated with a students t-test, followed by Benjamini-Hochberg correction. * p<0.05, ** p<0.01, *** p<0.001. (SQLE, Squalene Epoxidase; GAPDH, glyceraldehyde 3-phosphate dehydrogenase; C, control conditions; C-, lipid free control conditions; R, 100 nM rotenone; R-, lipid-free 100 nM rotenone)

7.3 Cholesterol sensing enzymes on ER membrane

The reduced activation of SREBP2 may be explained by a reduced sensitivity of SREBP2 to cholesterol or by an increase of cholesterol on the ER-membrane. Multiple enzymes on the ER membrane react to changes in ER-membrane cholesterol through specialised sterol sensing

domains, such as the enzymes SQLE and HMGCR. When excess cholesterol binds to these proteins, they are rapidly ubiquitinated and degraded. Conversely they are stabilised by lower abundance of sterols (see introduction chapter 1.4.4). If the earlier observed inability of SREBP2 to activate fully is a response to changes in cholesterol levels, we hypothesised that other ER-bound cholesterol sensors would likely also be affected. To investigate this, we measured the abundance of SQLE and HMGCR in various lipid conditions by Western Blot. As in earlier experiments we measured the abundance of these proteins from 8 hours to 2 days to see time dependent changes.

We observed that low-lipid culture conditions indeed increases the abundance of SQLE (figure 7.4-A, B), confirming its sensitivity to intracellular cholesterol changes. This protein is stabilised in a time dependent manner, with noticeable changes after 24 hours. Inhibiting complex I reduced the abundance of SQLE in the low-lipid culture conditions in a similar fashion to the SREBP2 protein, with a significant decrease measurable after 24 hours

The protein HMGCR showed a similar pattern of abundance (figure 7.5-A, B), with seemingly a relative decrease after 24 hours, but only a measurable significant decrease after 48 hours due to technical limitations. For both proteins is it supposed that rotenone has analogous effects in the normal lipid conditions, but the low protein abundance under normal lipid conditions, observed in the figures as displaying faint bands, made difficult to confirm the reduced expression of both proteins in presence of rotenone. Together our results show that several cholesterol sensors residing on the ER are unable to induce a normal response to lower levels of cholesterol, similar to the effects observed with SREBP2. This extends the effects of complex I inhibition beyond SREBP2 to other cholesterol sensors on the ER.

7.4 Conclusion

The transcription factors SREBP2 is an important transcription factor in cholesterol homeostasis, driving the transcription of enzymes in the mevalonate pathway. In our models we can see that fibroblasts have normally functioning SREBP2, and this protein is cleaved in response to the lowering of intracellular sterols. Inhibition of complex I reduces the activation SREBP2 in response to lowering of intracellular sterols. It is suspected complex I inhibition also lowers SREBP2 activation under normal lipid conditions. The gene expression of the mevalonate transcripts closely mirrors the degree of activation, indicating that there is no defect in the nuclear translocation of the cleaved fragment, and its transcriptional activity remains intact. The cholesterol sensing enzymes SQLE and HMGCR were also degraded following complex I inhibition, confirming that the suppression was at the level of the ER-membrane. Overall, this shows that respiratory chain inhibition affects multiple cholesterol sensing molecules on the ER, inhibiting the processing of SREBP2 and lowering the abundance of SQLE and HMGCR.

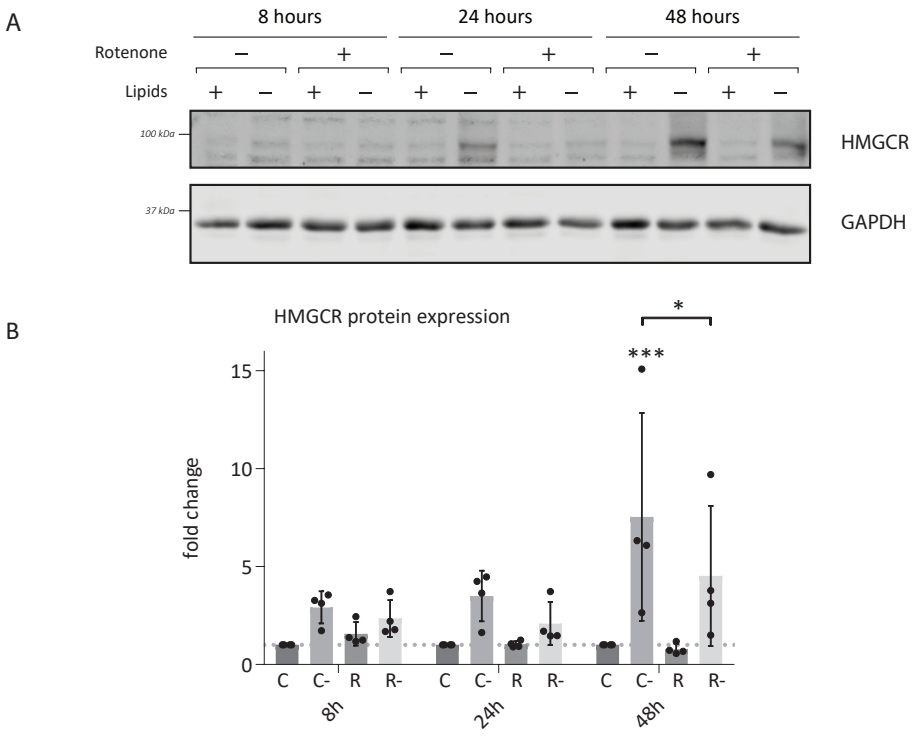

Figure 7.5 – **Complex I impairment reduces induced HMGCR accumulation.** (A) Western blot showing HMGCR protein following culture in normal or lipid free conditions (see materials and methods) supplemented with empty vehicle (DMSO) or 100 nM rotenone in primary human fibroblasts. Cells were treated for the times indicated. (B) Quantification of A. Data shown as fold change from control. Bars indicate mean of three independent experiments ± standard deviation, black points indicate individual replicates. Significance was calculated with a students t-test, followed by Benjamini-Hochberg correction. * p<0.05, ** p<0.01, *** p<0.001. (HMGCR, 3-Hydroxy-3-Methylglutaryl-CoA Reductase; GAPDH, glyceraldehyde 3-phosphate dehydrogenase; C, control conditions; C-, lipid free control conditions; R, 100 nM rotenone; R-, lipid-free 100 nM rotenone)

8 Intracellular cholesterol levels

The previous chapters established a clear consequence of mitochondrial respiratory chain dysfunction on cholesterol metabolism. Respiratory chain complex deficiency lowers expression of transcripts encoding enzymes of the mevalonate pathway through a reduced proteolytic activation of SREBP2. Other cholesterol sensing enzymes on the ER membrane were also less abundant in conditions of complex I impairment. Together these findings pointed in the direction that complex I deficient cells adapted to changes in the intracellular cholesterol levels. We thus questioned if intracellular cholesterol concentrations changed following complex I inhibition.

8.1 Changes in total cellular cholesterol

To assess if total cholesterol was affected by respiratory chain dysfunction, we measured the levels of cholesterol by gas chromatography. To artificially induce a pronounced increase in intracellular cholesterol, we treated cells with the Niemann-Pick C1 protein (NPC1) inhibitor U18666a. This compound impairs the endosomal export of cholesterol, leading to an accumulation in late endosomes. Treatment with U18666a showed an strong increase of total intracellular cholesterol as expected (figure 8.1-A). Cells cultured in lipid deficient conditions displayed a lower amount of total cellular cholesterol. Treatment with rotenone, however, did not significantly alter the levels of total cholesterol in the cell.

Cholesterol is present in two forms in the cell, either in a metabolically inactive esterified form or in the free form. Much of the cellular cholesterol is in its inactive esterified form, however changes in signalling are induced by changes in free cholesterol. We questioned if perhaps respiratory chain dysfunction converts esterified cholesterol into free cholesterol altering the levels of intracellular free cholesterol. To measure this, we prepared samples with an alternative method, isolating the free cholesterol. We observed a decrease in free cholesterol when cells were treated with atorvastatin, a compound inhibiting the synthesis of cholesterol (figure 8.1-B). Inhibiting of complex I again showed no measurable effect on the total levels of intracellular cholesterol.

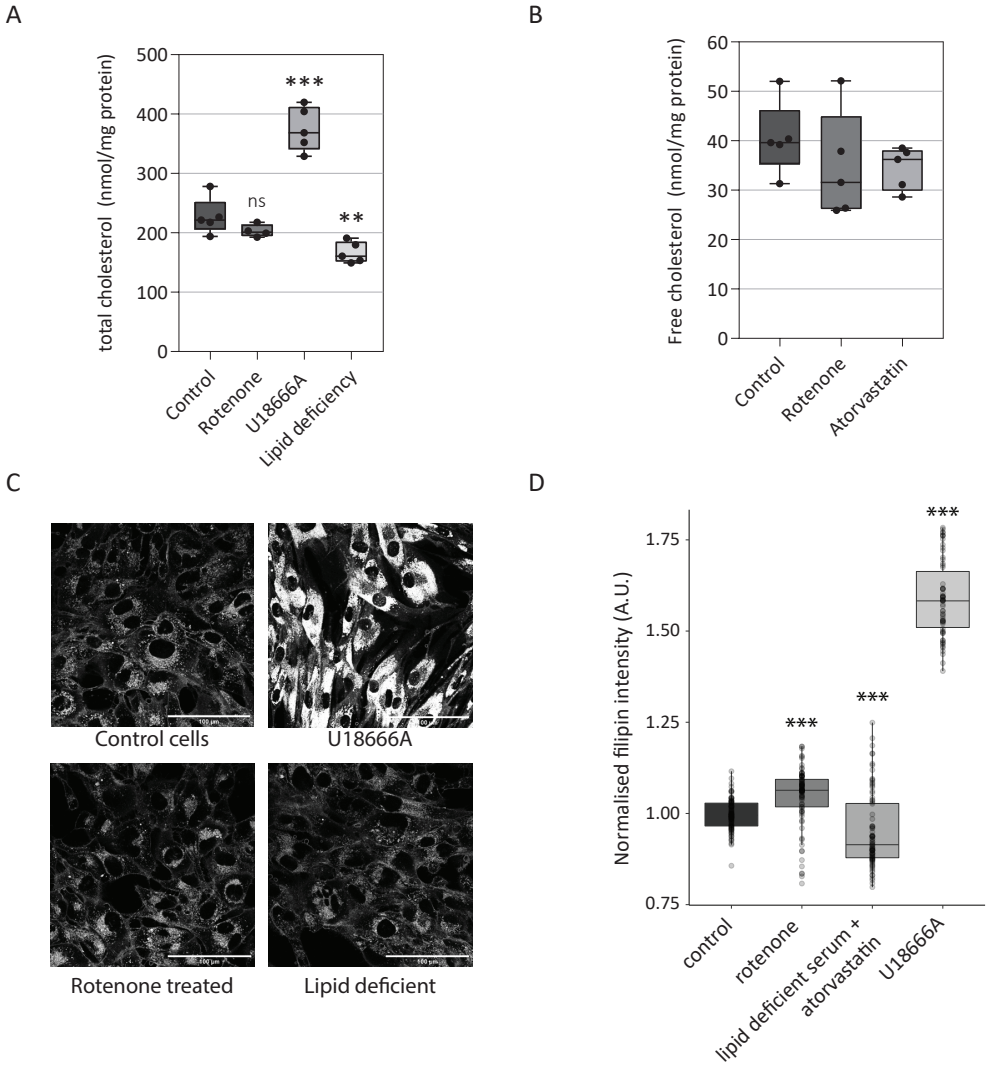

Figure 8.1 – **Complex I inhibition increases intracellular free cholesterol.** (A) Boxplot showing total cholesterol levels following treatment with control (DMSO), 100 nM rotenone, 500 nM U18666a or lipid deficient conditions for 48 hours in primary human fibroblasts, measured by gas chromatography. Data shown as nmol/mg protein. Boxes indicate interquartile ranges, median and 95th percentiles. N=5, individual data points are shown. (B) Boxplot showing total free-cholesterol levels following treatment with control (DMSO), 100 nM rotenone or 1 μM atorvastatin for 48 hours in primary human fibroblasts, as measured by mass spectrometry. Data shown as nmol/mg protein. Boxes indicate interquartile ranges, median and 95th percentiles. N=5, individual data points are shown. (C) Representative confocal fluorescent microscopy images following treatment with control (DMSO), 100 nM rotenone, 2 μM U18666a or lipid deficient conditions (see materials and methods) for 48 hours in human primary fibroblasts. Cells were fixed and stained with filipin prior to image acquisition. (D) Quantification of fluorescent signal in C. Data shown as filipin intensity normalised to control. Boxes indicate median and interquartile ranges. N=80 images from 2 separate replicates on 4 different days. (A,B,D) Significance calculated with an ANOVA (two-sided), followed by Tukey's HSD post-hoc test. * $p<0.05$, ** $p<0.01$, *** $p<0.001$.

8.2 Intracellular free cholesterol

A large fraction of the free cholesterol is bound in the plasma membrane, stored in specialised clusters called lipid rafts. In contrast, organelles such as the ER and mitochondria have the lowest amount of membrane cholesterol, making them very sensitive to changes in the intracellular environment. Subtle changes in the intracellular fraction can be responsible for strong alterations of intracellular signalling. We thus hypothesised that perhaps there are no changes in absolute levels, but instead complex I impairment initiates a redistribution of intracellular cholesterol. To measure the intracellular free cholesterol, we stained cells with the free-cholesterol binding fluorescent compound filipin and measured the fluorescent intensity with confocal microscopy. Filipin is a fluorescent polyene macrolide that specifically binds to free cholesterol. We developed a protocol adapted from (Wilhelm et al., 2019) to measure the intracellular cholesterol without interference from the plasma membrane.

Increasing the intracellular fraction of cholesterol with the compound U18666a as described in chapter 8.1 strongly increased intracellular fluorescence (figure 8.1-C, D). Cells cultured in sterol deficient conditions as described earlier displayed a significantly lower fluorescence, indicative of a reduced abundance of intracellular free cholesterol. Interestingly, inhibition of complex I increased the amounts of intracellular free cholesterol compared to control conditions as observed by an increase of fluorescent signal.

This shows that inhibition of mitochondrial respiratory chain function increases the cholesterol concentration in intracellular space, consequently rendering fibroblast unable to normally respond to changes in intracellular sterol levels. Due to the diffuse distribution of the ER and technical limitations, we failed to measure the amount of filipin staining specifically on the ER membrane. Nevertheless, likely the increase in intracellular cholesterol also occurs on the ER membrane, providing an explanation for the disruption of intracellular cholesterol signalling.

8.3 Intracellular trafficking

Cholesterol can enter the cell through the endocytosis of lipoprotein vesicles and is either transported back to the plasma membrane or released from late endosomes onto organelle membranes. The increase in free cholesterol may originate from an increased release from endosomes following complex I impairment. In cells where release from late endosomes was inhibited with the compound U18666a, cleaved SREBP2 was strongly induced confirming a depletion of ER-cholesterol (figure 8.2-A, B). This furthermore showed that the transport from the endosomes is an important supply of ER-cholesterol. Blocking endosomal release of cholesterol during complex I impairment, failed to abolish the SREBP2 suppressive effect of rotenone treatment. The combination showed a slight increase of SREBP2 cleavage relative to the complex I impairment alone, suggestive of a lower amount of ER cholesterol. However, it failed to rescue the levels of SREBP2 activation to the levels seen with U18666a alone,

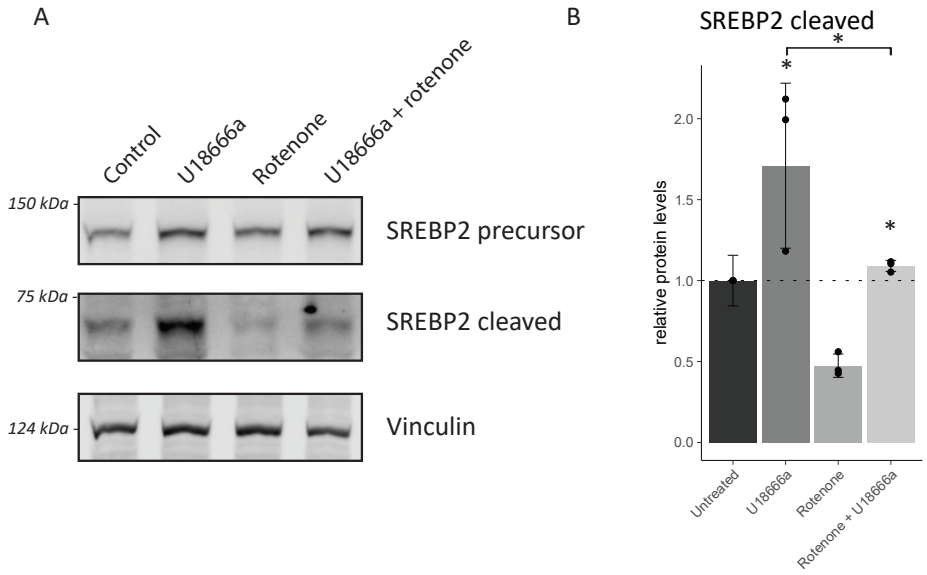

Figure 8.2 – **Complex I inhibition lowers mevalonate pathway transcripts independent of endosomal trafficking of cholesterol.** (A) Western blot showing SREBP2 precursor and activated SREBP2 cleavage product following treatment with 2 µM U18666a or 100 nM rotenone for 48 hours in primary human fibroblasts. Vinculin was used as loading control. (B) Quantification of protein signal as seen in A. Data shown as relative protein levels from DMSO control. Bars indicate mean of three independent experiments ± standard deviation. Individual data points are shown. Significance calculated as ANOVA (two-sided) with Tukey HSD post-hoc test. * p<0.05, ** p<0.01, *** p<0.001.

suggesting a complex I induced increase of cholesterol through a different mechanism. In conclusion, this shows that the increase in free cholesterol observed is not caused by an increased release from late-endosomes.

8.4 Conclusion

Cholesterol is divided into various compartments and forms in the intracellular space. Cholesterol can be esterified, rendering it metabolically inactive, and the free-cholesterol is distributed between the plasma membrane and organelles. We showed that impairing complex I does not affect total cholesterol levels in the cell. Neither does complex I impairment change the levels of free-cholesterol. A closer investigation of specifically the intracellular fraction of free cholesterol showed an increase in the intracellular compartments. This provides a rationale for the earlier observed effects on cholesterol homeostasis. We proposed that this increase may come from an increase in release from the endosomal compartment, however inhibiting the release of cholesterol from late endosomes did not abolish the suppression of SREBP2 processing.

9 Complex I dysfunction in hepatocarcinoma cells

The main site of cholesterol metabolism in the human body is the liver. This organ plays an important role in the management of the transport of lipoproteins and circulating cholesterol levels. To evaluate if the phenotype observed in fibroblasts also takes place in other cell types, we investigated the effect of respiratory chain inhibition on the human HepG2 hepatoma cell line.

9.1 Mevalonate pathway transcripts

To determine if the effect of mitochondrial respiratory chain dysfunction affects mevalonate pathway transcripts in HepG2 cells we repeated the measurements of key mevalonate pathway transcripts. To confirm the responsiveness of the cholesterol sensing mechanisms in these cell types we cultured these cells in lipid free conditions. We observed that the transcripts of key mevalonate pathway targets ACAT2, HMGCR, SQLE, HMGCS1 and DHCR7 were all strongly increased in sterol-depleted conditions (figure 9.1-A), indicating the HepG2 cells respond normally to changes in intracellular cholesterol. When complex I was impaired in the lipid free culture conditions, the levels of transcripts were drastically reduced in a more severe way than previously observed for the human fibroblasts.

9.2 Changes in SREBP2 activation

The drastic reduction in transcripts prompted the question if this effect was mediated by an equally marked effect on SREBP2. We measured the expression of SREBP2 protein and the degree of proteolytic cleavage by western blot. We inhibited the respiratory chain over a range of 8 hours to 2 days to reveal any time dependent effects. Transfer of the HepG2 cells into lipid free media increased the cleavage of SREBP2 as seen before in the fibroblasts, demonstrating adequate levels of the SREBP2 protein and its sensitivity to changing cellular cholesterol levels (figure 9.2-A). The effects of sterol reduction on SREBP2 cleavage are rapid, with a clear induction already visible after 8 hours. The inhibition of complex I lead to a severe decrease

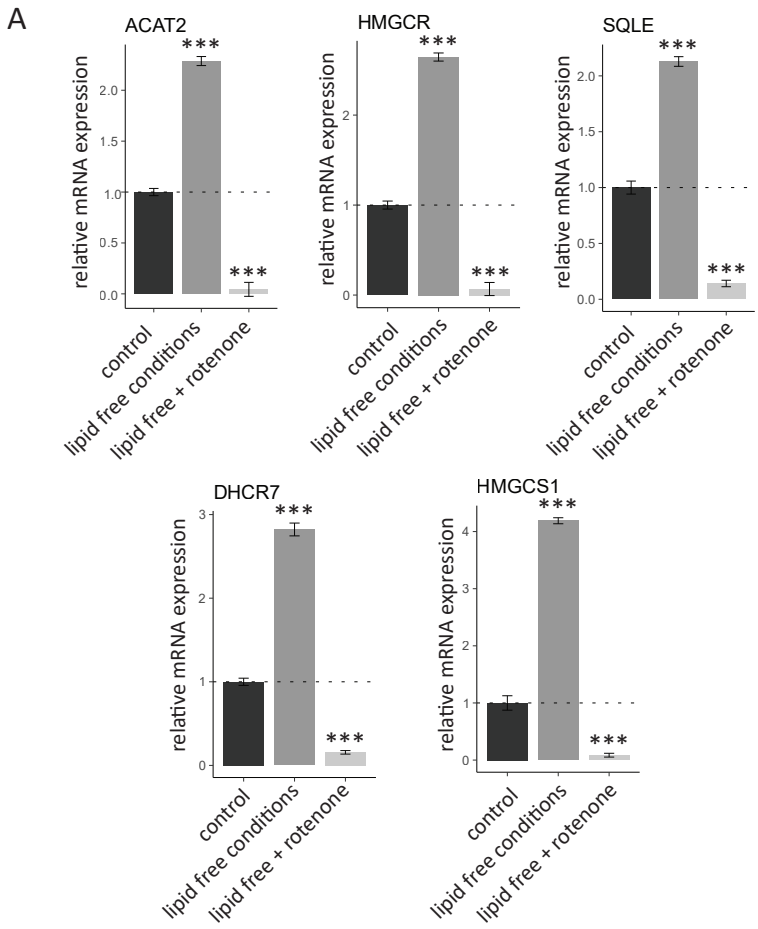

Figure 9.1 – **Complex I inhibition leads to a more severe phenotype in hepatocarcinoma cells.** (A) Relative mRNA expression of mevalonate pathway genes following treatment with empty vehicle (DMSO), culture in lipid-free conditions or treatment with 100 nM rotenone or a combination as shown for 48 hours in primary human fibroblasts. Data shown as relative mRNA expression from DMSO, normalised to housekeeping genes. Bars indicate mean of three independent experiments ± standard deviation. Significance was calculated with a students t-test, followed by Benjamini-Hochberg correction. * p<0.05, ** p<0.01, *** p<0.001. (ACAT2, Acetyl-CoA Acetyltransferase 2; HMGCR, 3-Hydroxy-3-Methylglutaryl-CoA Reductase; SQLE, Squalene Epoxidase; HMGCS1, 3-Hydroxy-3-Methylglutaryl-CoA Synthase 1; DHCR7, 7-Dehydrocholesterol Reductase)

of cleaved SREBP2 to near non-measurable levels in both normal and low sterol conditions. This effect was already present after 8 hours, where no induction of SREBP2 maturation was seen. After 48 hours we also observed a reduction in the SREBP2 precursor protein. This complete suppression of SREBP2 cleavage and a reduction of precursor protein is a more severe phenotype compared to the one observed in the fibroblast models.

To confirm the absence of the precursor we treated HepG2 cells with cyclodextrins to fully

prevent or stimulate the processing of SREBP2. We measured the effect of cyclodextrins in both normal and sterol depleted culture conditions. We observed that in control conditions the cleavage could be effectively prevented by treating with cholesterol loaded cyclodextrins and effectively stimulated by treatment with empty cyclodextrins (figure 9.2-B). All expression levels showed a similar pattern of activation in sterol free culture conditions, suggesting a higher abundance of total SREBP2. Inhibition of complex I showed a drastic decrease in abundance of all SREBP2 protein levels after 48 hours. A very minor induction of SREBP2 following complex I impairment was only seen in the sterol free culture conditions combined with empty cyclodextrin treatment. Overall, this confirmed our earlier findings that after 48 hours of treatment with rotenone reduces SREBP2 protein to very low levels.

9.3 Cholesterol sensing enzymes on the ER membrane

To validate that the effects were also extended to other ER-bound cholesterol sensors, we measured the abundance of HMGCR and SQLE following complex I inhibition. To reveal any time dependent effects we measured the protein levels over a range from 8 hours to 2 days. As earlier, the removal of lipids stabilised these proteins and increased their abundance (figure 9.3-A, B). We observed that removal of sterols induces protein abundance after roughly 24 hours and maintains this level up to 48 hours. Addition of rotenone to these cells again strongly reduced the abundance of the measured proteins to near non-measurable levels in both the normal sterol and low sterol conditions. The addition of rotenone prevented the stabilisation over all the timepoints measured, suggesting an effect after already 8 hours. This drastic effect prompted the question if this was a non-specific effect disturbing all ER-proteins. To address this concern, we measured the abundance of the calcium binding ER-membrane protein Calnexin. We measured the abundance of this protein under the same conditions as figure 9.3-A and B. We observed no decrease in the abundance of calnexin, proving that the effect was specific to the cholesterol binding proteins of the ER.

9.4 Conclusion

Overall, respiratory chain dysfunction drastically reduces the abundance of SREBP2 in HepG2 cells to near non-measurable levels. This reduction radically lowered the maximal activation of SREBP2 by empty cyclodextrins. This consequently reduced the expression of its target transcripts to equally low levels. This suppression is extended to the cholesterol sensors SQLE and HMGCR, where inhibition of the respiratory chain reduces the levels to equally low levels. For all affected proteins, the reduction is rapid in onset with a severe reduction already visible after 8 hours. This phenotype is more drastic than the one observed in the fibroblasts. These changes are assumed to be induced by a similar increase of intracellular cholesterol as seen in the fibroblasts. Likely, both post-translational regulation by cholesterol levels and a reduced transcription by impaired SREBP2 activation play a role in the regulation of these proteins.

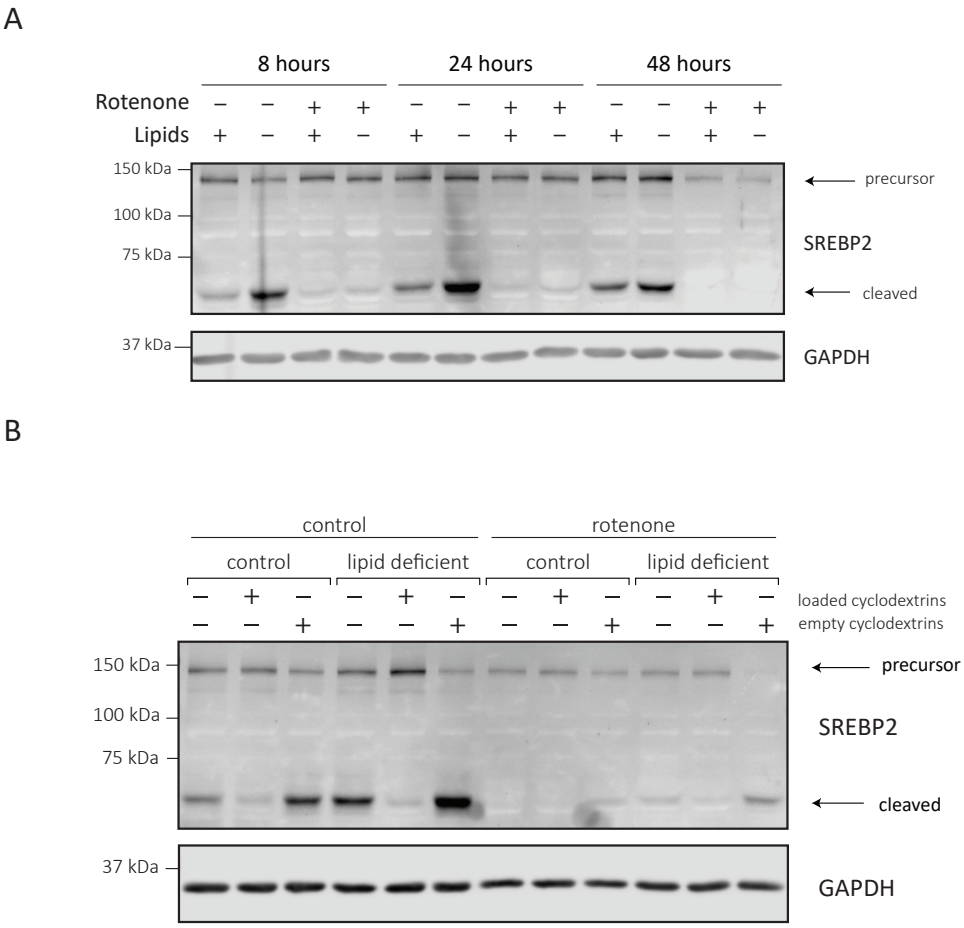

Figure 9.2 – **Complex I inhibition has a strong effect on the levels of SREBP2 in in hepatocarcinoma cells.** (A) Western blot showing SREBP2 precursor and activated SREBP2 cleavage product following culture in normal or lipid free conditions (see materials and methods) supplemented with empty vehicle (DMSO) or 100 nM rotenone in primary human fibroblasts. GAPDH was included as loading control. Cells were treated for the times indicated. (B) Western blot showing SREBP2 precursor and activated SREBP2 cleavage product following culture in lipid free conditions (see materials and methods) for 48 hours and supplemented with empty cyclodextrins, loaded cyclodextrins or vehicle (water) for 30 mins before collection of protein lysate in primary human fibroblasts. GAPDH was used as loading control.

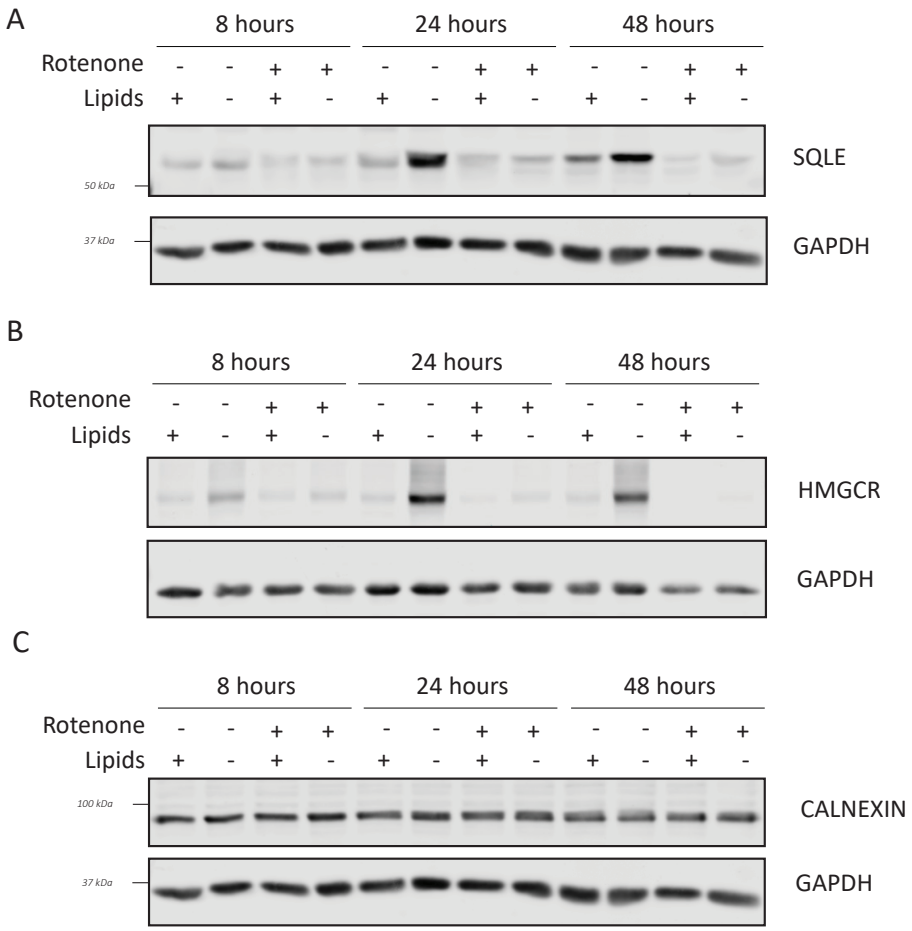

Figure 9.3 – **Complex I inhibition has a strong depletion on the levels of ER-membrane cholesterol sensors in hepatocarcinoma cells.** (A) Western blot showing SQLE protein following culture in normal or lipid free conditions (see materials and methods) supplemented with empty vehicle (DMSO) or 100 nM rotenone in HepG2 hepatocarcinoma cells. Cells were treated for the times indicated. GAPDH was used as loading control. (B) Western blot showing HMGCR protein following culture in normal or lipid free conditions (see materials and methods) supplemented with empty vehicle (DMSO) or 100 nM rotenone in HepG2 hepatocarcinoma. Cells were treated for the times indicated. GAPDH was used as loading control. (C) Western blot showing calnexing protein following culture in normal or lipid free conditions (see materials and methods) supplemented with empty vehicle (DMSO) or 100 nM rotenone in HepG2 hepatocarcinoma. Cells were treated for the times indicated. GAPDH was used as loading control.

10 Discussion

Mitochondria are best known for its respiratory chain and its role in ATP synthesis. However, this multifunctional organelle participates in many metabolic pathways shared between the mitochondrial matrix and the cytosol, contributing at many levels to cellular metabolism and homeostasis. These pathways maintain proper homeostasis such as the balance of nutrients, redox state and managing cellular fate in stress conditions. Coordinating these many aspects of cellular physiology requires close communication between mitochondria, the nucleus and the other metabolic pathways of the cell. When mitochondria are unable to function normally, this leads to changes in biochemical equilibria in the intracellular environment. These disruptions in cellular homeostasis are interpreted as signals by retrograde signalling pathways and translated into signals to inform the nucleus about the need for transcriptional responses to restore or maintain cellular health. When the retrograde signals can't restore cellular homeostasis, such as if the defect is too severe or if other environmental influences exacerbate the defect, it can lead to the dysfunction of whole tissues and lead to mitochondrial disease.

Although most mitochondrial mutations directly or indirectly cause a defect at the level of oxidative phosphorylation, mitochondrial diseases are highly variable with respect to severity, symptoms, age of onset and tissue specificity. The current consensus is that the observed variability in clinical presentation can be partially explained by differences in retrograde signaling and the resulting nuclear transcriptional response to mitochondrial dysfunction (Koopman et al., 2012; Rossignol et al., 2003). These differences prove promising for the treatment of mitochondrial diseases, as some tissues are often unaffected by the mitochondrial dysfunction suggesting that retrograde signalling can overcome the defect and maintain homeostasis. A comprehensive understanding of these retrograde signalling pathways may pave the way to novel treatments for specific mitochondrial diseases and in general for diseases where mitochondrial function is involved.

In this thesis we present a novel cellular adaptation to mitochondrial respiratory chain (RC) dysfunction. Taking advantage of QuantSeq 3'RNA sequencing we studied the retrograde transcriptional response in three models of respiratory chain dysfunction with different

underlying complex deficiencies. Transcriptomics is an ideal tool to compare adaptive transcriptional responses due to its high precision of identifying genes and its completeness of mapping the entire transcriptome. We used specific inhibitors of complex I, III and V of the respiratory chain at concentrations that cause a marked inhibition of respiration to induce a severe phenotype, thereby strongly activating retrograde signaling pathways.

In these disease models we identified downstream transcriptional programs that were affected by mitochondrial RC dysfunction, by all of the respiratory complexes impaired. We discovered activation of stress responses and apoptotic pathways in response to respiratory chain dysfunction, in line with previous studies (Marín-Buera et al., 2015; Mick et al., 2020; Quirós et al., 2017). We discovered a downregulation of transcripts involved in cholesterol biosynthetic pathways in all models of mitochondrial RC dysfunction, which has been noted in earlier studies, but never studied in detail. Upon closer examination this affected all the transcripts of the mevalonate pathway. Further research into the mechanisms involved, revealed this was caused by a suppression of SREBP2 processing. Impairment of complex I dampened the normal response of SREBP2 in normal and low-lipid conditions. The effect of the complex I inhibition was extended to post-translational regulation of the ER-bound sterol sensing proteins SQLE and HMGCR. This post-translational regulation was later identified to be caused by an increase of intracellular free cholesterol, which occurred without changing total sterol levels.

10.1 Cellular models of mitochondrial disease

Chemical models Studying the transcriptional adaptations to mitochondrial dysfunctions induced with respiratory chain inhibitors is a robust way to study retrograde signalling in fibroblasts. Treating fibroblasts with respiratory chain inhibitors induces a disbalance in cellular homeostasis and a strong activation of retrograde signalling pathways which aim to correct the disbalance. Many studies have looked at the effects of these chemical inhibitors in human fibroblasts. The long-term treatment of cells with rotenone has been shown to increase superoxide levels, the abundance of complex I, complex V, porin and mtHSP70 and change mitochondrial dynamics (Koopman et al., 2007). The prolonged treatment of rotenone mimics a lot of characteristics of cells derived from patients with complex I deficiency such as an increase in NADH, a depolarisation of the mitochondrial membrane, a normal amount of mitochondria and reduced peak concentrations of ATP.

There are slight differences in biochemical effects between chemically induced mitochondrial dysfunction and the cellular homeostasis in patients suffering from mitochondrial dysfunction. Important differences are that chemically induced complex I deficiency shows higher rather than lower complex I abundance, no changes in complex V expression and no change in cytosolic thiol status (Koopman et al., 2010). Due to the large overlap in cellular effects, it can be expected that many retrograde signalling pathways will be similarly activated. The use of these models should go paired with a thorough understanding of the differences to

avoid confounding by possible model-specific effects.

To increase the likelihood of finding disease relevant adaptations, we explored the transcriptional responses in three models of mitochondrial dysfunction. This has the advantage of excluding specific confounding effects inherent to the use of inhibitors. We also examined treated cells for two different timepoints, as another confounding effect of using inhibitors is the sudden change in cellular dynamics. By using a short and longer timepoint in our models we were able to identify genes whose response was rapid in onset and continued for the duration of treatment.

Genetic models To further strengthen the discovery, we developed and characterised genetic models of mitochondrial respiratory chain dysfunction. The respiratory impairment was induced by knocking out either the complex I subunits NDUFS4 or NDUFS6 in immortalised human fibroblasts. Both these subunits have been targets to successfully generate mouse models of mitochondrial dysfunction and have been reviewed in detail elsewhere (Torraco et al., 2015). The genetic models of mitochondrial dysfunction had a more moderate phenotype with baseline respiration ranging from 30%-70% of normal controls. This value more closely represents the residual respiration seen in fibroblasts derived from patients with complex I deficiency, which has been reported to be between 18% to 75% in a cohort of 16 patients (Koopman et al., 2010). Here we studied four single-cell derived clones, two separate clones of each the target genes NDUFS4 and NDUFS6. We observed some heterogeneity in the phenotypes, measuring differences between the expression of mitochondrial proteins and the proliferation rates. Possible explanations for these differences are heterogeneity in the cell line used to derive the single-cell clones or from non-specific off-site effects of Cas9, which may induce DNA damage and activate cellular signalling to compensate for this. Slight differences in the culture conditions could also in the long term induce certain adaptive pathways differently in each of the clones. Overall comparing the findings of the chemical model with the knockout cells proved useful in strengthening the discovery of the downregulated mevalonate pathway.

10.2 The mevalonate pathway is unaffected by a traditional retrograde signalling

By comparing the differentially expressed genes in our QuantSeq data, we found that a 10% subset of differentially expressed genes behaved similarly in all three models of mitochondrial dysfunction. We reasoned this shared subset of genes would likely be enriched for downstream effectors of retrograde signaling. Among the upregulated genes of this shared fraction there was a strong enrichment of gene sets linked to apoptosis, response to oxidative stress and a negative regulation of metabolism. Specifically, this included transcripts for Activating Transcription Factors (ATFs) and their downstream targets. These findings are consistent with earlier published work on the induction of the integrated stress response in models of mitochondrial dysfunction (Guo et al., 2020; Mick et al., 2020; Quirós et al., 2017). In the

downregulated fraction, we observed an enrichment in cholesterol biosynthesis pathways which encompassed a coordinated downregulation of almost all mevalonate pathway genes.

The mevalonate pathway is very relevant for mitochondrial function. This pathway is the main site for synthesis of isoprenoids, ubiquinone, and cholesterol. Isoprenoids play a key role in the prenylation of RhoGTPases, which in turn activate the YAP/TAZ proteins to promote glucose and amino acid uptake into cells (Gong et al., 2019; Sorrentino et al., 2014). The YAP/TAZ signalling pathway also mediates calcium signalling and controls the switch between aerobic glycolysis and oxphos respiration (White et al., 2019). The other main metabolite produced by the mevalonate pathway, ubiquinone, directly plays an essential role in the electron transport chain, accepting electrons from complex I and II, transferring them to complex III.

Earlier research with other cellular models of mitochondrial dysfunction has revealed a similar reduction in cholesterol biosynthesis gene expression (Kühl et al., 2017; Mick et al., 2020; Quirós et al., 2017), but the underlying molecular mechanisms were not further investigated. In spite of the clonal differences, the knockout clones also all show a mild suppression of the mevalonate pathway genes, suggesting that a similar mechanism is activated as in the pharmacological models of RC dysfunction. This would also imply that the adaptations observed in the pharmacological model are not just of short duration, but indicative of a more long-term impairment in conditions of malfunctioning respiratory chain. We thus concluded the observed suppression of mevalonate pathway genes must be the consequence of an impaired respiratory chain.

Proliferation The three most enriched pathways after pharmacological inhibition of oxidative phosphorylation in fibroblasts were cholesterol biosynthesis, cell cycle and DNA replication pathways. This simultaneous downregulation raised the concern that reduced expression of mevalonate pathway genes is simply the secondary consequence of slowed proliferation, which lowers the need for de novo cholesterol and lipid biogenesis. To address this concern, we measured the effect of complex I inhibition on mevalonate pathway genes in contact-inhibited fibroblasts. Intercellular contact in highly confluent fibroblasts cultures activates biochemical and physical mechanisms that arrest cell growth (Ribatti, 2017). We observed that complex I inhibition lowered mevalonate pathway genes expression to a similar extent in exponentially growing and confluent human primary fibroblasts. Based on these findings we think it is unlikely that reduced proliferation rate is responsible for the here observed reduction of mevalonate pathway gene expression. In fact, the opposite may be equally likely, where a reduction in isoprenoids produced by the mevalonate pathway reduces the activity of important RHO and RAS small-GTPases, which are important regulators of cell-cycle (Coleman et al., 2004).

AMPK Another consideration that arose from the model characterisation and the data exploration is that the observed effect was mediated through the activity of AMPK. AMPK has been shown to phosphorylate SREBP1 and SREBP2 (Li et al., 2011; Liu et al., 2015). Our notion was that inhibiting the respiratory chain activated AMPK, which in turn would inhibit SREBP2 and thus drive the reduction in gene expression. To study this, we looked at the effects of modifying AMPK activity on the mevalonate pathway transcripts during control conditions and complex I impairment. We observed that chemically inhibiting AMPK with compound C led to increased transcription of mevalonate pathway genes. Activation of AMPK with 991 showed a strong activation of AMPK while having no effect on gene transcription. Similarly, under conditions of complex I impairment, inhibition of AMPK lead to an increased expression whereas further activation had no effect. Inhibiting of complex I had a stronger effect on the lowering of transcripts, however it had a lower inducive effect on the levels of phosphorylated AMPK compared to activation of AMPK with 991. Considering that the activation of AMPK alone did not affect the expression of genes and that mitochondrial dysfunction had a lower activation of AMPK but a stronger effect on the gene expression, we proposed that this is not the main mechanism of regulation of SREBP2.

This independence of the mevalonate pathway gene suppression from AMPK was further confirmed in AMPK-α double knockout (AMPK-null) mouse embryonal fibroblasts. These cells lacked all AMPK activity, as we shown by the complete absence of phosphorylated AMPK and downstream substrates. Even in these conditions, inhibiting complex I shows a decrease in the mevalonate pathway transcripts providing conclusive evidence that the mechanism observed is not solely mediated by AMPK. The difference between our observed effect and the earlier studies can be attributed to the fact that the earlier work looked at SREBP2 in the liver extracted from mice that were on a high-fat diet and were treated with a non-specific activator of AMPK (Li et al., 2011). This experimental set-up has many variables that are different to ours, making a direct comparison prone to bias.

10.3 Potential mechanisms

After concluding the observed phenotype was robust and reproducible, we questioned the mechanism upstream of the transcriptional changes. The general downregulation of mevalonate pathway genes strongly implied inhibitory effects on the Sterol Responsive Element Binding Protein 2 (SREBP2). The N-terminal fragment of the full-length protein is released after proteolytic cleavage and binds to specific DNA-motifs called Sterol Regulatory Elements upstream of mevalonate pathway genes to initiate the transcription of these genes.

Transcriptional and post-translational regulation We used processing of SREBP2 and expression of SREBP2 target genes as a read-out of SREBP2 regulation to study the effects of mitochondrial dysfunction on SREBP2 processing. After complex I inhibition SREBP2 activity was reduced and was unable to activate to normal levels when stimulated by reducing sterol

abundance. However, acute addition of cholesterol retained SREBP2 in its inactive precursor form while cholesterol depletion induced maturation, showing that SREBP2 retained sensitivity to changes in cholesterol. Quantitatively however, the amount of SREBP2 processed when cholesterol was depleted was much lower in conditions of impaired complex I compared to control cells (figure 7.1). The reduced SREBP2 response was even more pronounced in the hepatoma cell line HepG2 (figure 9.2). When complex I was inhibited, the cleaved form of SREBP2 was close to undetectable even under conditions that would maximally induce SREBP2 activation in control cells. In addition, the total levels of SREBP2 were markedly reduced in HepG2 cells under conditions of complex I inhibition. This was much less apparent in fibroblasts.

SREBP2 is known to regulate its own expression (Sato et al., 1996). Impaired SREBP2 processing and activation therefore likely causes a negative feed-back loop also reducing SREBP2 transcription, with a gradual depletion of the protein as consequence. This is in line with the observation that HepG2 cells show a pronounced inhibition of SREBP2 already after 8 hours with a following progressive depletion of the precursor. In fibroblasts this suppression of SREBP2 is slower and thus shows no apparent depletion of total SREBP2. We propose that after complex I inhibition primary human fibroblasts as well as HepG2 cells SREBP2 responds to changes in sterol levels but are unbale to provoke the same degree of activation as control conditions.

Connecting mitochondrial function to SREBP2 How inhibition of mitochondria affects SREBP2 function remains unknown. There are to my knowledge no studies that have directly looked at the influence of mitochondrial dysfunction on SREBP2 signalling. Indirectly there is evidence which connects mitochondrial dysfunction to cholesterol metabolism, such as how mTORC1 activates SREBP2 by reducing cholesterol trafficking from lysosomes (Eid et al., 2017; Peterson et al., 2011). Furthermore, mitochondrial dysfunction induces ER-stress (Lim et al., 2009), which in turn had been shown to activate SREBP2 (Colgan et al., 2007), reduce expression of ABCA1 and also regulate ATF4-mediated transcriptional modulation of transcripts involved in cholesterol metabolism (Fusakio et al., 2016). One study discovered that a primary defect in mitochondrial dynamics lead to a respiratory chain dysfunction through inhibitory effects on the cholesterol biosynthesis pathway (Mourier et al., 2015). All these studies have hinted at an interaction between mitochondrial function but to date no follow-up studies have specifically focussed on this crosstalk.

Other cholesterol sensors We then established whether other ER localized cholesterol sensing proteins were dysregulated as a result of respiratory chain dysfunction. The proteins HMGCR and SQLE are two key regulatory enzymes of the mevalonate pathway, both of which are under transcriptional control of SREBP2. In addition, both are able to bind sterols for posttranslational regulation by cholesterol or precursors. When ER cholesterol levels are high HMGCR and SQLE are ubiquitinated and targeted for degradation by the proteasome.

Consistent with this dual regulation, we observe a marked accumulation of HMGCR and SQLE protein when the cells were shifted to a medium lacking cholesterol. When mitochondrial respiration was inhibited in human fibroblasts, removal of cholesterol from the media resulted in a much lower accumulation of these proteins. In HepG2 cells the impact of mitochondrial function on HMGCR and SQLE protein expression was again even more dramatic. HMGCR and SQLE were barely detectable even after removal of cholesterol from the medium. Taken together, we demonstrate that altered sterol sensing on the ER is not limited to SREBP2 activation but extended to the two mevalonate pathway enzymes HMGCR and SQLE, with the effect much more striking in HepG2 cells. As observed in the regulation of SREBP2 in HepG2 cells, likely both transcriptional and posttranslational regulation of mevalonate pathway enzymes plays a role in the observed cholesterol homeostasis remodelling in our cellular models of mitochondrial dysfunction.

Model comparisons The advantage of using multiple models of mitochondrial dysfunction is that hints towards the mechanism can be obtained by comparing the specific biochemical effects inherent to the use of these compounds. There are complex specific effects of three inhibitors, such as a much stronger effect on redox metabolism through altering the ratio of NADH/NAD+ levels after inhibition of complex III than complex I and again complex V. In figure 3.2-B we observed that all inhibitors affected the expression of mevalonate pathway transcripts, however there is a slightly more dramatic phenotype for antimycin A than rotenone and again than oligomycin A.

The amplitude of these differences closely match earlier measured NADH/NAD+ ratios after inhibition of the various complexes (Mick et al., 2020), where complex I and III inhibition show strong effects, which complex III the highest and complex V showing a more moderate phenotype. This makes it tempting to relate the effect observed on the mevalonate pathway to a disruption in NADH/NAD+ ratios and redox metabolism. Another biochemical comparison that can be made between the complexes is the amount of ROS that is produced by the individual complexes when impaired. The levels produced are again higher for antimycin A than for rotenone. Oligomycin A was not measured, but is known to produce less ROS (Goncalves et al., 2015; Siraki et al., 2002). Further research will have to focus on these specific biochemical changes to confirm the possible correlation between these observations.

Another correlation could be observed comparing the mevalonate pathway gene suppression and residual complex I activity. Of all the knockout cell lines, the clone NDUFS4 B displays the most dramatic effect, showing among the lowest baseline respiration, the lowest residual complex I respiration and the slowest proliferation rate. This clonal line also showed the strongest suppression of mevalonate pathway genes of all knockout cell lines. Pharmacologically inhibiting complex I strongly impairs the functioning of the complex, while also displaying a strong decrease in mevalonate pathway gene suppression. This difference in residual complex between the pharmacological model and the genetic models again mirrors the degree of reduction of mevalonate pathway transcripts, where the reduction in mevalonate

transcripts is also more pronounced in the pharmacological model. Comparing these models suggests that the degree of residual complex I respiration is determining for the severity of the phenotype and the mevalonate pathway suppression.

Oxysterols An interesting consideration is the link between mitochondria and oxysterols. The enzyme CYP27A1 on the mitochondrial membrane produce 27-hydroxycholesterol as a precursor for bile acid signaling (Hall and Pandak, 2005). Additionally, oxysterols have a cholesterol regulating role by binding to INSIG proteins on the ER membrane to inhibit SREBP2 processing and inducing degradation of HMGCR.

However, an increased production of oxysterols by mitochondrial function is unlikely the main mechanism involved as this does not explain the induced degradation of SQLE. This protein is regulated independently of INSIG and the binding of cholesterol itself induces this degradation. The increase in cholesterol is more likely upstream of the observed events. However, mitochondrially derived oxysterols may still be relevant, as cholesterol concentration is the rate-limiting parameter of oxysterol synthesis on the mitochondrial membrane by CYP27A1 and likely other oxysterol producing enzymes (Russell, 2000).

Summary Overall, we found that the reduction of mevalonate pathway transcripts was indeed the consequence of an inhibited SREBP2 processing. If this suppression was the consequence of transcriptional or post-translational regulation has yet to be clarified. In HepG2 cells we see a stronger and more rapid inhibition of SREBP2 which leads to a depletion of total SREBP2 suggesting a rapid post-translational regulation followed by reduced transcriptional activity, also the rapid degradation of other cholesterols sensors on the ER-membrane is more characteristic of post-translational regulation. Likely both mechanisms play a role. Exactly how mitochondrial dysfunction regulates SREBP2 function remains unknown. Some studies have shown effects of mitochondrial function on SREBP2 processing through the activation of metabolic pathways such as AMPK, ISR and mTOR. The investigation of these potential mechanisms however, showed that the observed downregulation is independent of these pathways.

10.4 Increased intracellular free cholesterol

We speculated that the response of SRBEP2 to intracellular cholesterol is proper but that for unknown reasons cholesterol is elevated in cells with mitochondrial respiratory chain dysfunction. Such an increase in intracellular cholesterol would make the cells more resistant to cholesterol lowering conditions. Yet, the total cholesterol levels were unaffected in human fibroblasts when respiration was inhibited with rotenone.

A large fraction of the total cellular cholesterol pool is stored in lipid droplets in the form of cholesterol esters and is not directly involved in cholesterol sensing on the ER. Free choles-

terol on the other hand is found in the membrane lipid bilayers and partakes in metabolic reactions. We find that total free cholesterol was also not significantly elevated in human primary fibroblasts after inhibition of complex I. However, most of cellular free cholesterol is found in the plasma membrane and only very little is present on the ER membrane. Slight changes in intracellular free cholesterol would thus not lead to a large relative change in plasma membrane cholesterol, but would have significant consequences if elevated on the ER membrane.

To follow the more relevant pool of cholesterol on intracellular membranes, we therefore also applied filipin staining of membrane cholesterol after brief extraction of the plasma membrane cholesterol with empty cyclodextrin. Blocking complex I activity elevated the intracellular cholesterol levels. These findings are in line with our model where after inhibition of respiratory chain activity ER-cholesterol sensors behave in a way resembling elevated cholesterol. In summary, our results show that inhibition of mitochondrial function augments the cholesterol concentration on intracellular membranes rendering sterol sensing in fibroblasts partially blunted to the acute or chronic removal of exogenous cholesterol.

10.5 Source of the intracellular cholesterol

Intracellular compartments The question remains open what the cause of the accumulation of cholesterol is in the intracellular environment. In general, after inhibition of mitochondrial function human fibroblasts seem to activate multiple mechanisms to lower cholesterol. A possible source for the observed increase of free cholesterol are cholesterol esters in lipid droplets. Retrograde signaling from mitochondria may stimulate the mobilization of cholesterol esters from this storage compartment to be hydrolyzed for cholesterol to be transferred onto other intracellular compartments. This process would leave the total cholesterol pool unchanged but perceived by the cell as if cholesterol was more abundant. Late-endosomes and lysosomes are another important site for intracellular cholesterol storage. Mitochondrial dysfunction has been shown to affect lysosomes by increasing ROS resulting in oxidative damage and lowering ATP, needed by the lysosomes to maintain the acidic pH (Stepien et al., 2020). This destabilisation of lysosomes may induce a leak of cholesterol. Future experiments should be designed to reveal whether and how mitochondrial dysfunction and retrograde signaling may be linked to mobilization of cholesterol from other intracellular compartments.

Plasma membrane A large part of the total free cholesterol is present in the plasma membrane. This pool of cholesterol can be very rapidly transported to the intracellular compartments by non-vesicular transport. Mitochondrial dysfunction may cause a shift of cholesterol from compartments with high or intermediate cholesterol concentrations such as plasma membrane to compartments such as the ER or mitochondria with low levels of cholesterol. The increase of intracellular free cholesterol could be accounted for by a redistribution of intracellular cholesterol. Using electronic image analysis of filipin staining, we failed to quantify

cholesterol specifically on ER membranes mostly because the concentration of cholesterol on the ER are low even when compared to the other intracellular compartments. In addition, the distribution of the ER is very broad and frequently in very close proximity to compartments strongly labeled with filipin. Therefore, the hypothesis that mitochondrial dysfunction shifts the free cholesterol onto ER membranes remains difficult to assess.

Vesicular trafficking One mechanism that may contribute to this shift is enhanced retrograde membrane trafficking of cholesterol from endosomes. We interfered with this process by blocking the function of the Niemann-Pick C1 protein using the compound U18666a. Consistent with earlier findings (Lu et al., 2015), treatment of human fibroblasts with U18666a causes accumulation of cholesterol in endosomes (data not shown) and reduced ER cholesterol as demonstrated by the induction of SREBP2 maturation and the stabilization of the ER cholesterol sensor SQLE. Under these conditions, complex I inhibition maintained its ability to interfere with sterol sensing. SQLE induction was less pronounced, SREBP2 processing inhibited, and mevalonate pathway gene expression reduced compared to control cells. We conclude that differences in retrograde cholesterol trafficking out of endosomes cannot explain alone why cholesterol sensing on the ER is affected in cells with mitochondrial dysfunction. Uptake of exogenous cholesterol can be ruled out in general as impaired cholesterol sensing on the ER was also observed in lipid free conditions, where the sterols were removed from the media.

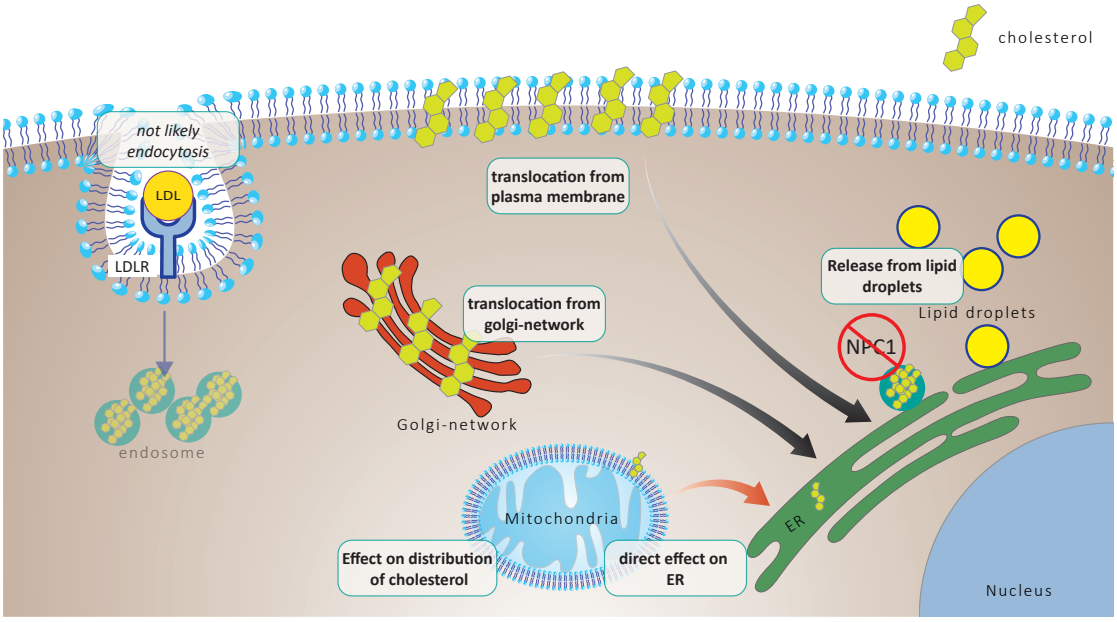

Figure 10.1 – **Schematic representation of proposed sources of intracellular cholesterol transport.** Illustration of the intracellular environment with indicated possible sources of cholesterol transport. Discussed mechanisms captioned in white boxes.

10.6 Clinical relevance

The here obtained results may extend beyond intracellular cholesterol metabolism to whole-body cholesterol management. There has been evidence in clinical studies suggesting a connection between mitochondrial function and systemic cholesterol metabolism. A large study that looked at Single Nucleotide Polymorphisms (SNPs) in mitochondrial DNA for example found a marked correlation in changes in patient in serum lipoprotein levels, clearly underlining a functional connection between the two (Flaquer et al., 2015; Kokaze et al., 2001). Secondly, the use of statins, an important family of cholesterol lowering drugs targeted to the mevalonate pathway, have been suspected to cause mitochondrially mediated side-effects in patients (Golomb and Evans, 2008), through reduced production of ubiquinol (Littarru and Langsjoen, 2007) or reduced protein prenylation (Rauthan et al., 2013). Furthermore, recent discoveries have associated mitochondrial cholesterol to well-known pathologies such as Alzheimer's disease. (Torres et al., 2019). This makes studying the interplay between mitochondrial function and cholesterol metabolism highly relevant area of research possibly leading to new therapies for well-known diseases.

11 Conclusions

In this thesis we provide novel insights into the complex signalling events that follow mitochondrial respiratory chain dysfunction. Mitochondrial respiratory chain dysfunction has been shown to impair the processing of SREBP2 and lower the abundance of mevalonate pathway enzymes SQLE and HMCGR. This led to a functional impairment of the mevalonate pathway, causing disbalances in the levels of mevalonate pathway metabolites. We show here that this is most likely the consequence of an increase in intracellular free cholesterol. Total levels of cholesterol remain unchanged. It is still under investigation what the signalling mechanism is by which mitochondria increase the intracellular free cholesterol pool. Relocation of cholesterol from membranes with high amounts of cholesterol or from lipid droplets though destabilisation of membrane contact sites are possible hypotheses. Well described signalling pathways ISR, AMPK and mTOR were not the main drivers. Comparing the amplitude of the effects on different complexes suggests a role of redox metabolism or ROS. More research will be needed to exactly dissect the mechanism by which mitochondrial dysregulates cholesterol metabolism. Future experiments with more subtle models of mitochondrial disease such as fibroblasts from disease patients will also provide insights to the translatability of the results.

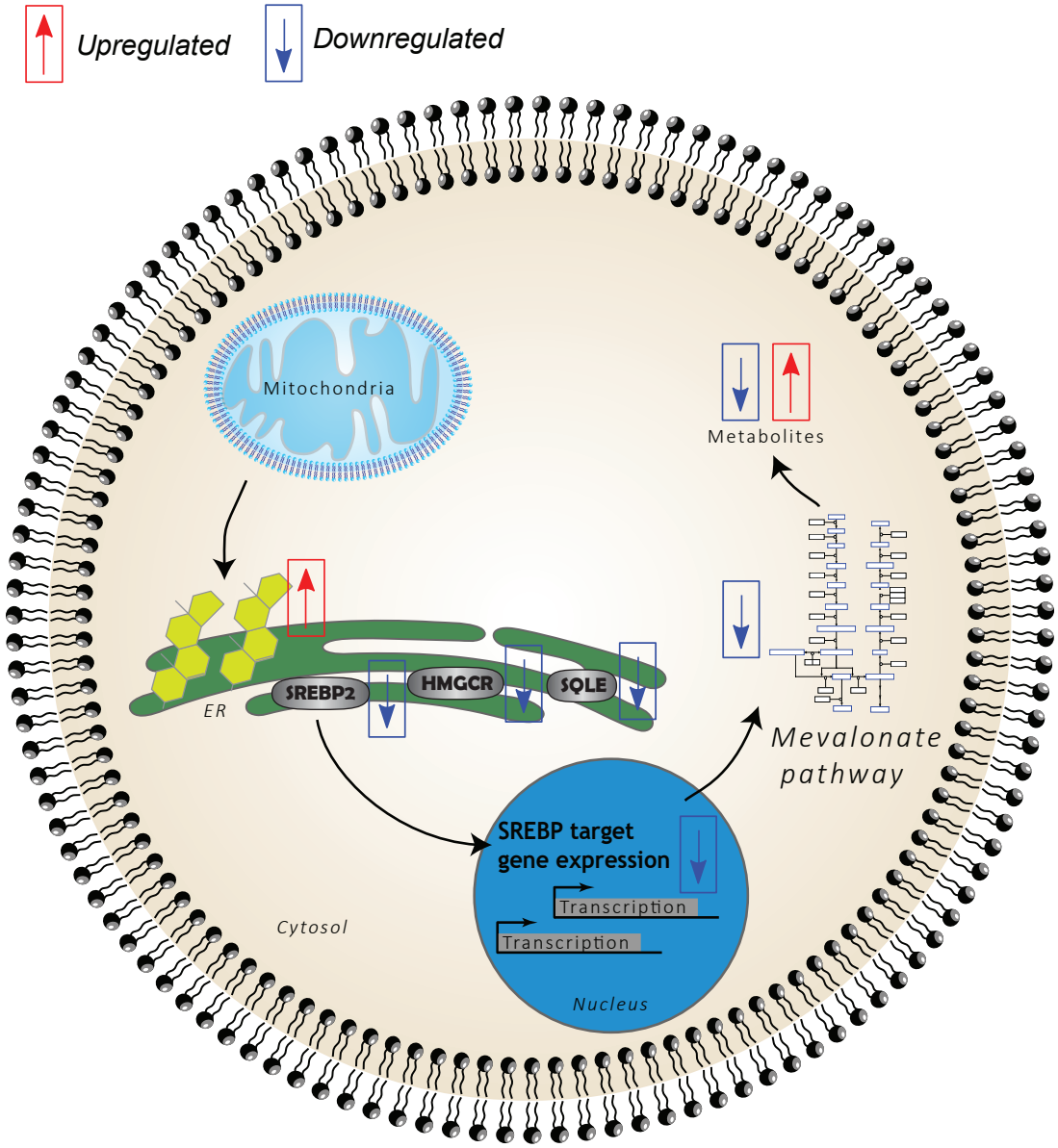

Figure 11.1 – **Schematic representation of discovered adaptations** Illustration of the intracellular environment showing the confirmed adaptaions of intracellular cholesterol metabolism in response to mitochondrial respiratory chain dysfunction. Suggested order of evens indicated by black arrows. Directionality of changes indicated by coloured boxed arrows (red; upregulated/increased. Blue; downregulated/decreased).

12 Future perspectives

The disruption of intracellular cholesterol homeostasis is a striking novel adaptive response to mitochondrial respiratory chain dysfunction. This work focussed on the discovery and validation of the observed downregulation of mevalonate pathway transcripts and the upstream mechanisms leading to the downregulation of the transcripts. Further research is warranted to elucidate the exact signals originating from the mitochondria that are interpreted to change the intrasellar free cholesterol. Comparing the biochemical differences with the degree of mevalonate pathway transcript changes between the separate chemical models, makes it tempting to imagine a role of redox metabolism of ROS. What would also be of interest is to dissect the role of transcriptional or post-translational regulation of the ER-resident cholesterol sensing enzymes. The downregulation of SREBP2 lowers the transcripts of all enzymes and there seems to be a sterol-mediated degradation, but exactly which contributes to the extended depletion of enzymes remains a mystery. Additional experiments will also shed light on the origin of the cholesterol that accumulated on the ER-membrane and validate the change with more sensitive assays. Here it was imagined that vesicular transport though the late endosomes may have been the source but inhibiting this trafficking did not abrogate the effect on SREBP2. More experiments through depleting certain pools of sterols may provide answers. Furthermore, the use of filipin is effective to measured differences in intracellular cholesterol, but the sensitivity of assay is moderate. More experiments should focus on extracting the intracellular fraction of cholesterol and quantifying with chromatographic methods.

Ultimately these findings must be translated into mitochondrial diseases, where the knowledge may provide new targets for treatments or supplements to alleviate symptoms of mitochondrial diseases. The first step would be to translate this into mouse models and observe the effect on a systemic level. Another first step to translating these findings is the careful characterisation of fibroblasts derived from mitochondrial disease patients to see if there are similar fingerprints of mevalonate pathway disruption. Here we have already confirmed the effect takes please in mouse tissue, proving the mechanism is conserved between human and mouse. A previous mitoGWAS has already identified mutations in the mitochondrial respiratory chain as a risk factor for the change in circulating lipoprotein levels, further strengthening

this discovery. Additional studies focussed on the plasma lipoprotein levels in mitochondrial disease patients may provide interesting findings. Lastly, the reversed may also be true that patients with chronically disrupted plasma lipoprotein levels have an underlying mitochondrial defect in the liver that may be diet-induced.

Altogether here we shed light on a clear link between mitochondrial dysfunction and cholesterol homeostasis, demonstrating that an impaired respiratory chain suppresses the mevalonate pathway. This work paves the way for a possible new therapeutic strategy for patients suffering from mitochondrial disease, or even inspire a new strategy for managing circulating cholesterol targeting mitochondria.

13 Materials and Methods

13.1 Reagents and chemicals

Unless otherwise stated all chemicals were from purchased from Merck KGaA (formerly Sigma Aldrich). See the tables of materials in the Annex for detailed information including supplier and product number. The AMPK activator 991 (5-[[6-Chloranyl-5-(1-Methylindol-5-Yl)-1h-Benzimidazol-2-Yl]oxy]-2-Methyl-Benzoic Acid; CAS no: 1219739-36-2) was custom synthesised by Spirochem. Assay specific reagents are included in the respective methods section.

13.2 Cyclodextrin loading

A stock solution of 5% methyl-beta-cyclodextrins (MBCD) (Merck, cat# C455) was prepared by dissolving in ultrapure water. A stock solution of 1% cholesterol (Merck, cat# C3045) was made in methanol:chloroform (2:1). To load the cyclodextrins the 5% aqueous MBCD solution was heated to 80°C to remove organic solvents. Under constant agitation cholesterol solution was dropwise added to a final concentration of 2.5 mM cholesterol. The solution was left to agitate until transparent between each addition of cholesterol solution. To ensure full encapsulation of the sterols in the cyclodextrins the solution was left shaking overnight.

13.3 Cell culture

Human primary fibroblasts (Cell Applications, cat# 106-05a), SV40 immortalised fibroblasts (ABM, cat# T0302) and HepG2 (ECACC, cat# 85011430) were cultured in Dulbecco's Modified Eagle Medium (DMEM, Gibco cat# 11966025), containing 4 mM glutamine in a humidified incubator with 5% CO2 at 37°C. The DMEM was supplemented with 5 mM glucose, 10% foetal bovine serum (FBS) and 100 IU/mL penicillin and 100 IU/mL streptomycin (Gibco, cat# 10270106, 15140122). For lipid deficient growth conditions, culture media was prepared as above, but the FBS was replaced with delipidised foetal bovine serum (Pan Biotech, cat#

P30-3401) and was supplemented with 1 μM of atorvastatin.

13.4 Transfections

For the transfection of plasmids molar ratios of 1:2 plasmid DNA were mixed with Lipofectamine 3000 reagents (Thermo Fisher, cat# L3000001) according to manufacturers protocol. A volume corresponding with 1 μg of total DNA was added to a suspension of 300.000 cells and immediately plated in a 6-well plate. After 30 hours the cells were trypsinised and GFP expressing cells were sorted into 96-wells plates, plating 1 cell per well. Cells were expanded using standard culture protocols.

13.5 Growth rate and apoptosis assays

Cells were plated at a density of 1x103 cells per well in a clear 96-well plate. After 24 hours 200 μL of media containing inhibitors or an equivalent volume of DMSO was added to the plate. For the apoptosis assays an additional 1:200 diluted Annexin V Green Reagent (Satorius, cat# 4642) was added to the base medium. Cellular growth and apoptosis was measured in the Incucyte ZOOM live cell analysis system. Growth metrics were calculated with the R package Growthcurver (Sprouffske and Wagner, 2016). Apoptosis counts were expressed as total fluorescent counts after 5 days.

13.6 Immunoblotting

Cells were routinely seeded at 1x106 cells in a 60 cm2 petri dish 24 hours before addition of chemical compounds. On the day of collection cells were washed twice with ice-cold PBS on ice, and lysed in 150 uL of Radio-Immunoprecipitation Assay (RIPA, Merck cat# R0278) buffer, supplemented with 10 mM sodium-fluoride, 2 mM sodium-orthovanadate, 0.1 μM phenylmethylsulfonyl fluoride, 1x "cOmplete Protease Inhibitor Cocktail" (Roche, Cat# 11697498001), 1x "PhosSTOP" (Roche, Cat# 4906845001). The resulting lysate was cleared by centrifugation at 8'000 x g for 20 minutes at 4°C. The protein content of the clear supernatant was quantified by Pierce™ BCA Protein Assay Kit (Thermofisher, Cat# 23225). Samples were diluted to 1 μg/μL and boiled for 5 minutes at 95°C in Laemmli sample buffer (Alfa Aesar, Cat# J60015). SDS-acrylamide gels were hand-casted according to manufacturer's guidelines using a Bio-Rad casting system (Bio-Rad, Cat#1658050). Routinely 25 μg of protein sample was separated on a 10% SDS-acrylamide gel. Following separation, proteins were transferred to nitrocellulose membrane paper (Li-Cor, Cat# 926-31092) in Bjerrum Schafer-Nielsen buffer (48 mM Tris, 39 mM glycine, pH 9.2) with 10% methanol on ice. Membranes were blocked for 1 hour in Odyssey blocking buffer (Li-Cor, Cat# 927-50000) and incubated with primary antibodies (see table) overnight in 5% bovine serum albumin (BSA) (Sigma, Cat#A2153) in Tris-buffered saline (20 mM Tris-HCL, 500 mM NaCl, pH 7.5) with 0.05% tween 20 (TBS-t).

Membranes were washed three times 10 minutes with TBS-t, after which the membrane was incubated with secondary antibody (Thermofisher, Cat# A11369, A32729. 1:10'000 in 5% BSA) for 1 hour. Westernblots were imaged with an Odyssey CLx imaging system (LI-COR Biosciences, USA) and quantified with the Image Studio v5.2 software.

13.7 Real-time qPCR

Fibroblasts were seeded at 1x106 cells in a 60 cm2 petri dish 24 hours before addition of chemical compounds. On the day of collection cells were washed 2x with ice-cold PBS on ice, and lysed in 1 mL of TRIzol reagent (Thermofisher, cat# 155960260). RNA was extracted from the lysate according to manufacturer's guidelines. RNA was resuspended in 32 uL of ultrapure RNase-free water. The concentration was assessed with a NanoDrop Microvolume Spectrophotometer (Thermo Fisher Scientific, USA). Immediately after quantification reverse transcription was performed with the PrimeScript™ RT Reagent Kit (Takara bio, cat#RR037B). Levels of mRNA were measured using SYBR Green LightCycler® 1536 DNA Green Master (Roche, cat# 05573092001). Relative quantification of Ct values was calculated with the $\Delta\Delta$Ct method (Livak and Schmittgen, 2001), normalising the Ct values to the housekeeping gene TBP.

13.8 Seahorse XF analyser

Cellular oxygen consumption rates were measured using a Seahorse XFe96 Analyser. The following protocol was adapted from the manufacturers protocol. Cells were seeded at 70'000 cells per well in a 96-well Seahorse XF cell culture plate. Cells were left at room temperature to evenly distribute the cells according to (Lundholt et al., 2003). The following day medium was exchanged for carbonate-free DMEM (Merck, cat# D5030) containing 5 mM glucose, 4 mM glutamine. Cells were left for 60 minutes to equilibrate in a CO2 free incubator at 37°C, before placing in the analyser. To measure the dose dependent decrease of respiration, a range of concentrations of the inhibitors were injected and the remaining respiration measured. Lastly rotenone (50 μM) and antimycin A (50 μM) were injected to measure non-mitochondrial respiration. After completion of the measurement the supernatant was aspirated and 25 μL of lysis buffer (1% SDS, 0.1 N NaOH) was added. The plate was briefly vortexed and the protein content was measured with a BCA protein assay (Thermo Fischer Scientific, cat# 23225). The respiration measurements were normalised to protein content per well and values are reported in residual respiration after compound injection, relative to baseline in each well.

13.9 DNA sequencing

Amplicon QC – Pooling and Purification steps. DNA from single-cell derived colonies was extracted with the DNeasy DNA-extraction kit according to manufacturers protocol. The three

target sites were amplified by the Q5® High-Fidelity DNA Polymerase kit (New England Biolabs, cat# M0491) using manufacturers protocol with 200 ng starting material for 30 cycles at 60°C. For each sample the 3 amplicons were pooled equal-volume then purified with AMPURE Beads (Beckman Coulter, cat# A63882) at ratio 1:1 and eluted in 20ul. The same volume 5 or 10 μL of each sample was used to prepare the libraries.

Celero DNA-Seq Library preparation The DNA libraries were prepared with the Celero EZ DNA-seq preparation kit (Tecan, cat# 0360-24). Brielfly, amplicons were end repaired to which specific indexed adaptor sequences were added. The libraries were amplified for 7 PCR cycles. The resulting libraries were again purified with two rounds of AMPURE bead in a ratio of 1:1. Libraries were quantified with the Nuquant system provided in the kit and usable directly on Qubit system to for quantification. Sequencing was performed on MiSeq System with MiSeq V2 500 cycles chemistry (Illumina, cat# MS-102-2001) and loaded at 12pM with 10% PhiX Control v3 library (Illumina, cat# FC-110-3001). The run was prepared with LRM (Local Run Manager), with FastQ only module. The resulting FastQ files were analysed with the online tool Cas-Analyser as published (Park et al., 2017).

13.10 3'RNAseq

The transcriptome of our studied models was measured with QuantSeq 3' RNA sequencing. Total RNA was extracted from the treated primary fibroblasts using Agencourt RNAdvance Tissue kit (Beckman Coulter Life sciences, cat# A32646) and quantified using a Quant-iT RiboGreen RNA Assay Kit (Invitrogen, cat# R11490). 250 ng RNA was used to generate libraries using the QuantSeq 3' mRNA-Seq library prep kit (FWD) HT for Illumina (Lexogen). The kit uses total RNA as input, hence no prior poly(A) enrichment or rRNA depletion is needed. The libraries were amplified for 17 cycles quantified with Quant-iT PicoGreen dsDNA Assay Kit (Invitrogen, cat# P7589). Size pattern was controlled with the High Sensitivity NGS Fragment Analysis kit on a Fragment Analyzer (Agilent DNF-474). Libraries were pooled at an equimolar ratio (i.e an equal quantity of each sample library) and clustered at a concentration of 9 pM on single read (SR) sequencing flow cell (Illumina). Sequencing was performed for 65 cycles on a HiSeq 2500 (Illumina) using the Rapid SBS Kit v2 (Illumina, cat# FC-402-4021). Sequencing reads were trimmed with BBDuk (BBTools version 35.85, Bushnell B., sourceforge.net/projects/bbmap/). Mapping to the human genome (built GRCh38.p2) was performed with RNA STAR version 2.3.0e (Dobin et al., 2013) using default parameters. Gene count was performed with HTSeq (Anders et al., 2015) version 0.5.4p3. Calculation of differentially expressed genes for each treatment were identified using the R package edgeR (Robinson et al., 2009). Clustering of GO-biological processes was performed with the ShinyGO online tool version 0.61 (Xijin Ge et al., 2020).

13.11 Metabolomics

Cells were plated at 3 million cells in a TPP300 peel-off flask (TPP, cat# 90303). After 24 hours 50 mL of media containing inhibitor or equivalent amounts of DMSO were added to the cells. After 48 hours the cells were placed on ice and rapidly the medium was aspirated, and the cells washed three times with ice-cold NaCl 0.9% solution. Immediately after washing, the cells were snap frozen on liquid nitrogen and placed on dry ice. Exactly 3.5 mL ice-cold methanol was added to the flask and all the material was collected by scratching and collected in a falcon tube. This step was repeated once to ensure maximal recovery of cellular material. Two identical flasks were pooled in one falcon tube and stored at -80°C until processing. Before sample preparation the samples were dried in a nitrogen evaporator at room temperature under a gentle nitrogen flow for 24 hours.

The cell pellet of each sample was resuspended in 200 μL of 50% methanol and then transferred to a 5-mL Eppendorf tube. The samples were lysed by homogenizing with the aid of two metal balls on a MM 400 mill mixer at a frequency of 30 Hz for 1 min three times. 0.8 mL of mixed methanol/chloroform (3:1, v/v) was then added to each tube. The homogenization step was repeated three times, followed by ultra-sonication in an ice-water bath for 5 min. The samples were centrifuged at 4,000 g for 45 min. The clear supernatants were collected and the residues were used for protein assay using a standardized Bradford procedure. 2. Quantitation of HMG-CoA and isoprenyl phosphates

250 μL of the supernatant of each sample was mixed with 200 μL of an internal standard solution of HMG-CoA-D3 and 100 μL of chloroform. The mixture was vortexed for 30 s, followed by centrifugal clarification for 5 min. After carful removal of the low organic phase using gel-loading tips, the upper aqueous phase was dried under a gentle nitrogen gas flow in a nitrogen evaporator. The residue was reconstituted in 200 μL of 50% methanol. A stock solution containing standard substances of HMG-CoA and isoprenyl phosphates was prepared in the internal standard solution. This standard solution was serially diluted in a ratio of 1 to 4 (v/v) to have calibration solutions in a range of 0.0001 to 10 μM. 10-μL aliquots of the calibration solutions and the sample solutions were injected to run LCMRM on a Water Acquity UPLC system coupled to a Sciex QTRAP 6500 mass spectrometer operated in the negative-ion mode, using a C18 column (2.1*150 mm, 1.8 μm) and a mobile phase composed of ammonium acetate buffer (A) and acetonitrile (B) as the mobile phase for binary-solvent gradient elution (5% to 80% B in 12) at 0.3 mL/min and 50 °C. Concentrations of the detected compounds were calculated by interpolating the constructed linear-regression, internal-calibration curves with the peak area ratios measured from sample solutions. Note: IPPP and DMAPP cannot be separated and their total amount in each sample was reported.

3. Quantitation of sterols 200 μL of the supernatant of each sample was dried under a gentle nitrogen gas flow. The residue was resuspended in 100 μL of a 13C3-cholesterol internal standard solution. Along with the sample preparation, serially diluted standard solutions of sterols were prepared in the same internal standard solution. 100 μL of each sample solution

or each standard solution was mixed with 100 μL of 20 mM dansyl chloride solution and 100 μL of 25-mM dimethylaminopyridine solution. The mixture was allowed to react at 50 C for 60 min. After reaction, the solution was dried in a speed-vac concentrator and the residue was reconstituted in 400 μL of acetonitrile. 10μL aliquots were injected onto a C18 UPLC column (2.1x50 cm, 1.7 μm) to run UPLC-MRM/MS on an Agilent 1290 UHPLC system coupled to n Agilent 6495B QQQ mass spectrometer operated in the positive-ion mode, using 0.1% formic acid in water acetonitrile/isopropanol (1:1) as the LC mobile phase for binary-solvent gradient elution at 0.35 mL/min and at 60 ^{o}C. Concentrations of individual sterols were calculated with the analyte-to-internal standard peak area ratios measured from injections of sample solutions to interpolate the constructed linear regression calibration curves of individual sterols in appropriate concentration ranges.

4. Quantitation of isoprenoids (dolichols, ubiquinones, squalene, oxidosqualene and MK4) 500 μL of each supernatant was mixed with 500 μL of 50% methanol and 1000 μL of hexane. After vortex mixing and centrifugal clarification, the organic phase was collected. The extraction was repeated with 1000 μL of hexane twice. The pooled hexane extractant of each sample was dried under a gentle nitrogen gas flow. The residue was dissolved in 100 μL of isopropanol. Along with the sample preparation, a standard solution of squalene, 2,3-oxidosqualene, MK-4, CoQ 6, 8, 9 and 10, and a mixture of dolichols 13-21, was prepared in isopropanol and was then serially diluted in a volume ratio of 1 to 4. 20 μL of each sample solution or each standard solution was injected to run LC-MRM/MS on a Water Acquity UPLC system coupled to a Sciex QTRAP 6500 mass spectrometer with positive-ion detection, using a C8 column (2.1*50 mm, 1.7 μm) and a mobile phase of 0.1% formic acid in water (A) and isopropanol (B) as the mobile phase for binary-solvent gradient elution (50% to 90% B in 15 min) at 0.25 mL/min and 50 °C. Molar concentrations of the detected compounds were calculated by interpolating the constructed linear-regression calibration curves from injection of calibration solutions, with the peak areas measured from sample solutions. Concentrations of dolichols were measured as the total weight amount of all detected dolichol compounds in each sample

13.12 Gas chromatography

Fibroblasts were seeded at 200'000 cells per well in a 6-well plate. The next day, media containing the interventions was added. After 48 hours the cells were trypsinised, washed once in PBS and the cell pellet was collected. The pellets were snap frozen at -80°C until analysis. On the day of analysis, the cell pellet was resuspended in 600 μL of 1M KOH in ethanol. A known amount of cholesterol was treated in the same way as calibration sample. To this solution 600 μL of a known concentration of epicoprostanol solution in cyclohexane was added as internal standard. For complete saponification the solution was left shaking overnight. This step ensures release of all cellular cholesterol and de-esterifies all cholesterol-esters. To this solution, 600 μL of 1 M KOH in water was added and was shaken for 15 minutes. The resulting solution was centrifuge for 15 min at 700g. The supernatant was transferred to clean autosampler vials and the liquid was completely dried under a nitrogen flow. To the vial

100 μL N,O-Bis(trimethylsilyl)trifluoroacetamide (BSTFA) and 25 μL of Trimethylsilyl chloride (TMCS) was added and the whole was heated to 80°C for 45 minutes. The vials were then cooled to room temperature and dried under a gentle nitrogen flow. Following this, 1 mL of 5% N,O-bis(trimethylsilyl)-acetamide in hexane was added and the vials were vortexed for 2 minutes. 1 μL of the samples were injected into an Agilent 7890B gas-chromatography system coupled to a flame ionisation detector. Samples were run in high purity helium gas through a 30 m DB-5 capillary column coated with (5 % phenyl)-methylpolysiloxane.

13.13 Confocal microscopy

Experimental procedures were adapted from a published protocol (Wilhelm Léa P. et al., 2019). Cells were seeded at 100.000 in 35 mm glass-bottom microscopy dishes (MaTek, cat# P35G-1.5-14-C). After 24 hours, the plating media was aspirated, cells were washed once with PBS and fresh media containing the interventions was added. After 48 hours a 5% cyclodextrin solution was added to a final concentration of 10 mM for 15 minutes to remove plasma membrane cholesterol. Cells were immediately washed three times with PBS and fixed with 4% PFA for 15 minutes at room temperature. After fixation the cells were again washed three times with PBS and a 50 μg/mL filipin solution in PBS was added. The cells were kept in the dark for three hours under gentle agitation on a rotary shaker to ensure complete penetration of the filipin compound. After staining the cells were again washed three times with PBS in a dark environment. Cells were kept in PBS during image acquisition. Filipin fluorescence intensity was captured on a confocal microscope (Leica, SP5) using a × 60 objective (oil; CFI Plan APO 1.4 NA). Filipin was excited with a Chameleon Ultra II multiphoton laser (Coherent) (1% transmission, 5% gain, 20% offset) at 700 nm (excitation) and the emission was collected at 380-535 nm. Images were acquired a scan resolution of 1024 x 1024 and a pinhole of 60 μm, at an 8-bit bit depth. Images were acquired at ten different positions per coverslip. Quantification of intensity was performed using FIJI software (Schindelin et al., 2012). The lower threshold of the intensity was set at 50 px for each image. Intensity was expressed as mean intensity per each image.

14 Resource tables

14.1 Chemicals

Chemical	Supplier	Product number
DMSO	Merck KGaA	D2650
Rotenone	Merck KGaA	R8875
Antimycin A	Merck KGaA	A8674
Oligomycin A	Merck KGaA	75351
U18666a	Merck KGaA	U3633
Atorvastatin	Chemie Brunschwig AG	TRCA791750
Glucose	Merck KGaA	G7021
Rapamycin	Merck KGaA	553210
Compound C	Merck KGaA	171260
Methanol	Merck KGaA	1.06018
Chloroform	Merck KGaA	1.02444

14.2 Antibodies

Target protein	Supplier	Product no.
SREBP2	BD Biosciences	557037
SQLE	Cell Signaling Technology	40659S
HMGCR	Thermo Fisher	MA5-31335
SERCA2	Cell Signaling Technology	4388S
Calnexin	Cell Signaling Technology	2679
Vinculin	Cell Signaling Technology	4650S
GAPDH	Cell Signaling Technology	2118S

14.3 plasmids

Target	Supplier	Product number
NDUFS4	Santa cruz biotechnology, inc	sc-405184
NDUFS6	Santa cruz biotechnology, inc	sc-410904

14.4 Primers

Gene	Fw	Rv
TBP	TGGTGTGCACAGGAGCCAAG	TTCACATCACAGCTCCCCAC
ACAT2	TCGCCATGGGAGCAACATAG	ATTGGCTGGGGTGACTGTTC
HMGCS1	TCTTGGGATGGACGGTATGC	CACGAAGCCCTCGTTCAAAA
HMGCR	GCCCTCAGTTCCAACTCACA	TTCAAGCTGACGTACCCCTG
DHCR7	GACAACTGGATCCCACTGCT	CGATGCCCATCATGTAGTTG
SQLE	GTCTCCGGAAAGCAGCTATG	AAAAGCCCATCTGCAACAAC

Bibliography

Acin-Perez R, Enriquez JA. 2014. The function of the respiratory supercomplexes: The plasticity model. Biochimica et Biophysica Acta - Bioenergetics. doi:10.1016/j.bbabio.2013.12.009

Acosta MJ, Vazquez Fonseca L, Desbats MA, Cerqua C, Zordan R, Trevisson E, Salviati L. 2016. Coenzyme Q biosynthesis in health and disease. Biochimica et Biophysica Acta - Bioenergetics 1857:1079–1085. doi:10.1016/j.bbabio.2016.03.036

Ahmadian M, Abbott MJ, Tang T, Hudak CSS, Kim Y, Bruss M, Hellerstein MK, Lee HY, Samuel VT, Shulman GI, Wang Y, Duncan RE, Kang C, Sul HS. 2011. Desnutrin/ATGL is regulated by AMPK and is required for a brown adipose phenotype. Cell Metabolism 13:739–748. doi:10.1016/j.cmet.2011.05.002

al Maruf A, Lee O, O'Brien PJ. 2014. Modifications of Mitochondrial Function by Toxicants Reference Module in Biomedical Sciences. Elsevier. doi:10.1016/B978-0-12-801238-3.01900-0

Alpy F, Tomasetto C. 2005. Give lipids a START: The StAR-related lipid transfer (START) domain in mammals. Journal of Cell Science 118:2791–2801. doi:10.1242/jcs.02485

Bando H, Atsumi T, Nishio T, Niwa H, Mishima S, Shimizu C, Yoshioka N, Bucala R, Koike T. 2005. Phosphorylation of the 6-phosphofructo-2-kinase/fructose 2,6-bisphosphatase/PFKFB3 family of glycolytic regulators in human cancer. Clinical Cancer Research 11:5784–5792. doi:10.1158/1078-0432.CCR-05-0149

Barrow JJ, Balsa E, Verdeguer F, Tavares CDJ, Soustek MS, Hollingsworth LR, Jedrychowski M, Vogel R, Paulo JA, Smeitink J, Gygi SP, Doench J, Root DE, Puigserver P. 2016. Bromodomain Inhibitors Correct Bioenergetic Deficiency Caused by Mitochondrial Disease Complex I Mutations. Molecular Cell 64:163–175. doi:10.1016/j.molcel.2016.08.023

Beg ZH, Stonik JA, Brewer HB. 1984. In vivo modulation of rat liver 3-hydroxy-3-methylglutaryl-coenzyme A reductase, reductase kinase, and reductase kinase kinase by mevalonolactone. Proceedings of the National Academy of Sciences 81:7293–7297. doi:10.1073/pnas.81.23.7293

Belevich I, Verkhovsky MI, Wikström M. 2006. Proton-coupled electron transfer drives the proton pump of cytochrome c oxidase. Nature 440:829–832. doi:10.1038/nature04619

Bodnar NO, Kim KH, Ji Z, Wales TE, Svetlov V, Nudler E, Engen JR, Walz T, Rapoport TA. 2018. Structure of the Cdc48 ATPase with its ubiquitin-binding cofactor Ufd1–Npl4. Nature Structural & Molecular Biology 25. doi:10.1038/s41594-018-0085-x

Bowden K, Ridgway ND. 2008. OSBP negatively regulates ABCA1 protein stability. Journal of Biological

Chemistry 283:18210–18217. doi:10.1074/jbc.M800918200

Boyer PD. 1997. The ATP synthase - a splendid molecular machine. Annu Rev Biochem 66:717–766.

Breuer ME, Willems PHGM, Smeitink JAM, Koopman WJH, Nooteboom M. 2013. Cellular and animal models for mitochondrial complex i deficiency: A focus on the NDUFS4 subunit. IUBMB Life 65:202–208. doi:10.1002/iub.1127

Brown MS, Goldstein JL. 1997. The SREBP Pathway: Regulation Review of Cholesterol Metabolism by Proteolysis of a Membrane-Bound Transcription Factor, Cell.

Buhaescu I, Izzedine H. 2007. Mevalonate pathway: A review of clinical and therapeutical implications. Clinical Biochemistry 40:575–584. doi:10.1016/j.clinbiochem.2007.03.016

Burg JS, Espenshade PJ. 2011. Regulation of HMG-CoA reductase in mammals and yeast. Progress in Lipid Research. doi:10.1016/j.plipres.2011.07.002

Butow RA, Avadhani NG. 2004. Mitochondrial Signaling: The Retrograde Response. Molecular Cell 14:1–15.

Calkin AC, Tontonoz P. 2012. Transcriptional integration of metabolism by the nuclear sterol-activated receptors LXR and FXR. Nature Reviews Molecular Cell Biology 13:213–224. doi:10.1038/nrm3312

Calvo SE, Clauser KR, Mootha VK. 2016. MitoCarta2.0: An updated inventory of mammalian mitochondrial proteins. Nucleic Acids Research 44:D1251–D1257. doi:10.1093/nar/gkv1003

Carling D, Zammit VA, Hardie DG. 1987. A common bicyclic protein kinase cascade inactivates the regulatory enzymes of fatty acid and cholesterol biosynthesis. FEBS Letters 223:217–222. doi:10.1016/0014-5793(87)80292-2

Cerutti R, Pirinen E, Lamperti C, Marchet S, Sauve AA, Li W, Leoni V, Schon EA, Dantzer F, Auwerx J, Viscomi C, Zeviani M. 2014. NAD+-dependent activation of Sirt1 corrects the phenotype in a mouse model of mitochondrial disease. Cell Metabolism 19:1042–1049. doi:10.1016/j.cmet.2014.04.001

Chambers CM, Ness GC. 1998. Dietary Cholesterol Regulates Hepatic 3-Hydroxy-3-methylglutaryl Coenzyme A Reductase Gene Expression in Rats Primarily at the Level of Translation. Archives of Biochemistry and Biophysics 354. doi:10.1006/abbi.1998.0689

Chang T-Y, Li B-L, Y Chang CC, Urano Y. 2009. Acyl-coenzyme A:cholesterol acyltransferases. Am J Physiol Endocrinol Metab 297:1–9. doi:10.1152/ajpendo.90926.2008

Chavez JA, Roach WG, Keller SR, Lane WS, Lienhard GE. 2008. Inhibition of GLUT4 translocation by Tbc1d1, a Rab GTPase-activating protein abundant in skeletal muscle, is partially relieved by AMP-activated protein kinase activation. Journal of Biological Chemistry 283:9187–9195. doi:10.1074/jbc.M708934200

Chua NK, Howe V, Jatana N, Thukral L, Brown AJ. 2017. A conserved degron containing an amphipathic helix regulates the cholesterol-mediated turnover of human squalene monooxygenase, a rate-limiting enzyme in cholesterol synthesis. Journal of Biological Chemistry. doi:10.1074/jbc.M117.794230

Clark BJ, Wells J, King SR, Stocco DM. 1994. The purification, cloning, and expression of a novel luteinizing hormone- induced mitochondrial protein in MA-10 mouse Leydig tumor cells. Characterization of the Steroidogenic Acute Regulatory protein (StAR). Journal of Biological Chemistry

269:28314–28322. doi:10.1016/s0021-9258(18)46930-x

Coleman ML, Marshall CJ, Olson MF. 2004. RAS and RHO GTPases in G1-phase cell-cycle regulation. Nature Reviews Molecular Cell Biology 5:355–366. doi:10.1038/nrm1365

Colgan SM, Tang D, Werstuck GH, Austin RC. 2007. Endoplasmic reticulum stress causes the activation of sterol regulatory element binding protein-2. International Journal of Biochemistry and Cell Biology 39:1843–1851. doi:10.1016/j.biocel.2007.05.002

Cunningham JT, Rodgers JT, Arlow DH, Vazquez F, Mootha VK, Puigserver P. 2007. mTOR controls mitochondrial oxidative function through a YY1-PGC-1α transcriptional complex. Nature 450:736–740. doi:10.1038/nature06322

Das A, Brown MS, Anderson DD, Goldstein JL, Radhakrishnan A. 2014. Three pools of plasma membrane cholesterol and their relation to cholesterol homeostasis. eLife 2014. doi:10.7554/eLife.02882

DeGrella RF, Simoni RD. 1982. Intracellular transport of cholesterol to the plasma membrane. Journal of Biological Chemistry 257:14256–14262. doi:10.1016/s0021-9258(19)45374-x

Deng Q, Guo T, Zhou X, Xi Y, Yang X, Ge W. 2016. Cross-talk between mitochondrial fusion and the Hippo pathway in controlling cell proliferation during Drosophila development. Genetics 203:1777–1788. doi:10.1534/genetics.115.186445

Distelmaier F, Valsecchi F, Liemburg-Apers DC, Lebiedzinska M, Rodenburg RJ, Heil S, Keijer J, Fransen J, Imamura H, Danhauser K, Seibt A, Viollet B, Gellerich FN, Smeitink JAM, Wieckowski MR, Willems PHGM, Koopman WJH. 2015. Mitochondrial dysfunction in primary human fibroblasts triggers an adaptive cell survival program that requires AMPK-α. Biochimica et Biophysica Acta - Molecular Basis of Disease 1852:529–540. doi:10.1016/j.bbadis.2014.12.012

Egan DF, Shackelford DB, Mihaylova MM, Gelino S, Kohnz RA, Mair W, Vasquez DS, Joshi A, Gwinn DM, Taylor R, Asara JM, Fitzpatrick J, Dillin A, Viollet B, Kundu M, Hansen M, Shaw RJ. 2011. Phosphorylation of ULK1 (hATG1) by AMP-Activated Protein Kinase Connects Energy Sensing to Mitophagy. Science 331. doi:10.1126/science.1196371

Eid W, Dauner K, Courtney KC, Gagnon AM, Parks RJ, Sorisky A, Zha X. 2017. mTORC1 activates SREBP-2 by suppressing cholesterol trafficking to lysosomes in mammalian cells. Proceedings of the National Academy of Sciences of the United States of America 114:7999–8004. doi:10.1073/pnas.1705304114

Elustondo P, Martin LA, Karten B. 2017. Mitochondrial cholesterol import. Biochimica et Biophysica Acta - Molecular and Cell Biology of Lipids 1862:90–101. doi:10.1016/j.bbalip.2016.08.012 Fassone E, Rahman S. 2012. Complex I deficiency: clinical features, biochemistry and molecular genetics. Journal of Medical Genetics 49:578–590. doi:10.1136/jmedgenet-2012-101159

Ferrari M, Jain IH, Goldberger O, Rezoagli E, Thoonen R, Chen KH, Sosnovik DE, Scherrer-Crosbie M, Mootha VK, Zapol WM. 2017. Hypoxia treatment reverses neurodegenerative disease in a mouse model of Leigh syndrome. Proceedings of the National Academy of Sciences of the United States of America 114:E4241–E4250. doi:10.1073/pnas.1621511114

Fessler E, Eckl EM, Schmitt S, Mancilla IA, Meyer-Bender MF, Hanf M, Philippou-Massier J, Krebs S, Zischka H, Jae LT. 2020. A pathway coordinated by DELE1 relays mitochondrial stress to the cytosol. Nature 579:433–437. doi:10.1038/s41586-020-2076-4

Fiorese CJ, Schulz AM, Lin YF, Rosin N, Pellegrino MW, Haynes CM. 2016. The Transcription Factor ATF5 Mediates a Mammalian Mitochondrial UPR. Current Biology 26:2037–2043. doi:10.1016/j.cub.2016.06.002

Foresti O, Ruggiano A, Hannibal-Bach HK, Ejsing CS, Carvalho P. 2013. Sterol homeostasis requires regulated degradation of squalene monooxygenase by the ubiquitin ligase Doa10/Teb4. eLife 2013. doi:10.7554/eLife.00953

Fusakio ME, Willy JA, Wang Y, Mirek ET, Baghdadi RJTA, Adams CM, Anthony TG, Wek RC. 2016. Transcription factor ATF4 directs basal and stress-induced gene expression in the unfolded protein response and cholesterol metabolism in the liver. Molecular Biology of the Cell 27:1536–1551. doi:10.1091/mbc.E16-01-0039

Gallegos AM, Schoer JK, Starodub O, Kier AB, Billheimer JT, Schroeder F. 2000. A potential role for sterol carrier protein-2 in cholesterol transfer to mitochondria. Chemistry and Physics of Lipids 105:9–29. doi:10.1016/S0009-3084(99)00128-0

García-Bartolomé A, Peñas A, Marín-Buera L, Lobo-Jarne T, Pérez-Pérez R, Morán M, Arenas J, Martín MA, Ugalde C. 2017. Respiratory chain enzyme deficiency induces mitochondrial location of actin-binding gelsolin to modulate the oligomerization of VDAC complexes and cell survival. Human molecular genetics 26:2493–2506. doi:10.1093/hmg/ddx144

Garza RM, Tran PN, Hampton RY. 2009. Geranylgeranyl Pyrophosphate Is a Potent Regulator of HRD-dependent 3-Hydroxy-3-methylglutaryl-CoA Reductase Degradation in Yeast. Journal of Biological Chemistry 284. doi:10.1074/jbc.M109.023994

Gatliff J, Campanella M. 2016. TSPO: Kaleidoscopic 18-kDa amid biochemical pharmacology, control and targeting of mitochondria. Biochemical Journal. doi:10.1042/BJ20150899

Gerards M, Sallevelt SCEH, Smeets HJM. 2016. Leigh syndrome: Resolving the clinical and genetic heterogeneity paves the way for treatment options. Molecular Genetics and Metabolism. doi:10.1016/j.ymgme.2015.12.004

Gill S, Stevenson J, Kristiana I, Brown AJ. 2011. Cholesterol-dependent degradation of squalene monooxygenase, a control point in cholesterol synthesis beyond HMG-CoA reductase. Cell Metabolism 13:260–273. doi:10.1016/j.cmet.2011.01.015

Goldstein JL, DeBose-Boyd RA, Brown MS. 2006. Protein sensors for membrane sterols. Cell 124:35–46. doi:10.1016/j.cell.2005.12.022

Golomb BA, Evans MA. 2008. Statin Adverse Effects A Review of the Literature and Evidence for a Mitochondrial Mechanism, Am J Cardiovasc Drugs.

Goncalves RLS, Quinlan CL, Perevoshchikova I v., Hey-Mogensen M, Brand MD. 2015. Sites of Superoxide and Hydrogen Peroxide Production by Muscle Mitochondria Assessed ex Vivo under Conditions Mimicking Rest and Exercise. Journal of Biological Chemistry 290:209–227. doi:10.1074/jbc.M114.619072

Gong L, Xiao Y, Xia F, Wu P, Zhao T, Xie S, Wang R, Wen Q, Zhou W, Xu H, Zhu L, Zheng Z, Yang T, Chen Z, Duan Q. 2019. The mevalonate coordinates energy input and cell proliferation. Cell Death and Disease 10. doi:10.1038/s41419-019-1544-y

Gropper SS, Smith JL, Carr TP. 2016. Advanced Nutrition and Human Metabolism. Cengage Learning.

Guo X, Aviles G, Liu Y, Tian R, Unger BA, Lin YHT, Wiita AP, Xu K, Correia MA, Kampmann M. 2020. Mitochondrial stress is relayed to the cytosol by an OMA1–DELE1–HRI pathway. Nature 579:427–432. doi:10.1038/s41586-020-2078-2

Gwinn DM, Shackelford DB, Egan DF, Mihaylova MM, Mery A, Vasquez DS, Turk BE, Shaw RJ. 2008. AMPK Phosphorylation of Raptor Mediates a Metabolic Checkpoint. Molecular Cell 30:214–226. doi:10.1016/j.molcel.2008.03.003

Hall EA, Pandak WM. 2005. Mitochondrial Cholesterol Transport: A Possible Targetin the Management of Hyperlipidemia. Lipids 40:1237–1244.

Hong YH, Varanasi US, Yang W, Leff T. 2003. AMP-activated protein kinase regulates HNF4α transcriptional activity by inhibiting dimer formation and decreasing protein stability. Journal of Biological Chemistry 278:27495–27501. doi:10.1074/jbc.M304112200

Horvath SE, Daum G. 2013. Lipids of mitochondria. Progress in Lipid Research. doi:10.1016/j.plipres.2013.07.002

Howe V, Sharpe LJ, Prabhu A v., Brown AJ. 2017. New insights into cellular cholesterol acquisition: promoter analysis of human HMGCR and SQLE, two key control enzymes in cholesterol synthesis. Biochimica et Biophysica Acta - Molecular and Cell Biology of Lipids 1862:647–657. doi:10.1016/j.bbalip.2017.03.009

Hua X, Nohturfft A, Goldstein JL, Brown MS. 1996. Sterol Resistance in CHO Cells Traced to Point Mutation in SREBP Cleavage-Activating Protein. Cell 87:415–426.

Huang S, Wang X, Wu X, Yu J, Li J, Huang X, Zhu C, Ge H. 2018. Yap regulates mitochondrial structural remodeling during myoblast differentiation. American Journal of Physiology - Cell Physiology 315:C474–C484. doi:10.1152/ajpcell.00112.2018

Hüttemann M, Lee I, Samavati L, Yu H, Doan JW. 2007. Regulation of mitochondrial oxidative phosphorylation through cell signaling. Biochimica et Biophysica Acta - Molecular Cell Research 1773:1701–1720. doi:10.1016/j.bbamcr.2007.10.001

Hüttemann M, Pecina P, Rainbolt M, Sanderson TH, Kagan VE, Samavati L, Doan JW, Lee I. 2011. The multiple functions of cytochrome c and their regulation in life and death decisions of the mammalian cell: From respiration to apoptosis. Mitochondrion 11:369–381. doi:10.1016/j.mito.2011.01.010

Hwang S, Nguyen AD, Jo Y, Engelking LJ, Brugarolas J, DeBose-Boyd RA. 2017. Hypoxia-inducible factor 1α activates insulin-induced gene 2 (Insig-2) transcription for degradation of 3-hydroxy-3-methylglutaryl (HMG)-CoA reductase in the liver. Journal of Biological Chemistry 292:9382–9393. doi:10.1074/jbc.M117.788562

Iaea DB, Mao S, Lund FW, Maxfield FR. 2017. Role of STARD4 in sterol transport between the endocytic recycling compartment and the plasma membrane. Molecular Biology of the Cell 28:1111–1122. doi:10.1091/mbc.E16-07-0499

Iaea DB, Mao S, Maxfield FR. 2014. Steroidogenic acute regulatory protein-related lipid transfer (START) proteins in non-vesicular cholesterol transportCholesterol Transporters of the START Domain Protein Family in Health and Disease: START Proteins-Structure and Function. Springer New York. pp. 173–188. doi:10.1007/978-1-4939-1112-7_8

Iannetti EF, Smeitink JAM, Willems PHGM, Beyrath J, Koopman WJH. 2018. Rescue from galactose-

induced death of Leigh Syndrome patient cells by pyruvate and NAD+. Cell Death and Disease 9. doi:10.1038/s41419-018-1179-4

Inoki K, Zhu T, Guan K-L. 2003. TSC2 Mediates Cellular Energy Response to Control Cell Growth and Survival. Cell 115:577–590.

Iommarini L, Peralta S, Torraco A, Diaz F. 2015. Mitochondrial Diseases Part II: Mouse models of OXPHOS deficiencies caused by defects in regulatory factors and other components required for mitochondrial function. Mitochondrion 22:96–118. doi:10.1016/j.mito.2015.01.008

Jain IH, Zazzeron L, Goli R, Alexa K, Schatzman-Bone S, Dhillon H, Goldberger O, Peng J, Shalem O, Sanjana NE, Zhang F, Goessling W, Zapol WM, Mootha VK. 2016. Hypoxia as a therapy for mitochondrial disease. Science 352:54–61. doi:10.1126/science.aad9642

Janowski BA, Willy PJ, Devi TR, Falck JR, Mangelsdorf DJ. 1996. An oxysterol signalling pathway mediated by the nuclear receptor LXRα. Nature 383. doi:10.1038/383728a0

Jiang LY, Jiang W, Tian N, Xiong YN, Liu J, Wei J, Wu KY, Luo J, Shi XJ, Song BL. 2018. Ring finger protein 145 (RNF145) is a ubiquitin ligase for sterol-induced degradation of HMG-CoA reductase. Journal of Biological Chemistry 293:4047–4055. doi:10.1074/jbc.RA117.001260

Johnson SC, Yanos ME, Kayser E-B, Quintana A, Sangesland M, Castanza A, Uhde L, Hui J, Wall VZ, Gagnidze A, Oh K, Wasko BM, Ramos FJ, Palmiter RD, Rabinovitch PS, Morgan PG, Sedensky MM, Kaeberlein M. 2013. mTOR Inhibition Alleviates Mitochondrial Disease in a Mouse Model of Leigh Syndrome. Science 342. doi:10.1126/science.1244360

Jovaisaite V, Auwerx J. 2015. The mitochondrial unfolded protein response-synchronizing genomes. Current Opinion in Cell Biology 33:74–81. doi:10.1016/j.ceb.2014.12.003

Kappler L, Hoene M, Hu C, von Toerne C, Li J, Bleher D, Hoffmann C, Böhm A, Kollipara L, Zischka H, Königsrainer A, Häring H-U, Peter A, Xu G, Sickmann A, Hauck SM, Weigert C, Lehmann R. 2019. Linking bioenergetic function of mitochondria to tissue-specific molecular fingerprints. American Journal of Physiology-Endocrinology and Metabolism 317:E374–E387. doi:10.1152/ajpendo.00088.2019

Kawaguchi T, Osatomi K, Yamashita H, Kabashima T, Uyeda K. 2002. Mechanism for fatty acid "sparing" effect on glucose-induced transcription: Regulation of carbohydrate-responsive element-binding protein by AMP-activated protein kinase. Journal of Biological Chemistry 277:3829–3835. doi:10.1074/jbc.M107895200

Kellogg BA, Poulter CD. 1997. Chain elongation in the isoprenoid biosynthetic pathway. Current Opinion in Chemical Biology 1:570–578. doi:10.1016/S1367-5931(97)80054-3

Khan NA, Nikkanen J, Yatsuga S, Jackson C, Wang L, Pradhan S, Kivelä R, Pessia A, Velagapudi V, Suomalainen A. 2017. mTORC1 Regulates Mitochondrial Integrated Stress Response and Mitochondrial Myopathy Progression. Cell Metabolism 26:419-428.e5. doi:10.1016/j.cmet.2017.07.007

Koo SH, Flechner L, Qi L, Zhang X, Screaton RA, Jeffries S, Hedrick S, Xu W, Boussouar F, Brindle P, Takemori H, Montminy M. 2005. The CREB coactivator TORC2 is a key regulator of fasting glucose metabolism. Nature 437:1109–1114. doi:10.1038/nature03967

Koopman WJH, Nijtmans LGJ, Dieteren CEJ, Roestenberg P, Valsecchi F, Smeitink JAM, Willems

PHGM. 2010. Mammalian Mitochondrial Complex I: Biogenesis, Regulation, and Reactive Oxygen Species Generation. Antioxidants & Redox Signaling 12:1431–1470. doi:10.1089/ars.2009.2743

Koopman WJH, Verkaart S, Visch HJ, van Emst-de Vries S, Nijtmans LGJ, Smeitink JAM, Willems PHGM. 2007. Human NADH:ubiquinone oxidoreductase deficiency: radical changes in mitochondrial morphology? American Journal of Physiology-Cell Physiology 293:C22–C29. doi:10.1152/ajpcell.00194.2006

Koopman WJH, Willems PHGM, Smeitink JAM. 2012. Monogenic Mitochondrial Disorders. New England Journal of Medicine 366:1132–1141. doi:10.1056/NEJMra1012478

Kops GJPL, Dansen TB, Polderman PE, Saarloos I, Wirtz KWA, Coffer PJ, Huang T-T, Bos JL, Medema RH, Burgering BMT. 2002. Forkhead transcription factor FOXO3a protects quiescent cells from oxidative stress. Nature 419:316–321. doi:10.1038/nature01036

Kühl I, Miranda M, Atanassov I, Kuznetsova I, Hinze Y, Mourier A, Filipovska A, Larsson N-G. 2017. Transcriptomic and proteomic landscape of mitochondrial dysfunction reveals secondary coenzyme Q deficiency in mammals. eLIFE. doi:10.7554/eLife.30952.001

Lagace TA, Byers DM, Cook HW, Ridgway ND. 1997. Altered regulation of cholesterol and cholesteryl ester synthesis in Chinese-hamster ovary cells overexpressing the oxysterol-binding protein is dependent on the pleckstrin homology domain. Biochem J 326:205–213.

Lange Y, Swaisgood MH, Ramos B v., Steck TL. 1989. Plasma membranes contain half the phospholipid and 90% of the cholesterol and sphingomyelin in cultured human fibroblasts. Journal of Biological Chemistry 264:3786–3793. doi:10.1016/s0021-9258(19)84918-9

Laplante M, Sabatini DM. 2009. mTOR signaling at a glance. Journal of Cell Science 122:3589–3594. doi:10.1242/jcs.051011

Lee JP, Brauweiler A, Rudolph M, Hooper JE, Drabkin HA, Gemmill RM. 2010. The TRC8 ubiquitin ligase is sterol regulated and interacts with lipid and protein biosynthetic pathways. Molecular Cancer Research 8:93–106. doi:10.1158/1541-7786.MCR-08-0491

Lee O, O'Brien PJ. 2010. Modifications of Mitochondrial Function by ToxicantsComprehensive Toxicology. Elsevier. pp. 411–445. doi:10.1016/B978-0-08-046884-6.00119-6

Lee YY, Cevallos RC, Jan E. 2009. An upstream open reading frame regulates translation of GADD34 during cellular stresses that induce eIF2phosphorylation. Journal of Biological Chemistry 284:6661–6673. doi:10.1074/jbc.M806735200

Lehto M, Laitinen S, Chinetti G, Johansson M, Ehnholm C, Staels B, Ikonen E, Olkkonen VM. 2001. The OSBP-related protein family in humans. Journal of Lipid Research 42:1203–1213. doi:10.1016/s0022-2275(20)31570-4

Leprivier G, Remke M, Rotblat B, Dubuc A, Mateo ARF, Kool M, Agnihotri S, El-Naggar A, Yu B, Prakash Somasekharan S, Faubert B, Bridon G, Tognon CE, Mathers J, Thomas R, Li A, Barokas A, Kwok B, Bowden M, Smith S, Wu X, Korshunov A, Hielscher T, Northcott PA, Galpin JD, Ahern CA, Wang Y, McCabe MG, Collins VP, Jones RG, Pollak M, Delattre O, Gleave ME, Jan E, Pfister SM, Proud CG, Derry WB, Taylor MD, Sorensen PH. 2013. The eEF2 kinase confers resistance to nutrient deprivation by blocking translation elongation. Cell 153:1064. doi:10.1016/j.cell.2013.04.055

Lerner C, Bitto A, Pulliam D, Nacarelli T, Konigsberg M, van Remmen H, Torres C, Sell C. 2013. Reduced mammalian target of rapamycin activity facilitates mitochondrial retrograde signaling and increases life span in normal human fibroblasts. Aging Cell 12:966–977. doi:10.1111/acel.12122 Li G, Gu HM, Zhang DW. 2013. ATP-binding cassette transporters and cholesterol translocation. IUBMB life 65:505–512. doi:10.1002/iub.1165

Li J, Pfeffer SR. 2016. Lysosomal membrane glycoproteins bind cholesterol and contribute to lysosomal cholesterol export. eLIFE. doi:10.7554/eLife.21635.001

Li Y, Xu S, Mihaylova MM, Zheng B, Hou X, Jiang B, Park O, Luo Z, Lefai E, Shyy JY-J, Gao B, Wierzbicki M, Verbeuren TJ, Shaw RJ, Cohen RA, Zang M. 2011. AMPK Phosphorylates and Inhibits SREBP Activity to Attenuate Hepatic Steatosis and Atherosclerosis in Diet-Induced Insulin-Resistant Mice. Cell Metabolism 13:376–388. doi:10.1016/j.cmet.2011.03.009

Lim MY. 2007. Crash Course: Metabolism and Nutrition, 3rd ed. Elsevier.

Littarru GP, Langsjoen P. 2007. Coenzyme Q10 and statins: Biochemical and clinical implications. Mitochondrion 7. doi:10.1016/j.mito.2007.03.002

Liu GY, Sabatini DM. 2020. mTOR at the nexus of nutrition, growth, ageing and disease. Nature Reviews Molecular Cell Biology. doi:10.1038/s41580-019-0199-y

Liu S, Jing F, Yu C, Gao L, Qin Y, Zhao J. 2015. AICAR-Induced Activation of AMPK Inhibits TSH/SREBP-2/HMGCR Pathway in Liver. PLOS ONE 10:e0124951. doi:10.1371/journal.pone.0124951

Liu Z, Butow RA. 2006. Mitochondrial Retrograde Signaling.
Annual Review of Genetics 40. doi:10.1146/annurev.genet.40.110405.090613

Long X, Lin Y, Ortiz-Vega S, Yonezawa K, Avruch J. 2005. Rheb Binds and Regulates the mTOR Kinase. Current Biology 15. doi:10.1016/j.cub.2005.02.053

Lu F, Liang Q, Abi-Mosleh L, Das A, de Brabander JK, Goldstein JL, Brown MS. 2015. Identification of NPC1 as the target of U18666A, an inhibitor of lysosomal cholesterol export and Ebola infection. eLIFE. doi:10.7554/eLife.12177.001

Luo J, Yang H, Song BL. 2020. Mechanisms and regulation of cholesterol homeostasis. Nature Reviews Molecular Cell Biology 21:225–245. doi:10.1038/s41580-019-0190-7

Luu W, Zerenturk EJ, Kristiana I, Bucknal MP, Sharpe LJ, Brown AJ. 2014. Signaling regulates activity of DHCR24, the final enzyme in cholesterol synthesis. Journal of Lipid Research 55:410–420. doi:10.1194/jlr.M043257

Ma XM, Blenis J. 2009. Molecular mechanisms of mTOR-mediated translational control. Nature Reviews Molecular Cell Biology 10:307–318. doi:10.1038/nrm2672

Marín-Buera L, García-Bartolomé A, Morán M, López-Bernardo E, Cadenas S, Hidalgo B, Sánchez R, Seneca S, Arenas J, Martín MA, Ugalde C. 2015. Differential proteomic profiling unveils new molecular mechanisms associated with mitochondrial complex III deficiency. Journal of Proteomics 113:38–56. doi:10.1016/j.jprot.2014.09.007

Martin LA, Kennedy BE, Karten B. 2016. Mitochondrial cholesterol: mechanisms of import and

effects on mitochondrial function. Journal of Bioenergetics and Biomembranes. doi:10.1007/s10863-014-9592-6

Martin S, Parton RG. 2006. Lipid droplets: a unified view of a dynamic organelle. Nature Reviews Molecular Cell Biology 7. doi:10.1038/nrm1912

McBride HM, Neuspiel M, Wasiak S. 2006. Mitochondria: More Than Just a Powerhouse. Current Biology. doi:10.1016/j.cub.2006.06.054

Mertens KL, Kalsbeek A, Soeters MR, Eggink HM. 2017. Bile acid signaling pathways from the enterohepatic circulation to the central nervous system. Frontiers in Neuroscience 11. doi:10.3389/fnins.2017.00617

Mesmin B, Pipalia NH, Lund FW, Ramlall TF, Sokolov A, Eliezer D, Maxfield FR. 2011. STARD4 abundance regulates sterol transport and sensing. Molecular Biology of the Cell 22:4004–4015. doi:10.1091/mbc.E11-04-0372

Meusser B, Hirsch C, Jarosch E, Sommer T. 2005. ERAD: the long road to destruction. Nature Cell Biology 7:766–772. doi:10.1038/ncb0805-766

Mick E, Titov D v., Skinner OS, Sharma R, Jourdain AA, Mootha VK. 2020. Distinct mitochondrial defects trigger the integrated stress response depending on the metabolic state of the cell. eLIFE 9. doi:10.7554/eLife.49178

Mitchell P. 1961. Coupling of Phosphorylation to Electron and Hydrogen Transfer by a Chemi-Osmotic type of Mechanism. Nature 191. doi:10.1038/191144a0

Morita M, Gravel SP, Chénard V, Sikström K, Zheng L, Alain T, Gandin V, Avizonis D, Arguello M, Zakaria C, McLaughlan S, Nouet Y, Pause A, Pollak M, Gottlieb E, Larsson O, St-Pierre J, Topisirovic I, Sonenberg N. 2013. MTORC1 controls mitochondrial activity and biogenesis through 4E-BP-dependent translational regulation. Cell Metabolism 18:698–711. doi:10.1016/j.cmet.2013.10.001

Mourier A, Motori E, Brandt T, Lagouge M, Atanassov I, Galinier A, Rappl G, Brodesser S, Hultenby K, Dieterich C, Larsson NG. 2015. Mitofusin 2 is required to maintain mitochondrial coenzyme Q levels. Journal of Cell Biology 208:429–442. doi:10.1083/jcb.201411100

Muller FL, Liu Y, van Remmen H. 2004. Complex III releases superoxide to both sides of the inner mitochondrial membrane. Journal of Biological Chemistry 279:49064–49073. doi:10.1074/jbc.M407715200

Nagaraj R, Gururaja-Rao S, Jones KT, Slattery M, Negre N, Braas D, Christofk H, White KP, Mann R, Banerjee U. 2012. Control of mitochondrial structure and function by the Yorkie/YAP oncogenic pathway. Genes and Development 26:2027–2037. doi:10.1101/gad.183061.111

Nakatsu F, Kawasaki A. 2021. Functions of Oxysterol-Binding Proteins at Membrane Contact Sites and Their Control by Phosphoinositide Metabolism. Frontiers in Cell and Developmental Biology 9. doi:10.3389/fcell.2021.664788

Nargund AM, Pellegrino MW, Fiorese CJ, Baker BM, Haynes CM. 2012. Mitochondrial Import Efficiency of ATFS-1 Regulates Mitochondrial UPR Activation. Science 337:587–590. doi:10.1126/science.1223560

Nathan JA. 2020. Squalene and cholesterol in the balance at the ER membrane. Proceedings of the National Academy of Sciences of the United States of America 117:8228–8230. doi:10.1073/pnas.2003388117

Ness GC. 2015. Physiological feedback regulation of cholesterol biosynthesis: Role of translational control of hepatic HMG-CoA reductase and possible involvement of oxylanosterols. Biochimica et Biophysica Acta (BBA) - Molecular and Cell Biology of Lipids 1851. doi:10.1016/j.bbalip.2015.02.008

Nunnari J, Suomalainen A. 2012. Mitochondria: In sickness and in health. Cell 148:1145–1159. doi:10.1016/j.cell.2012.02.035

Palam LR, Baird TD, Wek RC. 2011. Phosphorylation of eIF2 facilitates ribosomal bypass of an inhibitory upstream ORF to enhance CHOP translation. Journal of Biological Chemistry 286:10939–10949. doi:10.1074/jbc.M110.216093

Parks DJ, Blanchard SG, Bledsoe RK, Chandra G, Consler TG, Kliewer S, Stimmel JB, Wilson TM, Zavacki AM, Moore DD, Lehmann JM. 1999. Bile Acids: Natural Ligands for an Orphan Nuclear Receptor. Science 284. doi:10.1126/science.284.5418.1365

Pellegrino MW, Nargund AM, Haynes CM. 2013. Signaling the mitochondrial unfolded protein response. Biochimica et Biophysica Acta - Molecular Cell Research 1833:410–416. doi:10.1016/j.bbamcr.2012.02.019

Peng M, Ostrovsky J, Kwon YJ, Polyak E, Licata J, Tsukikawa M, Marty E, Thomas J, Felix CA, Xiao R, Zhang Z, Gasser DL, Argon Y, Falk MJ. 2015. Inhibiting cytosolic translation and autophagy improves health in mitochondrial disease. Human Molecular Genetics 24:4829–4847. doi:10.1093/hmg/ddv207

Pereira SP, Deus CM, Serafim TL, Cunha-Oliveira T, Oliveira PJ. 2018. Metabolic and phenotypic characterization of human skin fibroblasts after forcing oxidative capacity. Toxicological Sciences 164:191–204. doi:10.1093/toxsci/kfy068

Pessayre D. 2007. Role of mitochondria in non-alcoholic fatty liver diseaseJournal of Gastroenterology and Hepatology (Australia). Blackwell Publishing. doi:10.1111/j.1440-1746.2006.04640.x

Peterson TR, Sengupta SS, Harris TE, Carmack AE, Kang SA, Balderas E, Guertin DA, Madden KL, Carpenter AE, Finck BN, Sabatini DM. 2011. MTOR complex 1 regulates lipin 1 localization to control the srebp pathway. Cell 146:408–420. doi:10.1016/j.cell.2011.06.034

Pfeffer G, Majamaa K, Turnbull DM, Thorburn D, Chinnery PF. 2012. Treatment for mitochondrial disorders. Cochrane Database of Systematic Reviews. doi:10.1002/14651858.cd004426.pub3

Picca A, Lezza AMS. 2015. Regulation of mitochondrial biogenesis through TFAM-mitochondrial DNA interactions. Mitochondrion 25:67–75. doi:10.1016/j.mito.2015.10.001

Pol A, Luetterforst R, Lindsay M, Heino S, Ikonen E, Parton RG. 2001. A Caveolin Dominant Negative Mutant Associates with Lipid Bodies and Induces Intracellular Cholesterol Imbalance 7, The Journal of Cell Biology.

Prabhu A v., Luu W, Li D, Sharpe LJ, Brown AJ. 2016. DHCR7: A vital enzyme switch between cholesterol and vitamin D production. Progress in Lipid Research 64:138–151. doi:10.1016/j.plipres.2016.09.003

Quinzii CM, Hirano M. 2010. Coenzyme Q and mitochondrial disease. Developmental Disabilities Research Reviews 16:183–188. doi:10.1002/ddrr.108

Quirós PM, Prado MA, Zamboni N, D'Amico D, Williams RW, Finley D, Gygi SP, Auwerx J. 2017. Multi-omics analysis identifies ATF4 as a key regulator of the mitochondrial stress response in mammals.

Journal of Cell Biology 216:2027–2045. doi:10.1083/jcb.201702058

Rabinovitch RC, Samborska B, Faubert B, Ma EH, Gravel SP, Andrzejewski S, Raissi TC, Pause A, St.-Pierre J, Jones RG. 2017. AMPK Maintains Cellular Metabolic Homeostasis through Regulation of Mitochondrial Reactive Oxygen Species. Cell Reports 21:1–9. doi:10.1016/j.celrep.2017.09.026

Radhakrishnan A, Goldstein JL, McDonald JG, Brown MS. 2008. Switch-like Control of SREBP-2 Transport Triggered by Small Changes in ER Cholesterol: A Delicate Balance. Cell Metabolism 8:512–521. doi:10.1016/j.cmet.2008.10.008

Radhakrishnan A, Ikeda Y, Joo Kwon H, Brown MS, Goldstein JL. 2007. Sterol-regulated transport of SREBPs from endoplasmic reticulum to Golgi: Oxysterols block transport by binding to Insig.

Ramanathan A, Schreiber SL. 2009. Direct control of mitochondrial function by mTOR. PNAS 29:22229–22232. doi:10.1073/pnas.0912074106

Rauthan M, Ranji P, Pradenas NA, Pitot C, Pilon M. 2013. The mitochondrial unfolded protein response activator ATFS-1 protects cells from inhibition of the mevalonate pathway. Proceedings of the National Academy of Sciences of the United States of America 110:5981–5986. doi:10.1073/pnas.1218778110

Raychaudhuri S, Prinz WA. 2010. The Diverse Functions of Oxysterol-Binding Proteins. Annual Review of Cell and Developmental Biology 26. doi:10.1146/annurev.cellbio.042308.113334

Ribatti D. 2017. A revisited concept: Contact inhibition of growth. From cell biology to malignancy. Experimental Cell Research 359:17–19. doi:10.1016/j.yexcr.2017.06.012

Richter JD, Sonenberg N. 2005. Regulation of cap-dependent translation by eIF4E inhibitory proteins. Nature 433:477–480. doi:10.1038/nature03205

Ridgway ND. 2010. Oxysterol-Binding ProteinsCholesterol Binding and Cholesterol Transport Proteins. Springer-Verlag. doi:10.1007/978-90-481-8622-8_6

Rodriguez-Agudo D, Malacrida L, Kakiyama G, Sparrer T, Fortes C, Maceyka M, Subler MA, Windle JJ, Gratton E, Pandak WM, Gil G. 2019. StarD5: An ER stress protein regulates plasma membrane and intracellular cholesterol homeostasis. Journal of Lipid Research 60:1087–1098. doi:10.1194/jlr.M091967

Rodriguez-Agudo D, Ren S, Hylemon PB, Redford K, Natarajan R, Castillo A del, Gil G, Pandak WM. 2005. Human StarD5, a cytosolic StAR-related lipid binding protein. Journal of Lipid Research 46:1615–1623. doi:10.1194/jlr.M400501-JLR200

Röhrl C, Eigner K, Winter K, Korbelius M, Obrowsky S, Kratky D, Kovacs WJ, Stangl H. 2014. Endoplasmic reticulum stress impairs cholesterol efflux and synthesis in hepatic cells. Journal of Lipid Research 55:94–103. doi:10.1194/jlr.M043299

Rone MB, Fan J, Papadopoulos V. 2009. Cholesterol transport in steroid biosynthesis: Role of protein–protein interactions and implications in disease states. Biochimica et Biophysica Acta (BBA) - Molecular and Cell Biology of Lipids 1791:646–658. doi:10.1016/j.bbalip.2009.03.001

Rossignol R, Faustin B, Rocher C, Malget M, Mazat J-P, Letellier T. 2003. Mitochondrial threshold effects. Biochemical Journal 370:751–762. doi:10.1042/bj20021594

Russell D. 2000. Oxysterol biosynthetic enzymes. Biochimica et Biophysica Acta (BBA) - Molecular

and Cell Biology of Lipids 1529:126–135. doi:10.1016/S1388-1981(00)00142-6

Sarbassov DD, Ali SM, Sabatini DM. 2005. Growing roles for the mTOR pathway. Current Opinion in Cell Biology 17:596–603. doi:10.1016/j.ceb.2005.09.009

Sato R, Inoue J, Kawabe Y, Kodama T, Takano T, Maeda M. 1996. Sterol-dependent transcriptional regulation of sterol regulatory element-binding protein-2. Journal of Biological Chemistry 271:26461–26464. doi:10.1074/jbc.271.43.26461

Schieke SM, Phillips D, McCoy JP, Aponte AM, Shen RF, Balaban RS, Finkel T. 2006. The mammalian target of rapamycin (mTOR) pathway regulates mitochondrial oxygen consumption and oxidative capacity. Journal of Biological Chemistry 281:27643–27652. doi:10.1074/jbc.M603536200

Sever N, Song B-L, Yabe D, Goldstein JL, Brown MS, DeBose-Boyd RA. 2003. Insig-dependent Ubiquitination and Degradation of Mammalian 3-Hydroxy-3-methylglutaryl-CoA Reductase Stimulated by Sterols and Geranylgeraniol. Journal of Biological Chemistry 278:52479–52490. doi:10.1074/jbc.M310053200

Sharpe LJ, Brown AJ. 2013. Controlling cholesterol synthesis beyond 3-hydroxy-3-methylglutaryl-CoA reductase (HMGCR). Journal of Biological Chemistry. doi:10.1074/jbc.R113.479808

Shpilka T, Haynes CM. 2018. The mitochondrial UPR: Mechanisms, physiological functions and implications in ageing. Nature Reviews Molecular Cell Biology. doi:10.1038/nrm.2017.110

Simons K, Ikonen E. 2000. How Cells Handle Cholesterol. Science 290:1721–1726. doi:10.1126/science.290.5497.1721

Simons K, Ikonen E. 1997. Functional rafts in cell membranes. Nature 387:569–572. doi:10.1038/42408

Siraki AG, Pourahmad J, Chan TS, Khan S, O'Brien PJ. 2002. Endogenous and endobiotic induced reactive oxygen species formation by isolated hepatocytes. Free Radical Biology and Medicine 32:2–10. doi:10.1016/S0891-5849(01)00764-X

Skladal D, Halliday J, Thorburn DR. 2003. Minimum birth prevalence of mitochondrial respiratory chain disorders in children. Brain 126:1905–1912. doi:10.1093/brain/awg170

Smeitink JA, Zeviani M, Turnbull DM, Jacobs HT. 2006. Mitochondrial medicine: A metabolic perspective on the pathology of oxidative phosphorylation disorders. Cell Metabolism. doi:10.1016/j.cmet.2005.12.001

Soccio RE, Breslow JL. 2004. Intracellular cholesterol transport. Arteriosclerosis, Thrombosis, and Vascular Biology. doi:10.1161/01.ATV.0000131264.66417.d5

Solsona-Vilarrasa E, Fucho R, Torres S, Nuñez S, Nuño-Lámbarri N, Enrich C, García-Ruiz C, Fernández-Checa JC. 2019. Cholesterol enrichment in liver mitochondria impairs oxidative phosphorylation and disrupts the assembly of respiratory supercomplexes. Redox Biology 24. doi:10.1016/j.redox.2019.101214

Song BL, Javitt NB, DeBose-Boyd RA. 2005. Insig-mediated degradation of HMG CoA reductase stimulated by lanosterol, an intermediate in the synthesis of cholesterol. Cell Metabolism 1:179–189. doi:10.1016/j.cmet.2005.01.001

Sorrentino G, Ruggeri N, Specchia V, Cordenonsi M, Mano M, Dupont S, Manfrin A, Ingallina E, Sommaggio R, Piazza S, Rosato A, Piccolo S, del Sal G. 2014. Metabolic control of YAP and TAZ by the mevalonate pathway. Nature Cell Biology 16:357–366. doi:10.1038/ncb2936

Sousa JS, D'Imprima E, Vonck J. 2018. Mitochondrial respiratory chain complexesSubcellular Biochemistry. Springer New York. pp. 167–227. doi:10.1007/978-981-10-7757-9_7

Spinelli JB, Haigis MC. 2018. The multifaceted contributions of mitochondria to cellular metabolism. Nature Cell Biology. doi:10.1038/s41556-018-0124-1

Stepien KM, Roncaroli F, Turton N, Hendriksz CJ, Roberts M, Heaton RA, Hargreaves I. 2020. Mechanisms of Mitochondrial Dysfunction in Lysosomal Storage Disorders: A Review. Journal of Clinical Medicine 9:2596. doi:10.3390/jcm9082596

Stöckl P, Hütter E, Zwerschke W, Jansen-Dürr P. 2006. Sustained inhibition of oxidative phosphorylation impairs cell proliferation and induces premature senescence in human fibroblasts. Experimental Gerontology 41:674–682. doi:10.1016/j.exger.2006.04.009

Sugii S, Reid PC, Ohgami N, Du H, Chang TY. 2003. Distinct endosomal compartments in early trafficking of low density lipoprotein-derived cholesterol. Journal of Biological Chemistry 278:27180–27189. doi:10.1074/jbc.M300542200

Sun LP, Li L, Goldstein JL, Brown MS. 2005. Insig required for sterol-mediated inhibition of Scap/SREBP binding to COPII proteins in vitro. Journal of Biological Chemistry 280:26483–26490. doi:10.1074/jbc.M504041200

Sun L-P, Seemann J, Goldstein JL, Brown MS. 2007. Sterol-regulated transport of SREBPs from endoplasmic reticulum to Golgi: Insig renders sorting signal in Scap inaccessible to COPII proteins.

Sundqvist A, Bengoechea-Alonso MT, Ye X, Lukiyanchuk V, Jin J, Harper JW, Ericsson J. 2005. Control of lipid metabolism by phosphorylation-dependent degradation of the SREBP family of transcription factors by SCFFbw7. Cell Metabolism 1:379–391. doi:10.1016/j.cmet.2005.04.010

Suomalainen A, Battersby BJ. 2018. Mitochondrial diseases: The contribution of organelle stress responses to pathology. Nature Reviews Molecular Cell Biology 19:77–92. doi:10.1038/nrm.2017.66

Tee AR, Manning BD, Roux PP, Cantley LC, Blenis J. 2003. Tuberous Sclerosis Complex Gene Products, Tuberin and Hamartin, Control mTOR Signaling by Acting as a GTPase-Activating Protein Complex toward Rheb. Current Biology 13:1259–1268. doi:10.1016/S

Thomas C, Pellicciari R, Pruzanski M, Auwerx J, Schoonjans K. 2008. Targeting bile-acid signalling for metabolic diseases. Nature Reviews Drug Discovery 7:678–693. doi:10.1038/nrd2619

Torraco A, Peralta S, Iommarini L, Diaz F. 2015. Mitochondrial Diseases Part I: Mouse models of OXPHOS deficiencies caused by defects in respiratory complex subunits or assembly factors. Mitochondrion 21:76–91. doi:10.1016/j.mito.2015.01.009

Trevisson E, Dimauro S, Navas P, Salviati L. 2011. Coenzyme Q deficiency in muscle. Current Opinion in Neurology 24:449–456. doi:10.1097/WCO.0b013e32834ab528

Trzaskos JM. 1995. Oxylanosterols as modifiers of cholesterol biosynthesis. Progress in Lipid Research 34. doi:10.1016/0163-7827(94)00008-A

Vafai SB, Mootha VK. 2012. Mitochondrial disorders as windows into an ancient organelle. Nature 491:374–383. doi:10.1038/nature11707

Valsecchi F, Monge C, Forkink M, de Groof AJC, Benard G, Rossignol R, Swarts HG, van Emst-De Vries

SE, Rodenburg RJ, Calvaruso MA, Nijtmans LGJ, Heeman B, Roestenberg P, Wieringa B, Smeitink JAM, Koopman WJH, Willems PHGM. 2012. Metabolic consequences of NDUFS4 gene deletion in immortalized mouse embryonic fibroblasts. Biochimica et Biophysica Acta - Bioenergetics 1817:1925–1936. doi:10.1016/j.bbabio.2012.03.006

Voilquin L, Lodi M, di Mattia T, Chenard M-P, Mathelin C, Alpy F, Tomasetto C. 2019. STARD3: A Swiss Army Knife for Intracellular Cholesterol Transport. Contact 2:251525641985673. doi:10.1177/2515256419856730

Walther TC, Farese R v. 2012. Lipid Droplets and Cellular Lipid Metabolism. Annual Review of Biochemistry 81. doi:10.1146/annurev-biochem-061009-102430

Wang C, Youle R. 2016. Form follows function for mitochondria. Nature 530. doi:10.1038/530288a

Wang C, Youle RJ. 2009. The Role of Mitochondria in Apoptosis. Annual Review of Genetics 43. doi:10.1146/annurev-genet-102108-134850

Wang M, Casey PJ. 2016. Protein prenylation: Unique fats make their mark on biology. Nature Reviews Molecular Cell Biology 17:110–122. doi:10.1038/nrm.2015.11

Wang Y, Hekimi S. 2016. Understanding Ubiquinone. Trends in Cell Biology 26. doi:10.1016/j.tcb.2015.12.007
Weissig V. 2020. Drug Development for the Therapy of Mitochondrial Diseases. Trends in Molecular Medicine. doi:10.1016/j.molmed.2019.09.002

Wek RC. 2018. Role of eIF2α kinases in translational control and adaptation to cellular stress. Cold Spring Harbor Perspectives in Biology 10. doi:10.1101/cshperspect.a032870 Wek RC, Jiang H-Y, Anthony TG. 2006. Coping with stress: eIF2 kinases and translational control. Biochemical Society Transactions.

White SM, Avantaggiati ML, Nemazanyy I, di Poto C, Yang Y, Pende M, Gibney GT, Ressom HW, Field J, Atkins MB, Yi C. 2019. YAP/TAZ Inhibition Induces Metabolic and Signaling Rewiring Resulting in Targetable Vulnerabilities in NF2-Deficient Tumor Cells. Developmental Cell 49:425-443.e9. doi:10.1016/j.devcel.2019.04.014

Wiley CD, Velarde MC, Lecot P, Liu S, Sarnoski EA, Freund A, Shirakawa K, Lim HW, Davis SS, Ramanathan A, Gerencser AA, Verdin E, Campisi J. 2016. Mitochondrial dysfunction induces senescence with a distinct secretory phenotype. Cell Metabolism 23:303–314. doi:10.1016/j.cmet.2015.11.011

Wilhelm LP, Voilquin L, Kobayashi T, Tomasetto C, Alpy F. 2019. Intracellular and Plasma Membrane Cholesterol Labeling and Quantification Using Filipin and GFP-D4 In: Drin G, editor. Intracellular Lipid Transport: Methods and Protocols. Springer. doi:10.1007/978-1-4939-9136-5_11

Wirth C, Brandt U, Hunte C, Zickermann V. 2016. Structure and function of mitochondrial complex i. Biochimica et Biophysica Acta - Bioenergetics 1857:902–914. doi:10.1016/j.bbabio.2016.02.013

Wu S-B, Wei Y-H. 2012. AMPK-mediated increase of glycolysis as an adaptive response to oxidative stress in human cells: Implication of the cell survival in mitochondrial diseases. Biochimica et Biophysica Acta (BBA) - Molecular Basis of Disease 1822:233–247. doi:10.1016/j.bbadis.2011.09.014

Wu S-B, Wu Y-T, Wu T-P, Wei Y-H. 2014. Role of AMPK-mediated adaptive responses in human cells with mitochondrial dysfunction to oxidative stress. Biochimica et Biophysica Acta (BBA) - General Subjects 1840:1331–1344. doi:10.1016/j.bbagen.2013.10.034

Wullschleger S, Loewith R, Hall MN. 2006. TOR signaling in growth and metabolism. Cell. doi:10.1016/j.cell.2006.01.016

Yabe D, Brown MS, Goldstein JL. 2002. Insig-2, a second endoplasmic reticulum protein that binds SCAP and blocks export of sterol regulatory element-binding proteins. Proceedings of the National Academy of Sciences 99. doi:10.1073/pnas.162488899

Yan D, Mäyränpää MI, Wong J, Perttilä J, Lehto M, Jauhiainen M, Kovanen PT, Ehnholm C, Brown AJ, Olkkonen VM. 2008. OSBP-related protein 8 (ORP8) suppresses ABCA1 expression and cholesterol efflux from macrophages. Journal of Biological Chemistry 283:332–340. doi:10.1074/jbc.M705313200

Yang T, Espenshade PJ, Wright ME, Yabe D, Gong Y, Aebersold R, Goldstein JL, Brown MS. 2002. Crucial Step in Cholesterol Homeostasis: Sterols Promote Binding of SCAP to INSIG-1, a Membrane Protein that Facilitates Retention of SREBPs in ER. Cell 110:489–500.

Ylikallio E, Suomalainen A. 2012. Mechanisms of mitochondrial diseases. Annals of Medicine 44:41–59. doi:10.3109/07853890.2011.598547

Yu W, Gong JS, Ko M, Garver WS, Yanagisawa K, Michikawa M. 2005. Altered cholesterol metabolism in Niemann-Pick type C1 mouse brains affects mitochondrial function. Journal of Biological Chemistry 280:11731–11739. doi:10.1074/jbc.M412898200

Zanconato F, Forcato M, Battilana G, Azzolin L, Quaranta E, Bodega B, Rosato A, Bicciato S, Cordenonsi M, Piccolo S. 2015. Genome-wide association between YAP/TAZ/TEAD and AP-1 at enhancers drives oncogenic growth. Nature Cell Biology 17:1218–1227. doi:10.1038/ncb3216

Zelcer N, Hong C, Boyadjian R, Tontonoz P. 2009. LXR Regulates Cholesterol Uptake Through Idol-Dependent Ubiquitination of the LDL Receptor. Science 325:100–104. doi:10.1126/science.1168974

Zelcer N, Sharpe LJ, Loregger A, Kristiana I, Cook ECL, Phan L, Stevenson J, Brown AJ. 2014. The E3 Ubiquitin Ligase MARCH6 Degrades Squalene Monooxygenase and Affects 3-Hydroxy-3-Methyl-Glutaryl Coenzyme A Reductase and the Cholesterol Synthesis Pathway. Molecular and Cellular Biology 34:1262–1270. doi:10.1128/MCB.01140-13

Zhang DW, Lagace TA, Garuti R, Zhao Z, McDonald M, Horton JD, Cohen JC, Hobbs HH. 2007. Binding of proprotein convertase subtilisin/kexin type 9 to epidermal growth factor-like repeat A of low density lipoprotein receptor decreases receptor recycling and increases degradation. Journal of Biological Chemistry 282:18602–18612. doi:10.1074/jbc.M702027200

Zhao Q, Hogenraad N. 2002. A mitochondrial specific stress response in mammalian cells. The EMBO Journal 21. doi:10.1093/emboj/cdf445

Zhou D, Palam LR, Jiang L, Narasimhan J, Staschke KA, Wek RC. 2008. Phosphorylation of eIF2 directs ATF5 translational control in response to diverse stress conditions. Journal of Biological Chemistry 283:7064–7073. doi:10.1074/jbc.M708530200

Zhou Q, Liu C, Liu W, Zhang H, Zhang R, Liu J, Zhang J, Xu C, Liu L, Huang S, Chen L. 2015. Rotenone induction of hydrogen peroxide inhibits mTOR-mediated S6K1 and 4E-BP1/eIF4E pathways, leading to neuronal apoptosis. Toxicological sciences : an official journal of the Society of Toxicology 143:81–96. doi:10.1093/toxsci/kfu211

Zorova LD, Popkov VA, Plotnikov EY, Silachev DN, Pevzner IB, Jankauskas SS, Babenko VA, Zorov SD,

Balakireva A v., Juhaszova M, Sollott SJ, Zorov DB. 2018. Mitochondrial membrane potential. Analytical Biochemistry 552:50–59. doi:10.1016/j.ab.2017.07.009

CHRISTOPHER WALL

PharmD

@ ctj.wall@gmail.com Lausanne, Switzerland www.linkedin.com/in/ctjwall/

RESEARCH EXPERIENCE

Ph.D. candidate in Molecular Life Science

EPFL & Nestlé Research

2017 – Ongoing Lausanne, Switzerland

- Set up and interpreted various omics experiments in the context of mitochondrial disease
- Adapted RNAseq analysis pipelines for hypothesis testing
- Ran chromatographic techniques for metabolite quantification

Post-graduate research intern

Hubrecht Institute

Sept 2016 – Mar 2017 Utrecht, The Netherlands

- Investigated endonuclease-null Cas9 (dCas9) for the transdifferentiation of mouse embryonal fibroblasts.
- Applied cell-culture and molecular biology technologies such as Cas9.

Graduate research intern

National University of Singapore

Aug 2014 – Mar 2015 Singapore, Singapore

- Characterised the immunogenic properties of various nanoparticles intended for drug delivery.

PUBLICATIONS

Journal Articles

- Chareyron, I., Wall, C., Thevenet, J., Santo-Domingo, J., & Wiederkehr, A. (2019). Cellular stress is a prerequisite for glucose-induced mitochondrial matrix alkalinization in pancreatic beta-cells. *Mol Cell Endocrinol*, *481*, 71–83.

WORK EXPERIENCE

Assistant pharmacist

University Hospital Amsterdam (AMC)

2012 – 2016 Amsterdam, The Netherlands

- Responsible for dug surveillance and distribution of parenteral medication for pediatric ICU and oncology departments

EDUCATION

Ph.D. candidate in Molecular Life Science

EPFL

2017 – Ongoing Lausanne, Switzerland

- Completed course on biostatistics, main project running a GWAS
- Completed courses on programming in python, ImageJ and R.

M.Sc. Major in Pharmacy

Utrecht University

2013-2016 | Utrecht, The Netherlands

- Specialised in analytical chemistry and drug dosage design.

B.Sc. Major in Pharmacy

Utrecht University

2009-2013 | Utrecht, The Netherlands

- Education in healthcare, human anatomy and biology.

PROJECTS

Faces of Industrial Research 2021 symposium

Virtual event https://fir-2021.com/

2020-2021 | Lausanne, Switzerland

- Lead organiser of the Faces of Industrial Research symposium.

Faces of Industrial Research 2020 symposium

EPFL Rolex Learning Center

2019-2020 | Lausanne, Switzerland

- Head of finances of the Faces of Industrial Research symposium.

Faces of Industrial Research 2019 symposium

EPFL campus

2018-2019 | Lausanne, Switzerland

- Head of media and advertisement of the Faces of Industrial Research symposium.

LANGUAGES

English
Dutch
French